profile). Roughness and waviness are differentiated by means of profile filters.

Profile height P_t, R_t, W_t
Maximum excursion above the centerline Z_p plus the maximum excursion below the centerline Z_v within the traversing length l_n.

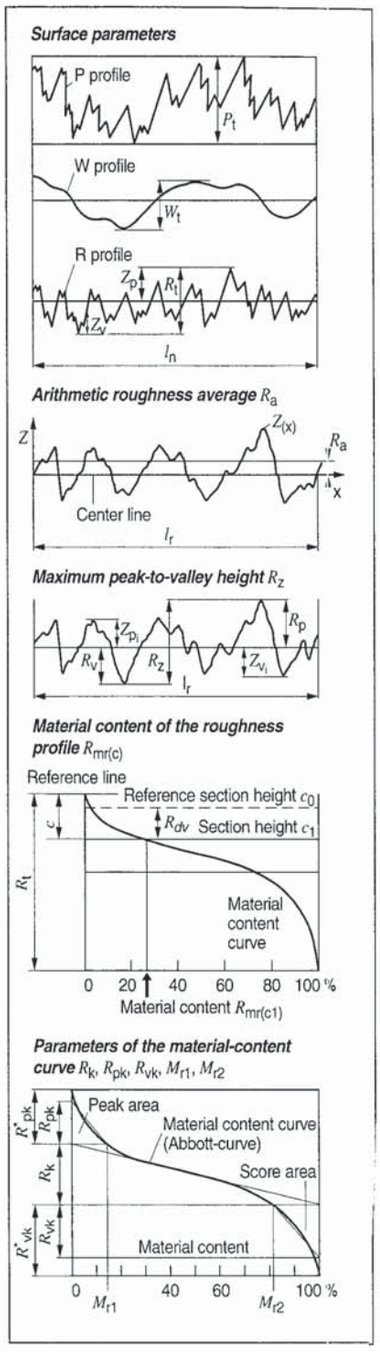
The traversing length l_n can consist of one or more sampling lengths l_r. The value of a parameter is computed from the measured data for its sampling length. As a rule, five sampling lengths are required for computing the roughness and waviness parameters. The standardized measuring conditions are based on the maximum roughness peak-to-valley height and include, for example, limit wave length λ_c, sampling length l_r, traversing length l_n, profile length l_t, stylus-tip radius $r_{SP\,max}$ and digitizing cutoff Δx_{max}). For industrial purposes, the parameters generally employed in describing surfaces are as follows:

Arithmetic roughness average R_a
Arithmetic average of the absolute values of the ordinates of the roughness profile.

Maximum peak-to-valley height R_z
Maximum excursion above the centerline R_p plus the maximum excursion below the centerline R_v within a sampling length. As the vertical distance between the highest peak and the lowest valley, R_z is a measure of scatter of the roughness ordinates.

Material content of the roughness profile $R_{mr(c)}$
The material-content curve reflects the material content as a function of section height c. The characteristic is formed by a percentage relationship between the sum of the material lengths Ml(c) of the profile elements in a specified section height c and traversing length l_n..

Parameters of the material-content curve R_k, R_{pk}, R_{vk}, Mr_1, Mr_2
The material-content curve derived from the filtered roughness profile is divided into three sections characterized by parameters (core peak-to-valley height R_k, reduced peak height R_{pk} and reduced score depth R_{vk}). The parameters Mr_1 and Mr_2 reflect the material content at the limits of the roughness core profile.



PETITIONER'S EXHIBIT 1002
US PATENT NO. 6,557,540

Sliding bearings and rolling bearings

Sliding bearings

Different types of sliding bearings range from bearings with usually complete separation of the sliding surfaces by a lubrication film (fluid friction), through self-lubricating bearings, most of which exhibit mixed friction i.e. some of the bearing load is transformed to solid contact between the sliding surfaces), to dry sliding-contact bearings which exhibit dry friction (i.e. completely without an effective fluid lubricating film), but which nevertheless have an adequate service life.

Most of the hydrodynamic sliding bearing types used in automotive applications are circular cylindrical radial-sleeve bearings (often with oval clearance) for holding the crankshaft and camshaft, and turbocharger bearings. Thrust bearings are usually used only as axial locators, and are not subjected to large forces.

Hydrodynamic sliding bearings

Symbols (DIN 31 652)

Designation	Symbols	Unit
bearing length bearing diameter	B	m
nal diameter) diameter (nominal	D	m
ter) tricity (displacement	d	m
en shaft and bearing s)	e	m
	F	N
bricant depth	h_0	m
ubricant pressure	p	Pa = N/m²
load $\bar{p} = F/(B \cdot D)$	$\bar{p}$	Pa
clearance $s = (D - d)$	s	m
rfeld number	So	–
eccentricity 2 e/s	ε	–
dynamic viscosity		
bricant	η_{eff}	Pa · s
bearing clearance		
	ψ	–
ment angle	β	°
namically effective elocity	ω_{eff}	s⁻¹

A hydrodynamic sliding bearing is reliable in service if it remains sufficiently unaffected by the following:
- Wear (sufficient separation of the contact surfaces by the lubricant),
- Mechanical stress (bearing material of sufficient strength),
- Thermal loading (observance of thermal stability of bearing material and viscosity/temperature behavior of lubricant).

The dimensionless Sommerfeld number So is used when determining loadability, i.e. when assessing the formation of the lubricating film

$$So = D \cdot \psi^2/(D \cdot B \cdot \eta_{eff} \cdot \omega_{eff})$$

As the Sommerfeld number So increases, relative eccentricity ε rises and minimum lubricating-film thickness h_0 drops:

$$h_0 = (D - d)/2 - e = 0.5\, D \cdot \psi \cdot (1 - \varepsilon)$$

with relative eccentricity

$$\varepsilon = 2e/(D - d)$$

Table 1. Orders of magnitude of the coefficients of friction for different types of friction
The coefficients of friction given below are approximate values, and are intended solely for comparison of the different types of friction.

Type of friction	Coefficient of friction f
Dry friction	0.1 .. > 1
Mixed friction	0.01 .. 0.1
Fluid friction	0.01
Friction in roller bearings	0.001

Table 2. Empirical values for maximum approved specific bearing load (Maximum values only apply for very low sliding velocities)

Bearing materials	Maximum specif. bearing load $\bar{p}_{lim}$
Pb and Sn alloys (babbitt metals)	5 ... 15 N/mm²
Bronze, lead base	7 ... 20 N/mm²
Bronze, tin base	7 ... 25 N/mm²
AlSn alloys	7 ... 18 N/mm²
AlZn alloys	7 ... 20 N/mm²

PETITIONER'S EXHIBIT 1002
US PATENT NO. 6,557,540

The Sommerfeld number is also used to determine the coefficient of friction in the bearing, and thus for calculation of frictional power and thermal stress (cf. DIN 31 652, VDI Guideline 2204).

Because hydrodynamic bearings also operate with mixed friction a certain amount of the time, they must accommodate a certain amount of contamination without loss of function, and are additionally subjected to high dynamic and thermal stress (particularly in piston engines), the bearing material must meet a number of requirements, some of which are opposed to each another.

- Anti-seizure performance (resistance to welding),
- Conformability (compensation of misalignment without shortening service life),
- Embeddability (ability of the bearing surface to absorb particles of dirt without increasing bearing or shaft wear),
- Fatigue strength (under fatigue loading, particularly with high thermal stress),
- Mechanical loadability,
- Run-in performance (a combination of compatibility, resistance to wear and embeddability),
- Seizure resistance (bearing material must not weld to shaft material, even under high compressive load and high sliding velocity),
- Wear resistance (in the case of mixed friction),
- Wettability by lubricant.

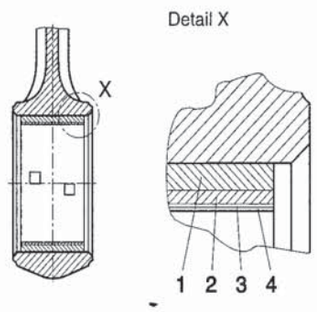
If a bearing (e.g. piston-pin bushing) is to be simultaneously subjected to high loads and low sliding velocities, high fatigue strength and wear resistance should take precedence over resistance to seizing. Bearing materials used in such cases are hard bronzes, e.g. leaded tin bronzes (Table 3).

Since they are subjected to high dynamic loads with high sliding velocities, connecting-rod and crankshaft bearings in internal-combustion engines must fulfill a number of different requirements. In these applications, **multilayer bearings**, above all trimetal bearings, have proved themselves in practice.

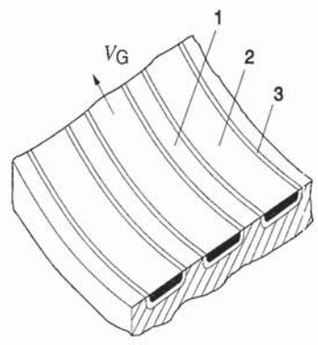
The service life of crankshaft bearings can be further increased through the use of **grooved sliding bearings**. In these bearings, fine grooves have been machined into the surface in the sliding direction, and filled with a liner made of soft material (an electroplated liner similar to that found in trimetal bearings). These contact areas are separated from one another by a harder light-alloy metal.

These bearings feature low rates of wear and high fatigue strength with good embeddability regarding lubricant impurities.

Multilayer bearing
(Design of a trimetal bearing)
1 Steel backing shell, 2 Cast lead bronze (0.4 mm), 3 Nickel barrier between lead bronze and babbitt-metal (1...2 µm), 4 Electroplated babbitt-metal liner (overlay, e.g., 20 µm).



Section through a grooved friction bearing
(MIBA patent). The liner has very fine grooves in the running direction V_G.
1 Wear-resistant light-alloy metal, 2 Soft liner, 3 Nickel barrier.



PETITIONER'S EXHIBIT 1002
US PATENT NO. 6,557,540

Table 3. Selection of materials for hydrodynamic sliding bearings

Material	Alloy designation	Composition in %	HB hardness 20 °C	HB hardness 100 °C	Remarks, application examples
Tin-base babbitt metal	LgPbSn 80 (WM 80)	80 Sn; 12 Sb; 6 Cu; 2 Pb	27	10	Very soft, good conformance of contact surfaces to off-axis operation, excellent anti-seizure performance.
Lead-base babbitt metal	LgPbSn 10 (WM 10)	73 Pb; 16 Sb; 10 Sn; 1 Cu	23	9	Reinforcement necessary, e.g. as composite steel casting or with intermediate nickel layer on lead bronze.
Lead-base bronze	G-CuPb 25	74 Cu; 25 Pb; 1 Sn	50	47	Very soft, excellent anti-seizure performance, less resistant to wear.
	G-CuPb 22	70 Cu; 22 Pb; 6 Sn; 3 Ni	86	79	
Lead-tin-base bronze	G-CuPb 10 Sn	80 Cu; 10 Pb; 10 Sn	75	67	Improved anti-seizure performance by alloying with Pb. More resistant to off-axis performance than pure tin bronzes, therefore high-load Pb-Sn bronzes are preferable for use as crankshaft bearings. Composite bearings used in internal-combustion engine manufacture, piston-pins $\bar{p}$ to 100 N/mm².
	G-CuPb 23 Sn	76 Cu; 23 Pb; 1 Sn	55	53	Composite casting for low-load bearings (70 N/mm²). Also thick-wall bearing shells. Very good anti-seizure performance. Crankshaft and camshaft bearings, connecting-rod bearings.
Tin-base bronze	G-CuSn 10 Zn	88 Cu; 10 Sn; 2 Zn	85		Hard material. Friction-bearing shells can be subjected to moderate load at low sliding velocities. Worm gears.
	CuSn 8	92 Cu; 8 Sn	80 ... 220		High-grade wrought alloy. Good performance under high loads and in absence of sufficient lubrication. Steering-knuckle bearings. Particularly well suited for use as thin-wall sliding bearing bushings.
Red brass	G-CuSn7 ZnPb	83 Cu; 6 Pb; 7 Sn; 4 Zn	75	65	Tin partially replaced with zinc and lead. Can be used in place of tin bronze, but only for moderate loads (40 N/mm²). General sliding bearings for machinery. Piston pins, bushings, crankshaft and toggle-lever bearings.

PETITIONER'S EXHIBIT 1002
US PATENT NO. 6,557,540

Material	Alloy designation	Composition in %	HB hardness 20 °C	HB hardness 100 °C	Remarks, application examples
Brass	CuZn 31 Si	68 Cu: 31 Zn; 1 Si	90 ... 200		Zn content is disadvantageous at high bearing temperatures. Can be used in place of tin bronze; low loads.
Aluminum bronze	CuAl 9 Mn	88 Cu; 9 Al; 3 Mn	110 ... 190		Thermal expansion comparable to that of light alloys. Suitable for use as interference-fit bearings in light-alloy housings. Better wear resistance than tin bronze, but higher friction.
Aluminum alloy	AlSi 12 Cu NiMn	1 Cu; 85 Al; 12 Si; 1 Ni; 1 Mn	110	100	Piston alloy for low sliding velocities.
Rolled aluminum cladding	AlSn 6	1 Cu; 6 Sn; 90 Al; 3 Si	40	30	Liquated tin stretched by rolling, therefore high loadability and good anti-friction properties. Improved by electroplated layer.
Electro-plated liners	PbSn 10 Cu	2 Cu; 88 Pb; 10 Sn	50 ... 60		Used in modern trimetal bearings, electroplated to thickness 10 ... 30 µm, very fine grain. Intermediate nickel layer on bearing metal.

For materials, see also DIN 1703, 1705, 1716, 17 660, 17 662, 17 665, 1494, 1725, 1743.
ISO 4381, 4382, 4383.

Table 4. Sintered-metal bearing materials
Sint-B indicates 20 % P (porosity) (Sint-A: 25 % P; Sint-C: 15 % P).

Material group	Designation Sintered ...	Composition	Remarks
Sintered iron	B 00	Fe	Standard material which meets moderate load and noise requirements.
Sintered steel, containing Cu	B 10	< 0.3 C 1 ... 5 Cu Rest Fe	Good resistance to wear, can be subjected to higher loads than pure Fe bearings.
Sintered steel, higher Cu content	B 20	20 Cu Rest Fe	More favorably priced than sintered bronze, good noise behavior and $p \cdot v$ values.
Sintered bronze	B 50	< 0.2 C 9 ... 10 Sn Rest Cu	Standard Cu-Sn-base material, good noise behavior.

PETITIONER'S EXHIBIT 1002
US PATENT NO. 6,557,540

Sintered-metal sliding bearings

Sintered-metal sliding bearings consist of sintered metals which are porous and impregnated with liquid lubricants. For many small motors in automotive applications, this type of bearing is a good compromise in terms of precision, installation, freedom from maintenance, service life and cost. They are primarily used in motors with shaft diameters from 1.5...12 mm. Sintered-iron bearings and sintered-steel bearings (inexpensive, less likely to interact with the lubricant) are preferable to sintered-bronze bearings for use in the motor vehicle (Table 4). The advantages of sintered-bronze bearings are greater loadability, lower noise and lower friction indices (this type of bearing is used in phonograph equipment, office equipment, data systems and cameras).

The performance of sintered bearings over long periods of service is closely related to the use of optimum lubricants.

Mineral oils: Inadequate cold-flow properties, medium non-aging properties.

Synthetic oils: (e.g. esters, Poly-α olefins): Good cold-flow properties, high resistance to thermal stresses, low evaporation tendency.

Synthetic greases: (oils which include metal soaps): Low starting friction, low wear.

Dry sliding bearings

(see Table 5, P. 288)

Solid polymer bearings made of thermoplastics

Advantages: Economically-priced, no danger of seizure with metals.

Disadvantages: Low thermal conductivity, relatively low operating temperatures, possible swelling due to humidity, low loadability, high coefficient of thermal expansion.

The most frequently used polymer materials are: Polyoxymethylene (POM, POM-C), polyamide (PA), polyethylene and polybutylene terephthalate (PET, PBT), polyetheretherketone (PEEK).

The tribological and mechanical properties can be varied over a wide range by incorporating lubricants and reinforcements in the thermoplastic base material.

Lubricant additives: polytetrafluoroethylene (PTFE), graphite (C), silicone oil and other liquid lubricants.

Reinforcement additives: glass fibers (GF), carbon fibers (CF).

Application examples: windshield wiper bearings (PA and fiberglass), idle-position actuators (PEEK and carbon fiber, PTFE and other additives).

Polymer bearings made of duroplastics and elastomers

These materials, with their high levels of intrinsic friction, are seldom used as bearing materials in the motor vehicle. Duroplastics include: phenol resins (high friction, e.g. Resitex), epoxy resins (require the addition of PTFE or C in order to reduce their high intrinsic brittleness, reinforcement necessary usually by fibers), polyimides (high thermal and mechanical loadability).

Application examples: polyimide axial stop in wiper motor.

Metal-backed composite bearings

Composite bearings are combinations of polymer materials, fibers and metals. Depending upon bearing structure, they provide advantages over pure or filled polymer sliding bearings in terms of loadability, bearing clearance, thermal conductivity and installation (suitable for use with oscillating motion).

Example of bearing structure: Tinplated or copper-clad steel backing (several millimeters thick), onto which is sintered an 0.2...0.35 mm thick porous bronze layer with a porosity of 30...40%. A low-friction polymer material is rolled into this bronze layer as a liner. Liner made of a) acetal resin, either impregnated with oil or containing lubricating recesses, or b) PTFE + Pb or MoS_2 additive.

Metal-backed composite bearings are available in a number of different shapes and compositions. Metal-backed composite bearings with woven PTFE fiber inserts exhibit unusually high loadability

PETITIONER'S EXHIBIT 1002
US PATENT NO. 6,557,540

and are suitable for use in ball-and-socket joints.

Some motor-vehicle applications for this type of bearing are: Shock-absorber-piston bearings, release-lever bearings for clutch pressure plates, brake-shoe bearings in drum brakes, ball-and-socket bearings, door-hinge bearings, bearings for seat-belt winding shafts, steering-knuckle bearings, gear-pump bearings.

Carbon-graphite bearings

Carbon-graphite bearings are members of the ceramic bearing family due to their method of manufacture and material properties. The base materials are powdered carbon; tar or synthetic resins are used as binders.

Advantages: Heat-resistant up to 350 °C (hard-burnt carbon) or 500 °C (electro-graphite), good antifriction properties, good corrosion resistance, good thermal conductivity, good thermal shock resistance. They are highly brittle, however.

Examples of carbon-graphite bearing applications: Fuel-pump bearings, bearings in drying ovens, adjustable blades in turbochargers.

Metal-ceramic bearings

Metal-ceramic bearings consist of material manufactured by powder metallurgy processes; in addition to the metallic matrix, the bearing material also contains finely distributed solid lubricant particles.

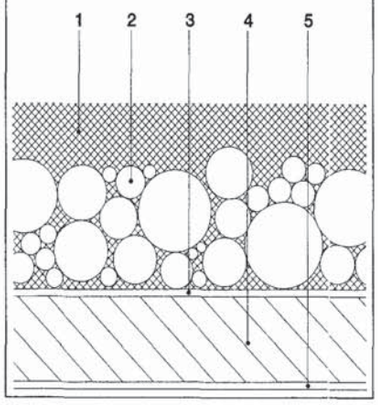
Matrix: e.g. bronze, iron, nickel.

Lubricant: e.g. graphite, MoS_2.

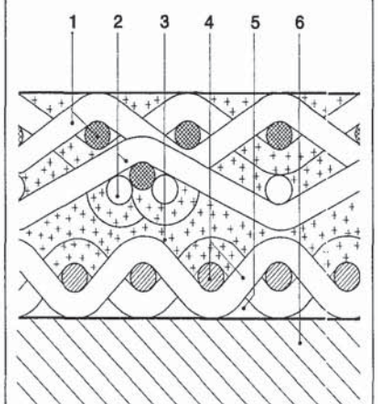
These materials are suitable for use under extremely high loads, and are at the same time self-lubricating.

Application example: Steering-knuckle bearings.

Cutaway view of a self-lubricated composite bearing
1 Polymer liner, 2 Porous bronze layer, 3 Copper layer, 4 Steel backing, 5 Tin layer.



Section through composite bearing with fabric insert made of PTFE and fiberglass
1 PTFE fiber fabric, 2 Adhesive fibers, 3 Resin, 4 Fiberglass backing, 5 Adhesive, 6 Steel backing.



PETITIONER'S EXHIBIT 1002
US PATENT NO. 6,557,540

Table 5. Properties of maintenance-free, self-lubricating bearings

	Sintered bearings oil-impregnated		Polymer bearings		Metal-backed composite bearings Liner		Synthetic carbons
	Sintered iron	Sintered bronze	Thermoplastic polyamide	Duroplastic polyimide	PTFE + additive	Acetal resin	
Compression strength N/mm²	80 ... 180		70	110	250	250	100 ... 200
Max. sliding velocity m/s	10	20	2	8	2	3	10
Typical load N/mm²	1 ... 4 (10)		15	50 (at 50 °C) 10 (at 200 °C)	20 ... 50	20 ... 50	50
Permissible operating temperature °C Short-term	– 60 ... 180 (depends on oil) 200		– 130 ... 100 120	– 100 ... 250 300	– 200 ... 280	– 40 ... 100 130	– 200 ... 350 500
Coefficient of friction without lubrication	with lubrication 0.04 ... 0.2		0.2 ... 0.4 (100 °C) 0.4 ... 0.6 (25 °C)	0.2 ... 0.5 (unfilled) 0.1 ... 0.4 (filled)	0.04 ... 0.2	0.07[1]) ... 0.2 [1]) PTFE filled	0.1 ... 0.35
Thermal conductivity W/(m · K)	20 ... 40		0.3	0.4 ... 1	46	2	10 ... 65
Corrosion resistance	poor	good	very good		good	good	very good
Chemical resistance	none		very good		conditional	conditional	good
max. $p \cdot v$ (N/mm²) · (m/s)	20		0.05	0.2	1.5 ... 2		0.4 ... 1.8
Embeddability of dirt and abraded material	poor		good	good	poor	good	poor

PETITIONER'S EXHIBIT 1002
US PATENT NO. 6,557,540

Rolling bearings

In rolling bearings, forces are transmitted by rolling elements (balls or rollers). Here, rolling is a form of movement comprising rolling and sliding. In rolling bearings a microslip (i.e. sliding) nearly always occurs in addition to the pure rolling movement. In the case of mixed friction, this sliding movement leads to increased wear.

Advantages:
Low static coefficient of friction (0.001...0.002), therefore particularly well suited to applications in which starting occurs frequently,
Low maintenance,
Suited to permanent lubrication,
Low lubricant consumption,
Small bearing width,
High precision.

Disadvantages:
Sensitive to impact loads, sensitive to dirt,
Bearing noise is too high for some applications,
Standard bearings are only 1-piece bearings.

Bearing materials

Bearing races and rolling elements are made of a special chromium-alloy steel (100 Cr6H) which has a high degree of purity and a hardness in the range of 58...65 HRC.

Depending upon application, the bearing cages are made of stamped sheet steel or brass. Cages made of polymer materials have come into recent use due to their ease of manufacture, improved adaptability to bearing geometry and other tribological advantages (e.g. antifriction properties). Polymer materials made of fiberglass-reinforced polyamide 66 can withstand continuous operating temperatures of up to 120 °C, and can be operated for brief periods at temperatures up to 140 °C.

Static loadability (ISO 76-1987)

The static load rating Co is used as a measure of the loadability of very slow-moving or static rolling bearings. Co is that load at which total permanent deformation of rolling elements and races at the most highly-loaded contact point amounts to 0.0001 of the diameter of the rolling element. A load equal to this load rating Co generates a maximum compressive stress of 4000 N/mm² in the center of the most highly-loaded rolling element.

Dynamic loadability

The basic load rating C is used for calculating the service life of a rotating rolling bearing. C indicates that bearing load for a nominal bearing service life of 1 million revolutions. In accordance with ISO 281:

Service life equation $L_{10} = \left(\frac{C}{P}\right)^p$

L_{10} Nominal service life in millions of revolutions achieved or exceeded by 90 % of a large batch of identical bearings,
C Basic load rating in N (determined empirically),
P Equivalent dynamic bearing load in N,
p Empirical exponent of the service life equation: for ball bearings, $p = 3$, for roller bearings, $p = 10/3$

Modified nominal service life

$$L_{na} = a_1 \cdot a_2 \cdot a_3 \cdot \left(\frac{C}{P}\right)^p$$

L_{na} Modified nominal service life in millions of revolutions,
a_1 Factor for survival probability, e.g. 90 %: $a_1 = 1$; 95 %: $a_1 = 0.62$,
a_2 Material coefficient of friction,
a_3 Coefficient of friction for operating conditions (bearing lubrication).

As the frictional coefficients a_2 and a_3 are not mutually independent, the combined coefficient a_{23} is employed.

Rolling bearings are subject to a fatigue stress. It is included, along with other influencing parameters such as contamination, in the calculation of service life (see catalogs issued by rolling-bearing manufacturers).

PETITIONER'S EXHIBIT 1002
US PATENT NO. 6,557,540

Spring calculations

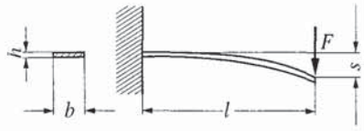
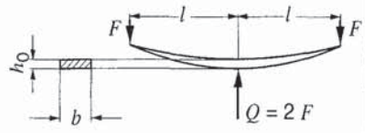
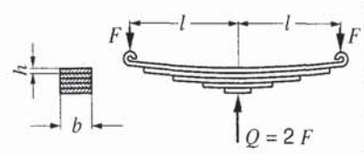
See PP. 14 ... 16 for names of units

Quantity		Unit
b	Width of spring leaf	mm
c	Spring rate (spring constant): For leaf springs and helical springs, increase in spring force per mm of spring deflection; For torsion bar springs, coiled torsion springs and flat spiral springs, increase in spring moment per degree of rotation	N/mm N · mm/°
d	Wire diameter	mm
D	Mean coil diameter	mm
E	Modulus of elasticity: for spring steel = 206,000 N/mm², for other materials, see P. 196	N/mm²

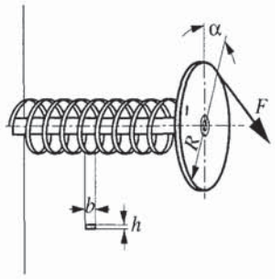
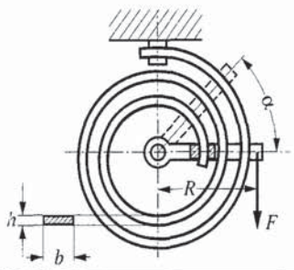
Quantity		Unit
F	Spring force	N
G	Shear modulus: for hot-formed springs ≈ 78,500 N/mm² for cold-formed springs ≈ 81,400 N/mm²	N/mm²
h	Height of spring leaf	mm
n	Number of active coils	–
M	Spring moment	N · mm
s	Spring deflection	mm
α	Angle of rotation	°
σ_b	Bending stress	N/mm²
τ	Torsional stress	N/mm²

Conversion of no longer permissible units:
1 kp = 9.81 N ≈ 10 N, 1 kp/mm ≈ 10 N/mm, 1 kp mm ≈ 10 N mm,
1 kp mm/° ≈ 10 N mm/°, 1 kp/mm² ≈ 10 N/mm².

Springs subjected to bending stress

Type	Bending stress	Spring rate
Rectangular cantilever spring (constant cross section) 	$\sigma_b = \frac{6\,l}{b \cdot h^2} F$	$c = \frac{F}{s} = \frac{E \cdot b \cdot h^3}{4 \cdot l^3}$
	See fatigue limit diagram on P. 291.	
Single-leaf spring, rolled out parabolically (vehicle spring) 	$\sigma_b = \frac{3\,l}{b \cdot h_0^2} Q$	$c = \frac{Q}{s} = \frac{E \cdot b \cdot h_0^3}{4 \cdot l^3}$
Multi-leaf spring, constant cross-section of the leaves (vehicle spring) 	$\sigma_b = \frac{3\,l}{n \cdot b \cdot h^2} Q$	$c = \frac{(2 + n'/n)\, E \cdot n \cdot b \cdot h^3}{6 \cdot l^3}$
	n = number of leaves n' = number of leaves at ends of spring	

PETITIONER'S EXHIBIT 1002
US PATENT NO. 6,557,540

Type	Bending stress	Spring rate
Coil spring (DIN 2088)	The same equations are used for torsion and spiral springs.	
	Rectangular cross-section: $\sigma_b = \frac{6}{b \cdot h^2} M$	$c = \frac{M}{\alpha} = \frac{E \cdot b \cdot h^3}{57.3 \cdot 12 \cdot l}$
	Circular section: $\sigma_b = \frac{32}{\pi \cdot d^3} M$	$c = \frac{M}{\alpha} = \frac{E \cdot \pi \cdot d^4}{57.3 \cdot 64 \cdot l}$
	where $M = F \cdot R$	
	l = straight length of spring material = $2 \pi \cdot r \cdot n$ (r mean coil radius)	
Spiral torsion spring (both ends clamped)	Under a pulsating load the stress increase due to curvature must be taken into consideration.	
		

Fatigue-limit diagram

For polished spring-steel strip (not for vehicle springs) in accordance with DIN 17 222 Ck 75 and Ck 85, hardened and tempered to 430...500 HV[1]), and Ck 85 and Ck 101, hardened and tempered to 500...580 HV.

Example (broken line in diagram):
For a leaf spring with a hardness of 430...500 HV, assuming a minimum stress of

$\sigma_U = 600$ N/mm²

the permissible stress range is

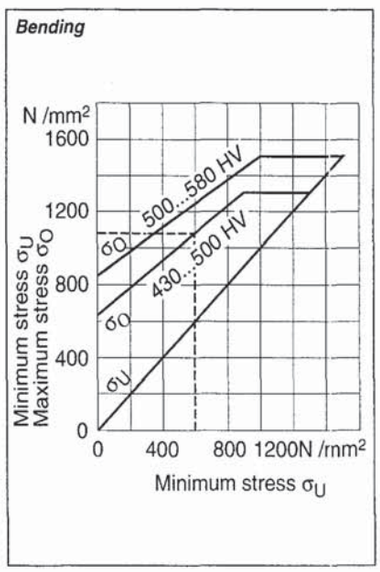
$\sigma_{hperm} = 480$ N/mm²

and the overstress is

$\sigma_O = \sigma_U + \sigma_{hperm} = 1080$ N/mm².

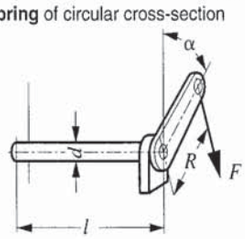
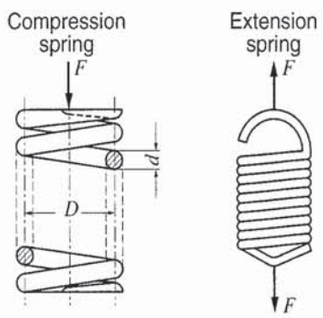
For reasons of safety, the stress range selected should be approximately 30% lower. Surface damage (corrosion pits, score marks) drastically reduces the fatigue limit.

[1]) Vickers hardness; see P. 276.



PETITIONER'S EXHIBIT 1002
US PATENT NO. 6,557,540

Springs subjected to torsional stress

Type	Torsional stress	Spring rate
Torsion-bar spring of circular cross-section (DIN 2091) 	$\tau = \frac{16}{\pi \cdot d^3} M$ where $M = F \cdot R$	$c = \frac{M}{\alpha} = \frac{G \cdot \pi \cdot d^4}{57.3 \cdot 32 \cdot l}$
Helical springs made of round wire (DIN 2089)  Above: half "German" loop, Below: hifo® hook (see P. 295)	a) In the case of a static or infrequently alternating load, allowance need not be made for the effect of the wire curvature: $\tau = \frac{8 \cdot D}{\pi \cdot d^3} F$ b) In the case of a pulsating load, the non-uniform distribution of torsional stresses must be taken into consideration: $\tau_k = k \cdot \tau = \frac{8 \cdot k \cdot D}{\pi \cdot d^3} F$	$c = \frac{F}{s} = \frac{G \cdot d^4}{8 \cdot n \cdot D^3}$ In the case of compression springs with only 1 ... 3 coils, the load deflection curve is no longer a straight line; spring rate c is initially smaller and then larger than the calculated rate.

The curvature correction factor k depends on the spring index D/d.

D/d	3	4	6	8	10	20
k	1.55	1.38	1.24	1.17	1.13	1.06

Avoid D/d < 3 and > 20.

The maximum permissible stresses τ_{k0} for various wire diameters at temperatures up to approximately 40 °C can be taken from the vertical boundary lines of the RDZ diagrams on the next pages (RDZ = relaxation, fatigue limit, fatigue strength for finite life). Interpolation is to be used for intermediate values. At higher temperatures, the relaxation curves (loss of load) must be considered. After 300 h, relaxation values are approximately 1.5 times as great as after 10 h. Values for other materials are given on P. 196.

In the case of extension springs with initial tension, maximum permissible stress values must be reduced to 90 % of the values indicated in the diagrams because so-called setting is not possible here.

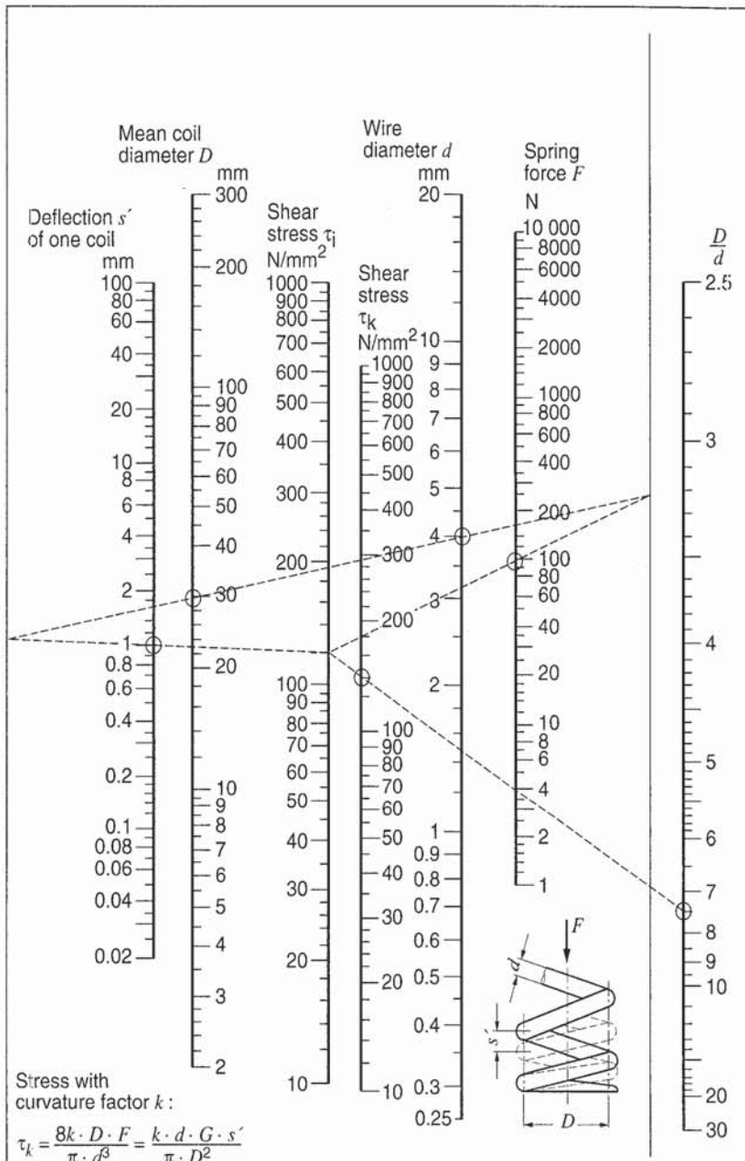
Explanation of the nomogram on the following page

The nomogram applies to cylindrical helical extension and compression springs made of round steel wire (shear modulus G = 81,400 N/mm²). In the case of materials with a different shear modulus G' spring deflection must be multiplied by G/G'.

The nomogram indicates the deflection s' of one coil. Total deflection s is obtained by multiplying (s') by the number of active coils n: $s = n \cdot s'$.

PETITIONER'S EXHIBIT 1002
US PATENT NO. 6,557,540

Nomogram for helical spring calculation



k see P. 292.

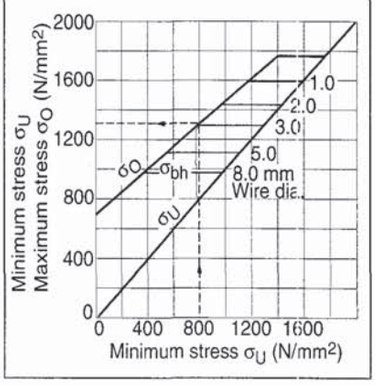
Example: given: D = 30 mm, d = 4 mm, F = 100 N
found: τ_i = 120 N/mm², τ_k = 140 N/mm², s' = 1.02 mm.

PETITIONER'S EXHIBIT 1002
US PATENT NO. 6,557,540

Fatigue-limit diagram for torsion springs

Spring-steel wire, type C (DIN 17 223, Sheet 1). Torsion springs not shot-peened.
Example (broken line in diagram):
For a torsion spring with a wire diameter d = 2 mm, the permissible stress range to which the spring can be subjected for 10^7 load cycles and more without fracture is σ_{bh} = 500 N/mm² at a minimum stress of σ_U = 800 N/mm².
The maximum stress is then
$\sigma_O = \sigma_U + \sigma_{bh}$ = 1300 N/mm².

Bending, Type C



Diagrams of relaxation fatigue limit and fatigue strength for finite life (RDZ)

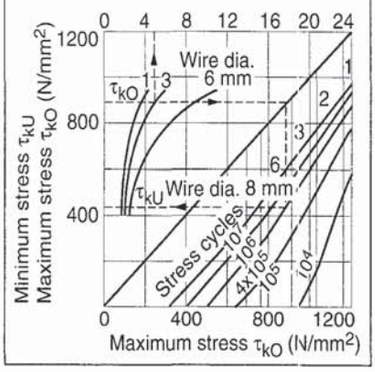
Spring-steel wire, type C (DIN 17 223, Sheet 1). Helical compression springs not shot-peened, cold-set.
Example (broken line in diagram):
A helical compression spring with a wire diameter of 3 mm a maximum stress of τ_{kO} = 900 N/mm² at an operating temperature of 80 °C, has a loss of spring force after 10 h of

ΔF_{10} = 5.5 %.

Given $N = 4 \times 10^5$ load cycles to failure, the stress range would be
$\tau_{kh} = \tau_{kO} - \tau_{kU}$ = 900 – 480 = 420 N/mm².

Torsion, Type C

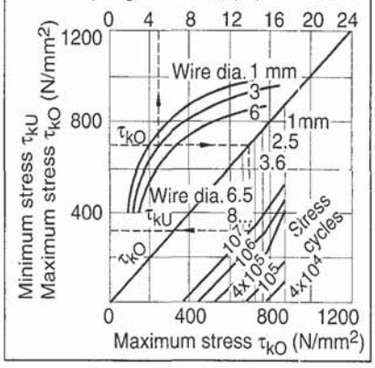
Loss of spring force ΔF_{10} (%) at t = 80 °C



Valve-spring steel wire, VD (DIN 17 223, Sheet 2). Helical compression springs not shot-peened, cold-set.
Example (broken line in diagram):
A helical compression spring with a wire diameter of 3 mm and a maximum stress of τ_{kO} = 700 N/mm² at an operating temperature of 80 °C, has a loss of spring force after 10 h of ΔF_{10} = 5 %.
For an infinite number of load cycles ($N \geq 10^7$), a stress range of
τ_{kh} = 700 – 320 = 380 N/mm²
is permissible.

Torsion, VD

Loss of spring force ΔF_{10} (%) at t = 80 °C



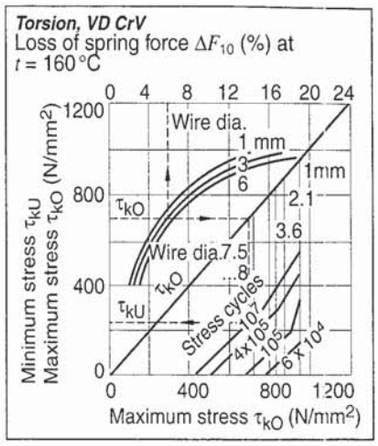
PETITIONER'S EXHIBIT 1002
US PATENT NO. 6,557,540

Valve-spring steel wire, VD CrV.[1])
Helical compression springs not shot-peened, cold-set.
Example (broken line in diagram):
A helical compression spring with a wire diameter of 3 mm and a maximum stress of τ_{kO} = 700 N/mm² at an operating temperature of 160 °C, has a loss of spring force after 10 h of ΔF_{10} = 6 %.

For an infinite number of load cycles ($N \geq 10^7$), a stress range of

τ_{kh} = 700 – 240 = 460 N/mm²

is permissible.

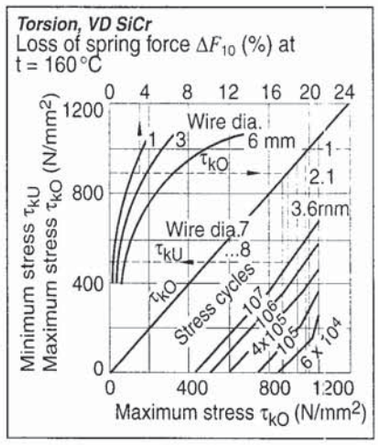


Valve-spring steel wire, VD SiCr.[1])
Helical compression springs not shot-peened, cold-set.
Example (broken line in diagram):
A helical compression spring with a wire diameter of 3 mm and a maximum stress of τ_{kO} = 900 N/mm² at an operating temperature of 160 °C, has a loss of spring force after 10 h of ΔF_{10} = 3.5 %.

For an infinite number of load cycles ($N \geq 10^7$), a stress range of

τ_{kh} = 900 – 510 = 390 N/mm²

is permissible.



If the danger of natural oscillation or other additional loads is present, reduce the selected stress range by approximately 30 %. Shot peening increases the permissible stress range by approximately 40 %.

In the case of **compression springs**, force eccentricity is reduced as far as possible by winding the spring such that the wire end at each end of the spring touches the adjoining coil (closed ends). Each end of the spring is then ground flat perpendicular to the axis of the spring (wire end ≈ $d/4$). The following values then apply:
Total number of coils $n_t = n + 2$.
The solid length from coil to coil ≤ $(n + 2)\ d$.

[1]) According to DIN 17 223, Part 2.

Helical extension springs are overstressed by roughly 50 % at standard hooks and loops when the body of the spring is subjected to permissible stress ranges. Hifo® hooks (German Patent, and others) exhibit infinite fatigue strength due to internal high initial force F_O.

Due to their favorable internal stresses, twist-wound extension springs can be subjected to stresses as high as those to which compression springs are subjected, and exhibit smaller relaxation than the latter. For high initial forces F_O (= hifo), these springs can be up to 50 % shorter at $F1$ than standard extension springs.

PETITIONER'S EXHIBIT 1002
US PATENT NO. 6,557,540

Gears and tooth systems

(with involute flanks)

Quantities and units (DIN 3960)

Quantity		Unit
a	Center distance	mm
b	Face width	mm
c	Bottom clearance	mm
d	Reference diameter	mm
d_a	Outside diameter	mm
d_b	Base circle diameter	mm
d_f	Root diameter	mm
d_w	Pitch diameter	mm
h_a	Addendum = $m \cdot h^*_{aP}$	mm
h_f	Dedendum = $m \cdot h^*_{fP}$	mm
i	Transmission ratio = z_2/z_1	–
j_n	Normal backlash	mm
m	Module m = d/z	mm
n	Rotational speed	min^{-1}
p	Pitch $p = \pi \cdot m$	mm
s	Tooth thickness (circular)	mm
W	Span measurement	mm
x	Addendum modification coefficient	–

Quantity		Unit
z	Number of teeth	–
α	Pressure angle	°
β	Helix angle	°
ε	Contact ratio	°
*	Specific value, to be multiplied by m	
Superscripts and subscripts		
1	referred to gear 1	
2	referred to gear 2	
a	referred to tooth tip	
b	referred to base circle	
f	referred to root	
n	referred to normal profile	
t	referred to transverse profile	
w	referred to operating pitch circle	
F	referred to root tooth load	
P	referred to basic rack	
W	referred to contact pressure	

Gear type and shape are determined by the position of the shafts which are joined by the gears in order to transmit forces or movements.

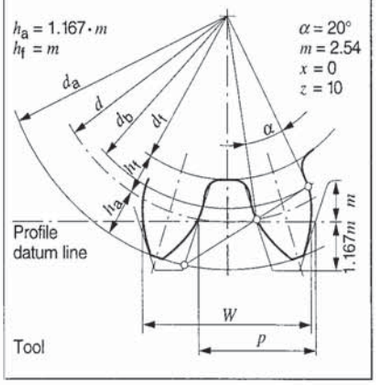
Cycloidal teeth: Cycloidal teeth are used primarily in the watch and clock industry. They permit small numbers of teeth without cutter interference (undercut). They are characterized by low contact pressure, but are sensitive to variations in the distance between centers.

Involute teeth: Involute teeth, on the other hand, are not sensitive to variations in the distance between centers.

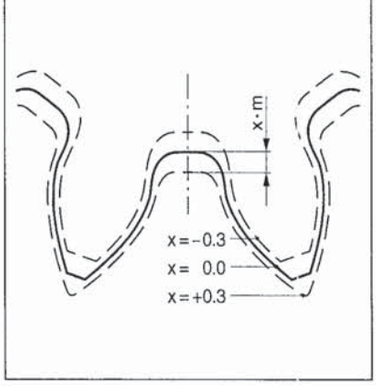
They can be produced with relatively simple tools using the generating method. The automobile industry uses involute teeth almost exclusively, therefore the following information is limited to this type of gear system.

All spur gears with the same module (and the same pressure angle) can be produced using the same generating tool, regardless of the number of teeth and addendum modification. A number of modules have been standardized in order to

Parameters for spur gears *(cycloidal teeth)*



Effect of addendum modification at spur gear *(cycloidal teeth)*



PETITIONER'S EXHIBIT 1002
US PATENT NO. 6,557,540

Definitions

Table 1. Gear types

Position of shafts	Gear type	Properties	Examples of application in automotive engineering
Parallel	External or internal spur-gear pair with straight or helical teeth	Helical teeth run more smoothly but are subject to axial thrust	Manual transmissions
Intersecting	Bevel-gear pair with straight, helical, or curved teeth	Sensitive to fluctuations in angular and axial clearance	Differentials
Crossing	Offset bevel-gear pair with helical or curved teeth		Rear-axle drives
	Crossed helical-gear pair	For small loads	Distributor drives
	Worm-gear pair	High-ratio, single-stage transmission	Windshield wiper drives
Coaxial	Toothed shaft and hub	Sliding shaft coupling	Starters (Bendix shaft and pinion)

limit the number of such tools and the number of master gears required for gear testing:

Module for spur and bevel gears: DIN 780 (see table on P. 299), module for worms and worm gears: DIN 780, module for toothed shafts and stubs: DIN 5480. The module in the normal profile for crossed helical gears is also selected in conformance with DIN 780 in most cases. A series of modules suited to the manufacturing process is generally used for curved-tooth bevel gears.

Tooth shape

Basic rack for spur gears: DIN 867, DIN 58 400; basic rack for bevel gears: DIN 3971; basic rack for worms and worm gears: DIN 3975; basic rack for toothed shafts and hubs: DIN 5480.

The tooth shape for crossed helical gears can also be designed in conformance with the basic rack as per DIN 867. In addition to the standardized pressure angles (20° for running gears and 30° for toothed shafts and hubs), pressure angles of 12°, 14°30', 15°, 17°30', 22°30' and 25° are used.

Table 2. List of standards

Standard	Title
DIN 3960	Definitions, parameters and equations for involute cylindrical gears and gear pairs
DIN 3961...4	Tolerances for cylindrical gear teeth
DIN 3990/1...5	Calculation of load capacity of cylindrical gears
DIN 58 405/1...4	Spur gear drives for precision engineering
DIN 3971	Definitions and parameters for bevel gears and bevel gear pairs
DIN 5480	Involute spline joints
DIN 3975	Terms and definitions for cylindrical worm gears with shaft angle 90°

PETITIONER'S EXHIBIT 1002
US PATENT NO. 6,557,540

Table 3. Basic equations for spur gears

Designation	Straight gear ($\beta = 0$)	Helical gear ($\beta \neq 0$)
Reference-circle diameter	$d = z \cdot m$ Module m, see P. 296	$d = \frac{z \cdot m_n}{\cos \beta}$ Module m_n, see P. 296
	The neg. value of z is to be used for internal teeth; center distance a becomes neg.	
Base-circle diameter	$d_b = d \cdot \cos \alpha_n$	$d_b = d \cdot \cos \alpha_t$ α_t from $\tan \alpha_t = \frac{\tan \alpha_n}{\cos \beta}$
Center distance, no backlash; if normal backlash $j_n = 0$	$a = m \frac{z_1 + z_2}{2} \cdot \frac{\cos \alpha}{\cos \alpha_w} = \frac{d_{b1} + d_{b2}}{2 \cdot \cos \alpha_w}$ as per DIN 867, $\alpha = 20°$ α_w from: $\text{inv}\, \alpha_w = \frac{2 (x_1 + x_2) \sin \alpha + j_n/m}{(z_1 + z_2) \cos \alpha} + \text{inv}\alpha$	$a = m_t \frac{z_1 + z_2}{2} \cdot \frac{\cos \alpha_t}{\cos \alpha_{wt}} = \frac{d_{b1} + d_{b2}}{2 \cdot \cos \alpha_{wt}}$ $m_t = \frac{m_n}{\cos \beta}$ $\cos \beta_b = \frac{\sin \alpha_n}{\sin \alpha_t}$ $\text{inv}\, \alpha_{wt} = \frac{m_n \cdot 2(x_1 + x_2) \sin \alpha_n + j_n/\cos \beta_b}{m_t (z_1 + z_2) \cos \alpha_t} + \text{inv}\alpha_t$
Involute	$\text{inv}\, \alpha = \tan \alpha - \text{arc}\, \alpha$ P. 146.	when $\alpha = 20°$, $\text{inv}\, \alpha = 0.014904$
Pitch-circle diameter	$d_w = d_b / \cos \alpha_w$	$d_w = d_b / \cos \alpha_{wt}$
Root-circle diameter	$d_f = d + 2\, xm - 2\, h^*_{fP} \cdot m$	$d_f = d_b + 2\, xm_n - 2\, h^*_{fP} \cdot m_n$
	with dedendum $h^*_{fP} \cdot m$ ($h^*_{fP} = 1.167$ or 1.25 as per DIN 3972)	
Tip-circle diameter	$d_a = d + 2\, xm + 2\, h^*_{aP} \cdot m$	$d_a = d \cdot 2\, xm_n + 2\, h^*_{aP} \cdot m_n$
	with addendum $h^*_{aP} \cdot m$ ($h^*_{aP} = 1.0$ as per DIN 867)	
Bottom clearance	$c_1 = a_{min} - d_{a1}/2 - d_{f2}/2$; $c_2 = a_{min} - d_{a2}/2 - d_{f1}/2$	$c \geq 0.15\, m_n$
Tooth thickness in pitch circle (circular)	$s = m\, (\pi/2 + 2\, x \cdot \tan \alpha)$	Normal profile $s_n = m_n (\pi/2 + 2\, x \cdot \tan \alpha_n)$
		Transverse profile $s_t = s_n / \cos \beta = m_t\, (\pi/2 + 2 \cdot x \cdot \tan \alpha_n)$
Ideal number of teeth	$z_i = z$	$z_i = z \frac{\text{inv}\, \alpha_t}{\text{inv}\, \alpha_n}$
Number of teeth spanned	$k \approx z_i \frac{\alpha_{nx}}{180} + 0.5$ for k take the next whole number	α_{nx} from $\cos \alpha_{nx} \approx \frac{z_i}{z_i + 2x} \cos \alpha_n$
Base tangent length over k teeth	$W_k = \{[(k' - 0.5)\, \pi + z_i\, \text{inv}\, \alpha_n] \cos \alpha_n + 2x \cdot \sin \alpha_n\}\, m_n$	
Back-reckoning of x from the base tangent	$x = \frac{(W/m_n) - [(k - 0.5) \cdot \pi + z_i \cdot \text{inv}\, \alpha_n] \cdot \cos \alpha_n}{2 \cdot \sin n\alpha}$	
Transverse contact ratio for gears without allowance for cutter interference	$\varepsilon_\alpha = \frac{\sqrt{d_{a1}^2 - d_{b1}^2} + \frac{z_2}{\lvert z_2 \rvert} \sqrt{d_{a2}^2 - d_{b2}^2} - (d_{b1} + d_{b2}) \tan \alpha_w}{2 \cdot \pi \cdot m_t \cdot \cos \alpha}$ (straight teeth)	
	$\varepsilon_\alpha = \frac{\sqrt{d_{a1}^2 - d_{b1}^2} + \frac{z_2}{\lvert z_2 \rvert} \sqrt{d_{a2}^2 - d_{b2}^2} - (d_{b1} + d_{b2}) \tan \alpha_{wt}}{2 \cdot \pi \cdot m_t \cdot \cos \alpha}$ (helical teeth)	
Overlap ratio	–	$\varepsilon_\beta = \frac{b \cdot \sin \lvert \beta \rvert}{m_n \cdot \pi}$
Total contact ratio	$\varepsilon_\gamma = \varepsilon_\alpha$	$\varepsilon_\gamma = \varepsilon_\alpha + \varepsilon_\beta$
	Apply only if: $\varepsilon_\gamma > 1$ for $d_{a\,min}$ and a_{max}	

PETITIONER'S EXHIBIT 1002
US PATENT NO. 6,557,540

Addendum modification
Addendum modification (see diagram) is used to avoid undercut when the number of teeth is small, to increase tooth root strength and to achieve a specific distance between centers.

Gear pair with reference center distance
With a gear pair at reference center distance, the addendum modifications to the gear and pinion are equal but opposite, such that the distance between centers does not change. This design is preferred for crossed helical and bevel gear pairs.

Gear pair with modified center distance
The addendum modifications to the gear and pinion do not cancel each other, so the distance between centers changes.

Terms and errors
Terms and errors are explained in detail in the following standards: DIN 3960, DIN 58 405 (spur gears), DIN 3971 (bevel gears), and DIN 3975 (worms and worm gears).

Inserting $j_n = 0$ in the preceding formulas results in gearing with zero backlash. The tooth thickness and span measurement deviations required to produce backlash can be specified in accordance with DIN 3967 and DIN 58 405, taking into consideration the quality of the gears. It is necessary to ensure that the minimum backlash is great enough to compensate for tooth error (such as total composite error, alignment deviation, center-to-center distance error, etc.) without reducing the backlash to zero, and without leading to gear jamming. Other parameters for which the tolerances must be determined (with reference to the tooth errors given above in parentheses) are those for (two-flank) total composite error and (two-flank) tooth-to-tooth composite error

DIN gear qualities (DIN 3961 to DIN 3964)

Table 4. Manufacture and applications

Quality	Examples of applications	Manufacture
2	Primary-standard master gears	Form grinding (50 ... 60 % scrap rate)
3	Master gears for the inspection department	Form grinding and generative grinding
4	Master gears for the workshop, measuring mechanisms	
5	Drives for machine tools, turbines, measuring equipment	
6	As 5, also highest gears of passenger-car and bus transmissions	
7	Motor-vehicle transmissions (highest gears), machine tools, rail vehicles, hoisting and handling equipment, turbines, office machines	Non-hardened gears (carefully manufactured) by hobbing, generative shaping and planing (subsequent shaving is desirable); additional grinding is required for hardened gears
8 and 9	Motor-vehicle transmissions (middle and lower gears), rail vehicles, machine tools and office machines	Hobbing, generative shaping and planing (non-ground but hardened gears)
10	Transmissions for farm tractors, agricultural machinery, subordinate gear units in general mechanical equipment, hoisting equipment	All of the usual processes apply, plus extrusion and sintering, and injection molding for plastic gears
11 and 12	General agricultural machinery	

PETITIONER'S EXHIBIT 1002
US PATENT NO. 6,557,540

(DIN 3963, DIN 58 405), alignment deviation (DIN 3962 T2, DIN 3967, DIN 58 405), and distance between centers (DIN 3964, DIN 58 405).

Module series for spur and bevel gears in mm (extract from DIN 780)

0.3	**1**	**3**	**10**	**32**
0.35	1.125	3.5	11	36
0.4	**1.25**	**4**	**12**	**40**
0.45	1.375	4.5	14	45
0.5	**1.5**	**5**	**16**	**50**
0.55	1.75	5.5	18	55
0.6	**2**	**6**	**20**	**60**
0.65	2.25	7	22	70
0.7	**2.5**	**8**	**25**	
0.75	2.75	9	28	
0.8				
0.85				
0.9				
0.95				

Modules given in bold type are preferred.

Addendum modification coefficient x

Table 5. Addendum modification coefficient x for straight-tooth gearing, $\alpha = 20°$,
Basic rack I, DIN 3972 ($h_{fP} = 1.167 \cdot m$)

1	2	3	4
Number of teeth z, for helical teeth z_i	Tooth free from undercut if $x \geq$	Top land width $0.2 \cdot m$ if $x \approx$	Tooth pointed if $x \geq$
7	+ 0.47	–	+ 0.49
8	+ 0.45	–	+ 0.56
9	+ 0.4	+ 0.4	+ 0.63
10	+ 0.35	+ 0.45	+ 0.70
11	+ 0.3	+ 0.5	+ 0.76
12	+ 0.25	+ 0.56	+ 0.82
13	+ 0.2	+ 0.62	+ 0.87
14	+ 0.15	+ 0.68	+ 0.93
15	+ 0.1	+ 0.72	+ 0.98
16	0	+ 0.76	+ 1.03

If the number of teeth is greater than
$z = 16$, x should not be less than
$x = (16 - z)/17$, for helical teeth
$x = (16 - z_i)/17$.

Starter-tooth design

The system of tolerances for gears "Standard distance between centers" as specified in DIN 3961, which is customary in mechanical engineering and by which the required backlash is produced by negative tooth thickness tolerances, cannot be used for starters. Starter gear teeth require far more backlash than constant-mesh gears due to the starter engagement process. Such backlash is best achieved by increasing the distance between centers.

The high torque required for starting necessitates a high transmission ratio (i = 10 to 20). For this reason, the starter pinion has a small number of teeth (z = 8...12). The pinion generally has positive addendum modification. In the case of pitch gears, this addendum modification is expressed using the following notation outside Germany: Number of teeth, for instance = 9/10.

This means that only 9 teeth are cut on a gear blank with a diameter for 10 teeth; this corresponds to an addendum modification coefficient of + 0.5. Slight deviations of $x = + 0.5$ are quite common and do not affect the above-mentioned notation method: Number of teeth = 9/10. (This notation is not to be confused with the P 8/10 notation, see below and next page.)

Table 6. Customary starter gearing

Module m mm	Diametral pitch P 1/inch	Pressure angle of basic rack	American standard	European standard
2.1167	12	12°	SAE J 543 c	ISO 8123 1991 E
2.5	–	15°		ISO 9457–1 1991 E
2.54	10	20°	SAE J 543 c	ISO 8123 1991 E
3	–	15°		ISO 9457–1 1991 E
3.175	8	20°	SAE J 543 c	ISO 8123 1991 E
3.5	–	15°		ISO 9457–1 1991 E
4.233	6	20°	SAE J 543 c	ISO 8123 1991 E

PETITIONER'S EXHIBIT 1002
US PATENT NO. 6,557,540

American gear standards

Instead of the module, in the USA standardization is based on the number of teeth on 1 inch of pitch diameter = diametral pitch (P).

$P = z/d$

The conversion is as follows:
Module m = 25.4 mm/P

The tooth spacing in the pitch circle is called circular pitch (CP):

$$CP = \frac{1 \text{ inch}}{P} \cdot \pi$$

Pitch p = 25.4 mm · $CP = \pi \cdot m$

Full-depth teeth
Full-depth teeth have an addendum $h_a = m$ in German standards, however the dedendum is frequently somewhat different.

Stub teeth
The formulas are the same as for full-depth teeth, however calculation of the addendum is based on a different module from that used for the other dimensions. Notation (example):

P 5/7 —— P 7 for calculation of the addendum
|
└—— P 5 for calculation of all other dimensions

Notation and conversions:

Outside Diameter:
$OD = da$

Pitch Diameter:
$PD = z/P = d$ in inches

Root Diameter:
$RD = d_f$

Layout Diameter:
$LD = (z + 2x)/P$ in inches
$LD = (z + 2x) \cdot$ m in mm
$LD \approx d_w$
d_w Pitch circle diameter

Measurement over D_M-pins:
M_d = measurement over D_M pins

Table 7. Diametral pitches P and modules derived from them

Diametral pitch P 1/inch	Corresponds to module m mm	Diametral pitch P 1/inch	Corresponds to module m mm	Diametral pitch P 1/inch	Corresponds to module m mm
20	1.27000	**6**	4.23333	**2**	12.70000
18	1.41111	5.5	4.61818	1.75	14.51429
16	1.58750	**5**	5.08000	**1.5**	16.93333
14	1.81429	4.5	5.64444	**1.25**	20.32000
12	2 11667	**4**	6.35000	**1**	25.40000
11	2.30909	3.5	7.25714	0.875	29.02857
10	2.54000	**3**	8.46667	**0.75**	33.86667
9	2.82222	2.75	9.23636	**0.625**	40.64000
8	3.17500	**2.5**	10.16000	**0.5**	50.80000
7	3.62857	2.25	11.28889		

PETITIONER'S EXHIBIT 1002
US PATENT NO. 6,557,540

Calculation of load-bearing capacity

The following can be employed for rough estimations as an alternative to DIN 3990 "Calculation of load-bearing capacity of spur bevel gears". It applies to 2-gear pairs in a stationary transmission unit.
The quantities which appear in the following formulas are to be entered for the units given below:

Term		Unit	Term		Unit
P	Power	kW	φ	Life factor	–
P_{PS}	Metric horsepower	PS*	HB	Brinell hardness	
M	Torque	N · m	HRC	Rockwell hardness	
n	Rotational speed	min^{-1}	b_N	Effective flank width	mm
F	Peripheral force	N	k	Contact pressure	N/mm^2
u	Gear ratio	–	L_h	Service life	h

Table 8. Calculating load-bearing capacity of spur gears

Power	$P = 0.736 \cdot P_{PS}$ $P = M \cdot n/9549$ $P = F_t \cdot d \cdot n/(19.1 \cdot 10^6)$
Peripheral force in pitch circle	$F_{tw} = 2000 \cdot M/d_w = 19.1 \cdot 10^6\ P/(d_w \cdot n)$
in reference circle	$F_t = 2000 \cdot M/d = 19.1 \cdot 10^6\ P/(d \cdot n)$
Gear ratio	$u = z_2/z_1 = n_1/n_2$ for pairs of internal gears $u < -1$
Life factor	$\varphi = \sqrt[6]{5000/L_h}$ or from the table on P. 303
Contact pressure for the small gear	$k_{perm} = \frac{(HB)^2}{2560 \cdot \sqrt[6]{n}} = \frac{(HRC)^2}{23.1 \cdot \sqrt[6]{n}}$ or from the table on P. 303
Straight teeth	$k_{actual} = \frac{F_{tw}}{b_N \cdot d_{w1}} \cdot \frac{4\,(u+1)}{u \cdot \sin 2\,\alpha_w}$
Helical teeth	$k_{actual} = \frac{F_{tw}}{b_N \cdot d_{w1}} \cdot \frac{4\,(u+1) \cdot \cos^2\beta}{u \sin 2\,\alpha_{wt}}$ $\cos^2\beta$ only for full contact, otherwise = 1
Resistance to pitting	$S_w = \varphi \cdot k_{perm}/k_{IST} \geq 1$

Resistance to pitting and wear due to excessive contact pressure is provided if the equations for S_w for the smaller gear (gear 1) yield a value equal to or greater than 1. In the case of gear pairs where $z_1 < 20$, select $S_w \geq 1.2 \ldots 1.5$ on account of the greater contact pressure at the inside single engagement point. Because the contact pressure k is equal in magnitude for both gears of the pair, for k_{perm} a material can be selected for gear 2 from the table which has at least the same contact pressure as for gear 1 at rotational speed n_2.

PETITIONER'S EXHIBIT 1002
US PATENT NO. 6,557,540

The k_{perm}-values in the table below apply when both gears are made of steel. For cast iron on steel or bronze on steel, the values should be roughly 1.5 times higher; for cast iron on cast iron or bronze on bronze, they should be approximately 1.8 times higher. For the gear with non-hardened surfaces, 20% higher k_{perm} values are permissible if the other gear in the pair has hardened tooth flanks. The values in the table apply to a service life L_h of 5000 hours. A different service life L_h is allowed for in the equation for resistance to pitting S_w by means of the life factor φ.

Table 9. Permissible contact pressure k_{perm} in N/mm² for a service life L_h = 5000 h

Hardness of teeth		Rotational speed min⁻¹ (for 1 load change per revolution)											
HB	HRC	10	25	50	100	250	500	750	1000	1500	2500	5000	10000
90		2.2	1.9	1.7	1.5	1.3	1.1	1.05	1.0	0.94	0.86	0.77	0.68
100		2.7	2.3	2.0	1.8	1.6	1.4	1.3	1.2	1.15	1.06	0.94	0.84
120		3.8	3.3	2.9	2.6	2.2	2.0	1.9	1.8	1.66	1.53	1.36	1.21
140		5.2	4.5	4.0	3.6	3.0	2.7	2.5	2.4	2.26	2.08	1.85	1.65
170		7.7	6.6	5.9	5.2	4.5	4.0	3.75	3.6	3.34	3.06	2.73	2.43
200		10.7	9.1	8.1	7.3	6.2	5.6	5.2	4.9	4.6	4.24	3.78	3.37
230		14.1	12.1	10.8	9.6	8.2	7.3	6.9	6.5	6.1	5.61	5.0	4.45
260		18.0	15.4	13.8	12.2	10.5	9.4	8.8	8.4	7.8	7.17	6.39	5.69
280		20.9	17.9	16.0	14.2	12.2	10.9	10.2	9.7	9.0	8.31	7.41	6.6
300		24.0	20.6	18.3	16.3	14.0	12.5	11.7	11.1	10.4	9.54	8.5	7.6
330		29.0	24.9	22.2	19.8	17.0	15.1	14.1	13.5	12.6	11.6	10.3	9.2
400		42.6	36.6	32.6	29.0	24.9	22.2	20.7	19.8	18.5	17.0	15.1	13.5
	57	96.0	82.3	73.3	65.3	56.0	49.9	46.7	44.5	41.6	38.2	34.0	30.3
	≥ 62	112	96.5	86.0	76.6	65.8	58.6	54.8	52.2	48.8	44.8	39.9	35.6

Corresponding materials are given in the table "Strength values" on P. 305.

Table 10. Life factor φ

The life factor is used to convert the values in the table (referred to a service life L_h of 5000 hours) to values which correspond to a different service life period.

Service life in hours of operation Lh	10	50	150	312	625	1200	2500	5000	10,000	40,000	80,000	150,000
Life factor φ	2.82	2.15	1.79	1.59	1.41	1.27	1.12	1	0.89	0.71	0.83	0.57

Guidelines for selection of service life: Drives in continuous operation at full load: 40,000...150,000 hours of operation; drives run intermittently at full load or only intermittently: 50...5000 hours of operation.

PETITIONER'S EXHIBIT 1002
US PATENT NO. 6,557,540

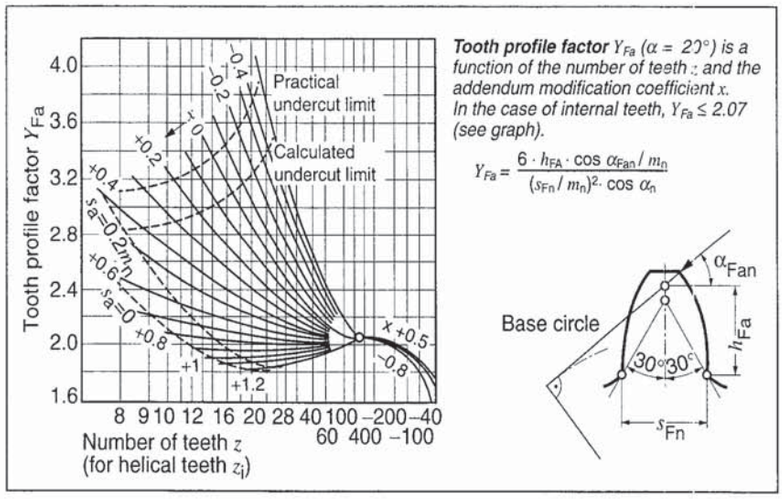
Teeth calculations for bending and tooth fracture

Table 11. Formulae for calculating the strength of spur gears

Peripheral velocity $v_1 = v_2$ m/s	$v_1 = \frac{\pi \cdot d_1 \cdot n_1}{60{,}000}$ d_1 in mm, n_1 in min^{-1}	
Velocity factor f_v	Take from table below, or calculate.	
Perm. root stress $\sigma_{F\,perm}$ N/mm²	Take $\sigma_{F\,lim}$ and Y_{NT} from table P. 305; estimate intermediate values. $\sigma_{F\,perm} = \sigma_{F\,lim} \cdot Y_{NT} \cdot Y_L$ $Y_L = 1$ for pulsating loads $Y_L = 0.7$ for alternating loads.	
Tooth profile factor Y_{Fa}	Take from graph below.	
Root stress of tooth $\sigma_{F\,actual}$ N/mm²	For straight teeth $\sigma_{F\,actual} = \frac{F_t}{b \cdot m} \cdot \frac{Y_{Fa}}{f_v \cdot \varepsilon_\alpha}$ ε_α, see P. 298 m, m_n, b in mm, F_t in N see P. 302	For helical teeth $\sigma_{F\,actual} = \frac{F_t}{b \cdot m_n} \cdot \frac{Y_{Fa}}{f_v \cdot \varepsilon_\alpha} \left(1 - \frac{\varepsilon_\beta \cdot \beta}{120°}\right)$ where $(1 - \varepsilon_\beta \cdot \beta/120°)$ must be ≥ 0.75. ε_β see P. 298, β in °
Resistance to tooth fracture S_F	$S_F = \sigma_{F\,perm}/\sigma_{F\,actual} \geq 1$	

Resistance to tooth fracture is provided if the equations for S_F for the smaller gear (gear 1) yield a value greater than or equal to 1.

If a better material is selected for gear 1 than for gear 2, the calculation for bending must also be made for gear 2.



Tooth profile factor Y_{Fa} *($\alpha = 20°$) is a function of the number of teeth z and the addendum modification coefficient x. In the case of internal teeth, $Y_{Fa} \leq 2.07$ (see graph).*

$$Y_{Fa} = \frac{6 \cdot h_{FA} \cdot \cos \alpha_{Fan} / m_n}{(s_{Fn}/m_n)^2 \cdot \cos \alpha_n}$$

Table 12. Velocity factor f_v

Materials	Peripheral velocity v m/s 0.25 | 0.5 | 1 | 2 | 3 | 5 | 10	Basic equation
Steel and other metals	Velocity factor f_v 0.96 | 0.93 | 0.86 | 0.75 | 0.67 | 0.55 | 0.38	$f_v = \frac{A}{A + v}$ [1]
Fabric-base laminates and other non-metals	0.85 | 0.75 | 0.62 | 0.5 | 0.44 | 0.37 | 0.32	$f_v = \frac{0.75}{1 + v} + 0.25$

PETITIONER'S EXHIBIT 1002
US PATENT NO. 6,557,540

Gear materials

Table 13. Material parameters

	Material	Condition	Tensile strength R_m N/mm² min.	Fatigue strength for reversed bending stress σ_{bW} N/mm² min.	Hardness HB or HRC min.	Permissible root stress[2] $\sigma_{F\,lim}$ N/mm²	Life factor Y_{NT}[3] at number of load changes $N_L = L_h \cdot 60 \cdot n$ ≥ 3 · 10⁶	10⁶	10⁵	10⁴	10³
Heat-treatable steel	St 60-2, C 45	annealed	590	255	170 HB	160	1	1.25	1.75	2.5	2.5
		heat-treat.	685	295	200 HB	185					
		heat-treat.	980	410	280 HB	245					
	St 70-2, C 60	annealed	685	295	200 HB	185					
		heat-treat.	785	335	230 HB	209					
		heat-treat.	980	410	280 HB	245					
	50 Cr V 4	annealed	685	335	200 HB	185					
		heat-treat.	1130	550	330 HB	294					
		heat-treat.	1370	665	400 HB	344					
	37 Mn Si 5	annealed	590	285	170 HB	160					
		heat-treat.	785	355	200 HB	230					
		heat-treat.	1030	490	300 HB	270					
Case-hardening steel	RSt 34-2, C 15	annealed	335	175	100 HB	110	1	1.25	1.75	2.5	2.5
		surf.-hard.[4]	590	255	57 HRC	160	1	1.2	1.5	1.9	2.5
	16 Mn Cr 5	annealed	800	–	150 HB	–	–	–	–	–	–
		surf.-hard.[4]	1100	–	57 HRC	300	1	1.2	1.5	1.9	2.5
	20 Mn Cr 5	annealed	590	275	170 HB	172	–	–	–	–	–
		surf.-hard.[4]	1180	590	57 HRC	330	1	1.2	1.5	1.9	2.5
	18 Cr Ni 8	annealed	640	315	190 HB	200	–	–	–	–	–
		surf.-hard.[4]	1370	590	57 HRC	370	1	1.2	1.5	1.9	2.5
Gray iron	GG-18	–	175		200 HB	50	1	1.1	1.25	1.4	1.6
	GS-52.1	–	510		140 HB	110	1	1.25	1.75	2.5	2.5
	G-SnBz 14		195		90 HB	100	1	1.25	1.75	2.5	2.5
	Polyamide PA 66	at 60 °C	–	40	–	27	1	1.2	1.75	–	–
	Pa 66 + 30 % GF		140	43	–	29					
	Fabric-base fine		–	–	–	75	1	1.15	1.4	1.65	2.0
	laminate coarse		–	–	–	50	1	1.2	1.6	2.1	2.8

For the heat-treatable steels, two values are given in each case for the heat-treated condition. For smaller gears up to roughly module 3, the larger of the two values can be specified. With very large gears, however, only the smaller value can be achieved with certainty.

---

[1]) Values are valid for $A = 6$ (average tooth quality). With cast gears and high-precision gears, $A = 3$ and 10 respectively.

[2]) For pulsating loads with a material fatigue strength $N_L \geq 3 \cdot 10^6$. In the case of alternating loads (idler gears), take into account the alternating load factor Y_L.

[3]) Within fatigue strength of finite life, root bending stress is multiplied by the factor Y_{NT}, depending upon the number of load changes $N_L = L_h \cdot 60 \cdot n$.

[4]) Surface-hardened.

PETITIONER'S EXHIBIT 1002
US PATENT NO. 6,557,540

Belt drives

Friction belt drives

Units and symbols

Quantity		Unit
A	Belt cross section	mm²
F	Contact force	N
F_1	Belt force on load side	N
F_2	Belt force on slack side	N
F_F	Centrifugal force of belt	N
F_f	Centrifugal force per side	N
F_R	Frictional force	N
F_u	Peripheral force	N
F_v	Pretensioning force	N
F_w	Tensioning force of shaft	N
P	Required power transmission	kW
k_1	Pretension factor, with reference to operating conditions and wrap angle	–
k_2	Factor for centrifugal force	–
v	Belt speed	m/s
z	Number of belts (V-belt drives) or ribs (V-ribbed belts)	–
α	Groove angle	°
β	Wrap angle	°
μ	Coefficient of friction	–
μ'	Wedge coefficient of friction	–
ϱ	Mean density of belt material	g/cm³

Transmission of force

The general equation for friction

$$F_R = \mu \cdot F$$

yields the following equation for V-belt pulleys (see illustration)

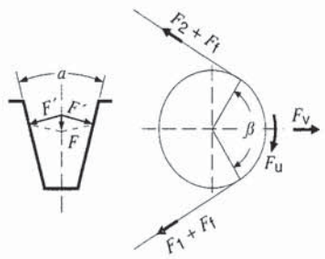
$$F_R = \mu \cdot 2 \cdot F'$$

or $F_R = \mu' \cdot F$

where $\mu' = \mu/\sin(\alpha/2)$

The Eytelwein equation describes the transition from static friction to sliding friction:

V-belt forces



$$F_1/F_2 = e^{\mu'\beta}$$

where $\mu' \approx 0.5 \pm 0.15$

according to the specifications of the V-belt manufacturers with the incorporation of various safety factors.

As long as the ratio of forces on the two belt sides is

$$F_1/F_2 \leq e^{\mu'\beta}$$

the belt will not slip during transmission of the peripheral force

$$F_u = F_1 - F_2 = P \cdot 1020/v$$

A pretensioning force F_v is required in order to transmit the peripheral force F_u; at high rotational speeds, the centrifugal force constituent F_F of the belt must be taken into consideration. The pretensioning force is

$$F_v = F_w \cdot F_F$$

where $F_w = F_u \cdot [(e^{\mu'\beta} + 1)/(e^{\mu'\beta} - 1)] \cdot \sin(\beta/2)$

$$F_F = 2 \cdot z \cdot F_f \cdot \sin(\beta/2)$$

$$F_f = \varrho \cdot A \cdot v^2 \cdot 10^{-3}$$

or in simplified form

$$F_F = 2 \cdot z \cdot k_2 \cdot v^2 \cdot \sin(\beta/2)$$

In practice, the following approximation process is frequently sufficient for calculating the pretensioning force (according to the Continental Co.):

$$F_v = (k_1 \cdot F_u + 2 \cdot z \cdot k_2 \cdot v^2) \cdot \sin(\beta/2)$$

The following rule of thumb can often be used for drives with 2 pulleys:

$$F_v = (1.5 \ldots 2) \cdot F_u$$

In order to check belt pretensioning, the static force applied to each side of each belt

$$F_s = F_v/[2z \cdot \sin(\beta/2)]$$

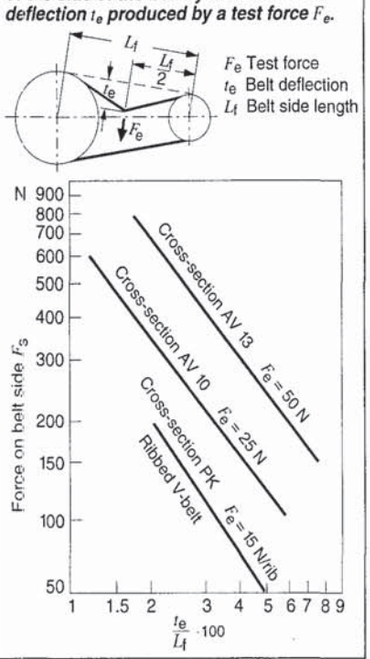
is compared with the value obtained by measuring belt deflection.

Belt drive calculations are performed in accordance with DIN 2218, or in accordance with the specifications supplied by the belt manufacturers. Manufacturer's belt performance specifications are based on a theoretical service life of 25,000 h. Computer programs are used to perform service life calculations. In properly designed drives, belt creep is less than 1%, and belt efficiency is 94...97%.

Belt service life is shortened if the maximum permissible belt speed and bending frequency are exceeded, if the belt pulleys are smaller than the minimum permissible pulley diameter or, in the case of V-belts, belt tensioners are used to apply force to the back of the belt.

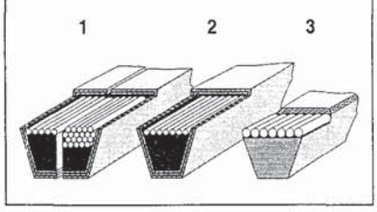
PETITIONER'S EXHIBIT 1002
US PATENT NO. 6,557,540

Determination of the static force F_S of the side of the belt by means of belt deflection t_e produced by a test force F_e.



Standard V-belts (classical V-belts)
In accordance with DIN 2215, for domestic appliances, agricultural machinery, heavy machinery. Ratio of top width to height: 1.6 : 1. Belt designs which use corded cable and bundled fibers as the tension members transmit considerably less power than equally wide narrow V-belts. Due to their high tensile strength and transverse stiffness, they are suitable for use under rough operating conditions with sudden load changes.

V-belt types
1 Wrapped standard V-belt
2 Wrapped narrow V-belt
3 Raw-edge narrow V-belt



Pretension factor k_1				
Belt	β	Drive: Light constant loads	Drive: Moderate loads	Drive: Heavy shock loads
V-belts	180°	1.5	1.7	1.9
	90°	2.6	2.8	3.0
V-ribbed belt	180°	1.8	2.0	2.2
	90°	3.3	3.5	3.7

Intermediate values for other wrap angles may be interpolated.

Belt	Cross section	Centrifugal factor k_2
V-belt	SPZ	0.07
	SPA	0.12
V-ribbed belt	K	0.02

Belt velocities up to 30 m/s and bending frequencies up to 40 s^{-1} are permissible. See DIN 2217 for corresponding pulley dimensions.

Narrow V-belts
In accordance with DIN 7753, Part 1; machine construction, motor vehicles built in the 1960s and 1970s. Ratio of top width to height: 1.2:1. The narrow V-belt is a modified version of the standard V-belt in which the central section, which in any case transmitted only limited forces, has been omitted. Higher capacity than standard V-belts of equal width. Toothed version exhibits less creep when bending around small pulleys. Belt velocities up to 42 m/s and bending frequencies up to 100 s^{-1} are permissible. (See DIN 2211 for corresponding pulley dimensions).

Raw-edge V-belts
Raw-edge standard V-belts in accordance with DIN 2215, and raw-edge narrow V-belts for motor vehicles in accordance with DIN 7753, Part 3 (draft). Subsurface belt fibers perpendicular to the direction of belt motion provide a high degree of flexibility while at the same time giving extreme transverse stiffness and high wear resistance. They also provide excellent support for the specially treated tension member. Particularly with small-diameter pulleys, this design increases belt capacity and provides a longer service life than wrapped narrow V-belts.

PETITIONER'S EXHIBIT 1002
US PATENT NO. 6,557,540

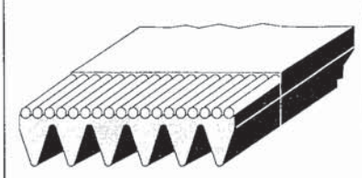
Further developments

The latest development are V-belts with tension members made of Kevlar. Kevlar has very high tensile strength with a very small degree of elongation, and is more highly temperature-resistant.

V-ribbed belts (poly-grooved belts)

In accordance with DIN 7867. Very flexible; the back of the belt may also be used to transmit power. This capability makes it possible for one such belt to be used to drive several vehicle accessories simultaneously (alternator, fan, water pump, air-conditioner compressor, power-steering pump, etc.) if the wrap angle around each driven pulley is sufficiently large. Optional cross sections include the PH, PJ, PK, PL, and PM, of which the PK cross section has been widely used in motor vehicles in recent years. This allows use of narrower pulley diameters ($d_{b\,min} \approx 45$ mm) than those possible with narrow V-belts (cross-section: AVX 10). A pretension approximately 20% greater than that employed on a narrow V-belt is recommended to provide the same force-transmission capabilities.

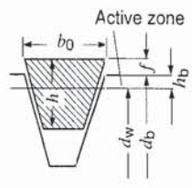
V-ribbed belts *(poly-grooved belts)*



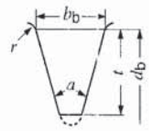
Narrow V-belts for motor vehicles in accordance with DIN 7753 Part 3
Example of designation: narrow V-belt DIN 7753 AVX 10 × 750 La,
Raw-edge, toothed with belt cross-section code AVX 10 L_a = 750 mm.

Narrow V-belt		Wrapped		Raw-edge Solid cross section (V)		Toothed (G)	
Belt cross-section	Code	9.5	12.5	AVP10	AVP13	AVX10	AVX13
	ISO code	AV 10	AV 13	AV 10	AV 13	AV 10	AV 13
Top width $b_0 \approx$		10	13	10	13	10	13
Belt height $h \approx$		8	10	7.5	8.5	8	9
Eff. line differential h_b		1.8	2.6	0.9			
Belt runout $h_{a\,max}$		–		2.4			
Effective length L_a		500 to 2550: in increments of 25 mm					

Dimensions in mm



Groove cross-section code		AV 10		AV 13	
Effective diameter	d_b	< 57	≥ 57	< 70	≥ 70
Groove angle	$\alpha \pm 0.5°$	34°	36°	34°	36°
Effective width	b_b	9.7		12.7	
Groove depth	t_{min}	11		14	
Radius of curvature	r	0.8			
Distance bet. grooves	e_{min}	12.6		16	



PETITIONER'S EXHIBIT 1002
US PATENT NO. 6,557,540

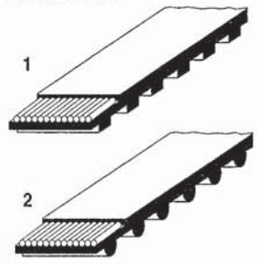
Positive belt drives

Synchronous drive belts (toothed belts) in accordance with DIN/ISO 5296
Toothed belts are used in motor vehicles as camshaft drives, and in some cases as ignition distributor drives.

Synchronous drive belts with trapezoidal or rounded teeth combine the advantages of a belt drive (any desired distance between pulley centers, quiet operation, low maintenance) with the advantages of a positive transmission (synchronous operation, low bearing stress due to low shaft load).

Synchronous drive belts must be guided on both sides to prevent them from running off. This is accomplished by using either a toothed pulley with two flanges or two toothed pulleys with one flange each on opposite sides.
See DIN/ISO 5294 for corresponding toothed-pulley dimensions.

Synchronous drive belts (toothed belts)
1 with trapezoidal teeth
2 with rounded teeth



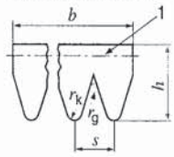
V-ribbed belts and pulleys as per DIN 7867

Designation for a 6-ribbed V-belt, cross-section code PK and reference length 800 mm:
V-ribbed belt DIN 7867-6 PK 800.

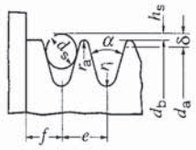
Designation for the corresponding V-belt pulley with 90 mm reference diameter:
V-ribbed belt pulley DIN 7867-6 Kx 90

Dimensions in mm	Belt	Groove profile
Cross-section code	PK	K
Rib or groove spacing s or e	3.56	3.56
Perm. deviation tolerance for s or e	± 0.2	± 0.05
Sum of deviation tolerances s or e	± 0.4	± 0.30
Groove angle α		40° ± 0.5°
r_k at rib / r_a at groove head	0.50	0.25
r_g at rib / r_i at groove seat	0.25	0.50
Belt height h	6	
Nominal dia. of test pin d_s		2.50
$2 \cdot h_s$ nominal dimension		0.99
$2 \cdot \delta$ (see illustration)		2.06
f (see illustration)		2.5

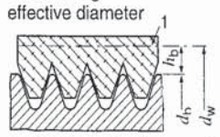
Belt cross-section



Groove cross-section



Determining effective diameter



1 Position of tension member

Belt width $b = n \cdot s$
with number of ribs = n

Effective diameter $d_w = d_b + 2\,h_b$
for K cross-section $h_b = 1.6$ mm

PETITIONER'S EXHIBIT 1002
US PATENT NO. 6,557,540

Basic principles of threaded fasteners

Units and symbols

Quantity		Unit
A_s	Stress area of thread, see P. 312	mm²
D_{Km}	Effective diameter for determining the friction torque at the fastener head or nut bearing surface	mm
F_M	Installed tension force (gen.)	N
F_{sp}	(Axial) installed tension force of threaded fastener at 90% of yield strength	N
M_M	Tightening torque for mounting	N · m
M_{sp}	Tightening torque required to load a threaded fastener to F_{sp}	N · m
P	Thread pitch	mm
d	Fastener diameter (major diameter of the thread)	mm
d_2	Mean flank diameter of the thread	mm
d_3	Root diameter of the thread	mm
μ_G	Coefficient of thread friction (friction factor)	–
μ_{tot}	Mean coefficient of friction for the fastener and head or nut bearing faces	–
μ_K	Coefficient of friction for the head and nut bearing faces	–
$\sigma_{0.2}$	0.2% yield strength of the fastener material (for low-strength fasteners, the yield point σ_s applies instead; see footnote[1]) on P. 43)	N/mm²

Basic rules

Threaded fasteners (screws, bolts, nuts) should clamp parts together with a force great enough to hold them in contact with one another without dislocation in spite of all applied operating forces. Bolts must not be subjected to shear.

A correctly preloaded fastener needs itself only to absorb a fraction of those operating forces which are applied roughly parallel to the bolt axis and which are usually dynamic in nature. When the parts to be joined are themselves as rigid as possible and elastic fasteners are used (viz. long and reduced in the body to d_3 and of property classes 8.8...12.9 with optimum tension force), the lowest fastener fatigue loading is achieved. Highly stressed joints are also the best provision against subsequent working loose (setting of the joint after tightening). As a rule of thumb, setting of the joint reduces the installed tension force of a joint using 8.8 fasteners by 10...20% if the maximum temperature is 100 °C and the parts so joined are metals with a tensile strength of at least 300 N/mm².

The tensioned section of the threaded fastener should have a minimum threaded length of 0.5 d, the object being to achieve 1.0 d whenever possible.

The spring force of installed locking devices (spring lock washers and the like) should be as great as the tension force of the fastener! Spring lock washers are usually disadvantageous when used with screws of property classes ≥ 8.8, grip lengths $> 2.5d$ and metallic components (because $F \ll F_{sp}$, and joint setting in the bearing faces additionally occurs). In the case of 4.8 and 5.6/5.8 fasteners, spring lock washers are generally superfluous if grip lengths are $\geq 5\ d$.

The compressive load per unit area under fastener heads and nuts must not exceed the crushing yield point (corresponds to at least the 0.2% permanent elongation limit or yield strength) of the material of the joint parts (if required, use large washers or flanged hex screws).

Flange mountings using four bolts are considerably more reliable than such joints which use 3 bolts in a 120° arrangement (in the latter case, failure of one bolt leads to failure of the entire bolted joint).

Property classes

The designation system for threaded fasteners consists of two numbers separated by a decimal point. The first number represents ≈ 1/100 of the minimum tensile strength in N/mm², while the second number is 10 times the ratio of the minimum yield point (or 0.2% yield strength) to the minimum tensile strength.

The property classes of standard nuts (with nominal heights ≥ 0.8 d and width across flats ≥ 1.45 d) are indicated by a number which corresponds to 1/100 of the stress under proof load in N/mm². This stress corresponds to the minimum tensile strength of a fastener in the same property class. The ability of a nut to with-

PETITIONER'S EXHIBIT 1002
US PATENT NO. 6,557,540

Table 1. Threaded fasteners: Mechanical strength properties and designations
Fasteners made of steels alloyed with boron which have a low carbon content are indicated by a solid line below the numerical designation, e.g. for property class: 10.9 (see also DIN-EN 20 898, Part 1).

Property class		3.6	4.6	4.8	5.6	5.8	6.8	8.8	10.9	12.9
Tensile strength σ_B N/mm²	min	330	400	420	500	520	600	800	1040	1220
	max ≈	490	550		700		800	1000	1200	1400
Yield point R_{el} N/mm²	min	180	240	320	300	400	480	–	–	–
0.2% yield strength $\sigma_{0.2}$	min	–	–	–	–	–	–	640	900	1080
Vickers hardness HV30	min	95	120	130	155	160	190	250	320	385
	max	250						320	380	435

stand the stress under proof load is determined using a bolt thread of greater strength (min. 45 HRC); after the stress is relieved, the nut must still be movable on the thread.

Property classes for nuts:

4	5	6	8	10	12

.

For nuts with limited loadability:

04	05

(e.g. flat nuts)

For thread diameters of 5 mm and larger,

- Fasteners in property class 8.8 and greater, as well as
- Nuts of all property classes

must be marked with the property class on the fastener head or nut face. If the fasteners are small, the decimal point between the two numbers can be omitted; for nuts, a code system can also be used, whereby the chamfers of the nuts are marked with notches and dots.

The fatigue limit of cold-formed steel fasteners of sizes up to M12 is $\sigma_D = \sigma_m \pm 50 \ldots 60$ N/mm² (referred to the root cross-section), and applies up to a mean stress of $\sigma_m = 0.6 \cdot \sigma_{0.2}$ and for all property classes from 4.8 to 12.9. Fasteners of sizes up to M8 whose threads are rolled after hardening and tempering can achieve σ_D values up to 450 ± 100 N/mm², whereas gray cast iron and aluminum nuts and fasteners can achieve values of ± 120 N/mm².

Table 2. Yield strength for threaded fasteners made of other materials

Material	Designation	Thread	0.2% yield strength N/mm²
X5CrNi 1911	A2-70	≤ M20	450
CuZn37	Cu2	≤ M6	340
		M8 ... M39	250
CuSn6	Cu4	≤ M12	340
		M14 ... M39	200
AlMgSi1	Al3	≤ M39	250

PETITIONER'S EXHIBIT 1002
US PATENT NO. 6,557,540

Tightening of threaded fasteners

Sufficient tightening torque for threaded fasteners can be realized by hand using a screwdriver up to sizes M5 – 8.8, using a hexagon socket up to a maximum of M8 – 10.9, and using a ring wrench or box-end wrench up to a maximum of M12 – 10.9 (provided that $\mu = \mu_G = \mu_K = 0.14$).

When fasteners are tightened using (conventional) torque measurement, variations in tension force occur in a ratio of approx. 1:2, and are caused by

- Variations in the coefficients of friction μ_K and μ_G (for screw head or nut and thread contact surface),
- Variations in the tightening torque (when tightened by hand and using power screwdrivers).

For $\mu_G = \mu_K = 0.1$, the effective force for producing the tension force is 17 % of the complete tightening torque, whereas the corresponding figure for $\mu_G = \mu_K = 0.2$ is only 9.5% of the complete tightening torque.

The highest possible tension forces with very small variations can be achieved with threaded fasteners using the angular tightening method and the yield-point-controlled tightening method. It must be noted that these procedures – employed to greatest advantages with grades 8.8 and above – necessitate the use of pre-calculations and empirical testing and/or special electronically-controlled wrenches. In addition, if the yield-point-controlled tightening method is used, the grip (total thickness of the bolted parts without female thread) should be at least as thick as the nominal diameter of the bolt which should be ≥ M4.

Basic formulas for tightening with torque measurement

The maximum permissible installed tension force in the fastener is limited by the effective stress (tension and torsion) which is equal to 0.9 times the minimum yield strength; this installed tension force is designated F_{sp}. The effective stress for the stress area is calculated according to the formula

$$A_s = \frac{\pi}{4} \cdot \left(\frac{d_2 + d_3}{2}\right)^2$$

with which the static, axial tensile stresses and the torsional stresses (generated by thread friction) can be viewed as if the fastener were a smooth component (A_s is greater than the root cross-section due to the fact that the threads inhibit deformation). Thus

$$F_{sp} = \frac{0.196\,(d_2 + d_3)^2 \cdot 0.9 \cdot \sigma_{0.2}}{\sqrt{1 + 4.86\left(\frac{P + \mu_G \cdot 3.63\,d_2}{d_2 + d_3}\right)^2}}$$

The values given in Table 5 for the installed tension forces F_{sp} were calculated for various coefficients of thread friction μ_G using the above formula.

In determining tightening torques it was formerly standard practice to assume that $\mu_G = \mu_K = \mu_{tot}$ in order to arrive at the simplified formula

$$M_{sp} = F_{sp}\left[0.16\,P + \mu_{tot}\left(0.58\,d_2 + \frac{D_{Km}}{2}\right)\right]$$

and corresponding graphs. In the case of differing fastener head and thread coefficients of friction (see example at end of chapter), however, this formula cannot be used to correctly determine the necessary tightening torque (see also the explanation above Table 4).

A simple, practical way of calculating tightening torque in the case of differing coefficients of friction μ_G and μ_K is the K method (proposed by Gill, used in the USA and contained in VDI Recommendation 2230, 1977 edition):
According to this method, the installed tightening torque is

$$M_M = K \cdot F_M \cdot d$$

and for tightening to 90% of the yield strength

$$M_{sp} = K \cdot F_{sp} \cdot d$$

where

$$K = \frac{0.16 \cdot P + \mu_G \cdot 0.58 \cdot d_2 + \mu_K \cdot D_{Km}/2}{d}$$

For differing coefficients of friction μ_G and μ_K and a wide range of fastener dimensions, K can be given independently of d in tabular form (see Table 4).

PETITIONER'S EXHIBIT 1002
US PATENT NO. 6,557,540

Coefficients of friction

Using Table 3 below, both the coefficient of friction for fastener head or nut (μ_K) and thread friction (μ_G) at the contact surface are determined separately and one after the other.

These coefficients of friction are significantly increased by the use of self-locking screws, washers with sharp roughly radial edges and lock nuts; connections using these fastening devices must be tightened according to special specifications.

Tightening threaded-fastener connections

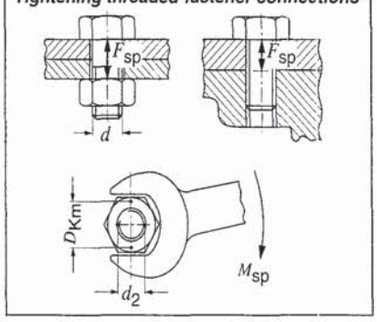


Table 3.
Coefficients of friction μ_K and μ_G for various surface and lubrication conditions
$\mu_{G\,min}$ (lower value in Table 3) is used to determine tension force F_{sp} in Table 5.

Surfaces on mating party: Bearing face on part (μ_K) or *nut thread* (μ_G)		Lubrication condition	Fastener surfaces: Bearing face of head or underside of nut (μ_K) or *fastener thread* (μ_G)		
			Steel, oil-quenched or Zn-phosph. pressed rolled	turned cut	Steel zinc-plated 6 µm
Steel,	rolled	Lightly oiled	0.13...0.19	0.10...0.18	0.10...0.18
	turned, cut planed, milled		0.10...0.18	–	0.10...0.18
	ground		0.16...0.22	0.10...0.18	0.10...0.18
Gray cast iron	planed, milled, turned, cut		0.10...0.18	–	0.10...0.18
All-black	malleable iron, ground		0.16...0.22	0.10...0.18	0.10...0.18
Steel	cadmium-electroplated, 6 µm		0.08...0.16	0.08...0.16	–
	zinc-electroplated, 6 µm		0.10...0.18	0.10...0.16	0.16...0.20
	zinc-electropl. female threads		–	–	0.10...0.18
	ground, rolled, phosphated		0.12...0.20	–	–
	machined, phosphated		0.10...0.18	–	–
Al-Mg	alloy, processed, cut		0.08...0.20	–	–
Steel,	cadmium-electroplated, 6 µm	Dry	0.08...0.16	–	–
	cadm.-electropl., fem. threads		0.08...0.14	–	–
	zinc-electroplated, 6 µm		0.10...0.18	–	0.20...0.30
	zinc-electropl., female threads		0.08...0.16	–	0.12...0.20

PETITIONER'S EXHIBIT 1002
US PATENT NO. 6,557,540

Table 4. K-Values

The K-values apply to standard threads of sizes M1.4 to M42 and bolt head and nut sizes corresponding to hexagon bolts and screws in accordance with DIN 931, 933; fillister-head slotted screws in accordance with DIN 84, hexagon cap screws in accordance with DIN 912, 6912, 7984; and nuts in accordance with DIN 934.

For M16 to M42 threads, the K-value is to be reduced by 5%, because the transition from M14 to M16 represents a significant jump in the coarseness of thread pitch a/P.

Intermediate values can be interpolated with sufficient accuracy.

Note: In special cases where only μ_{tot} has been determined previously, the K-value is determined for the case in which $\mu_K = \mu_G = \mu_{tot}$ (see also "Tightening of threaded fasteners" P. 304).

Coefficient of friction for threads μ_G	Coefficient of friction for fastener head and nut bearing face μ_K										
	0.04	0.06	0.08	0.10	0.12	0.14	0.16	0.18	0.20	0.24	0.28
0.08	0.094	0.108	0.120	0.134	0.148	0.162	0.176	0.190	0.204	0.232	0.260
0.10	0.104	0.118	0.132	0.146	0.158	0.172	0.186	0.200	0.214	0.242	0.270
0.12	0.114	0.128	0.142	0.156	0.170	0.184	0.196	0.210	0.224	0.252	0.280
0.14	0.124	0.138	0.152	0.166	0.180	0.194	0.208	0.222	0.234	0.262	0.290
0.16	0.134	0.148	0.162	0.176	0.190	0.204	0.218	0.232	0.246	0.272	0.300
0.18	0.146	0.160	0.172	0.186	0.200	0.214	0.228	0.242	0.256	2.284	0.312
0.20	0.156	0.170	0.184	0.198	0.210	0.224	0.238	0.252	0.266	0.294	0.322
0.24	0.176	0.190	0.204	0.218	0.232	0.246	0.260	0.274	0.286	0.314	0.342
0.28	0.198	0.212	0.224	0.238	0.252	0.266	0.280	0.294	0.308	0.336	0.362

Axial tension forces of bolted joints

Scope of Table 5 for installed tension forces F_{sp}

Table 5 applies only to

- Bolts with standard thread and $\frac{\text{shank diameter } d_1}{\text{minor diameter } d_3} \geq 1.05$
- With respect to material strength, the correct mating of nut and bolt, or female thread in housings;
- Nut height at least 0.8 x thread diameter and sufficient depth of thread in housings and the like.

Correction factors for tension forces and coefficients of friction (selection)

Flat nuts with a height of $0.5 \cdot d$ and the same hardness as the bolts allow a tension force of only 80 % of the values given in the table. In the case of low-strength flat nuts (04) on 12.9 bolts, only 33 % of F_{sp} is permissible.

In the case of fastener heads and nuts with smaller or larger bearing faces as well as adjusting screws and locating screws which do not have contact at their heads, the μ_K-value must be reduced or increased by the same ratio as the ratio of the mean friction diameter of their bearing faces to the mean friction diameter of the above-mentioned standard hexagon etc. fasteners and nuts. It is this corrected hypothetical μ_K-value which is used to determine the K-value (for this reason, Table 4 gives μ_K-values beginning with 0.04).

In the case of countersunk-head screws, allowance must be additionally made for the conical effect of the countersink angle as well as the greater elasticity of the outer edge of the head; thus the μ_K-value hypothetically increases by a factor of 1.25 in the case of standard countersunk screws (countersink angle: 90°).

PETITIONER'S EXHIBIT 1002
US PATENT NO. 6,557,540

Table 5. Tension forces F_{sp} in 10^3 N for standard threads and coefficients of friction μ_G in the threads (for 90 % utilization of $\sigma_{0.2}$ or σ_s)

Dimension (pitch)	Property class	F_{sp} (10^3 N) for coefficients of friction μ_G in the threads									
		0.06	0.08	0.10	0.12	0.14	0.16	0.18	0.20	0.24	0.28
	4.8	2.3	2.2	2.1	2.0	1.9	1.9	1.8	1.7	1.6	1.4
	5.8	2.8	2.7	2.6	2.5	2.4	2.3	2.2	2.1	2.0	1.8
M 4	8.8	4.5	4.4	4.2	4.1	3.9	3.7	3.6	3.4	3.2	2.9
	10.9	6.4	6.2	5.9	5.7	5.5	5.3	5.0	4.8	4.4	4.1
(0.7)	12.9	7.7	7.4	7.1	6.9	6.6	6.3	6.0	5.8	5.3	4.9
	4.8	3.7	3.6	3.5	3.3	3.2	3.1	2.9	2.8	2.6	2.4
	5.8	4.6	4.5	4.3	4.2	4.0	3.8	3.6	3.5	3.2	3.0
M 5	8.8	7.4	7.2	6.9	6.6	6.4	6.1	5.9	5.6	5.2	4.8
	10.9	10.4	10.1	9.7	9.4	9.0	8.6	8.3	7.9	7.3	6.7
(0.8)	12.9	12.5	12.1	11.7	11.2	10.8	10.3	9.9	9.5	8.7	8.1
	4.8	5.2	5.1	4.9	4.7	4.5	4.3	4.1	4.0	3.7	3.4
	5.8	6.6	6.3	6.1	5.9	5.6	5.4	5.2	5.0	4.6	4.2
M 6	8.8	10.5	10.1	9.8	9.4	9.0	8.6	8.3	7.9	7.3	6.7
	10.9	14.7	14.2	13.7	13.2	12.7	12.1	11.7	11.2	10.3	9.5
(1.0)	12.9	17.7	17.1	16.5	15.8	15.2	14.6	14.0	13.4	12.3	11.4
	4.8	9.6	9.3	8.9	8.6	8.3	7.9	7.6	7.3	6.7	6.2
	5.8	12.0	11.6	11.2	10.8	10.3	9.9	9.5	9.1	8.4	7.7
M 8	8.8	19.2	18.6	17.9	17.2	16.5	15.7	15.2	14.6	13.4	12.4
	10.9	27.0	26.1	25.2	24.2	23.2	22.3	21.4	20.5	18.9	17.4
(1.25)	12.9	32.4	31.3	30.2	29.0	27.9	26.8	25.7	24.6	22.6	20.9
	4.8	15.3	14.8	14.2	13.7	13.2	12.6	12.1	11.6	10.7	9.9
	5.8	19.0	18.5	17.8	17.1	16.5	15.9	15.1	14.5	13.4	12.3
M 10	8.8	30.5	29.5	28.5	27.4	26.3	25.3	24.2	23.2	21.4	19.7
	10.9	42.9	41.5	40.1	38.5	37.0	35.5	34.1	32.7	30.1	27.7
(1.5)	12.9	51.5	49.8	48.1	46.2	44.4	42.6	40.1	39.2	36.1	33.2
	4.8	22.2	21.5	20.8	20.0	19.2	18.4	17.7	16.9	15.6	14.4
	5.8	27.8	26.9	25.9	25.0	24.0	23.0	22.1	21.2	19.5	18.0
M 12	8.8	44.5	43.0	41.5	40.0	38.4	36.8	35.3	33.9	31.2	28.7
	10.9	62.5	60.5	58.4	56.2	54.0	51.8	49.7	47.7	43.8	40.4
(1.75)	12.9	75.0	72.6	70.0	67.4	64.8	62.2	59.6	57.2	52.6	48.5
	4.8	30.5	29.6	28.5	27.4	26.4	25.3	24.3	23.3	21.4	19.7
	5.8	38.1	36.9	35.6	34.3	32.9	31.6	30.3	29.1	26.8	24.7
M 14	8.8	61.0	59.1	57.0	54.9	52.7	50.6	48.5	46.5	42.8	39.5
	10.9	85.8	83.1	80.1	77.1	74.1	71.2	68.3	65.5	60.2	55.5
(2.0)	12.9	103	99.7	96.2	92.6	89.0	85.4	81.9	78.5	72.3	66.6
	4.8	41.8	40.5	39.2	37.7	36.3	34.8	33.4	32.1	29.5	27.2
	5.8	52.3	50.7	48.9	47.2	45.4	43.6	41.8	40.1	36.9	34.0
M 16	8.8	83.6	81.1	78.3	75.5	72.3	69.7	66.9	64.2	59.0	54.4
	10.9	118	114	110	106	102	98.0	94.1	90.2	83.0	76.5
(2.0)	12.9	141	137	132	127	122	118	113	108	99.6	91.9
	4.8	65.3	63.3	61.2	59.0	56.7	54.5	52.2	50.1	46.1	42.5
	5.8	81.7	79.2	76.5	73.7	70.9	68.1	65.3	62.7	57.7	53.2
M 20	8.8	131	127	122	118	113	109	105	100	92.3	85.1
	10.9	184	178	172	166	159	153	147	141	130	120
(2.5)	12.9	220	214	206	199	191	184	176	169	156	144

In contrast to 5.8 bolts, the tension forces F_{sp} for bolts in other (nonferrous) property classes must be converted based on their yield points or their yield strengths; e.g. for M6 Cu2 fastener with $\mu_G = 0.10$, $F_{sp} = (340/400) \cdot 6.1 \cdot 10^3 \approx 5.2 \cdot 10^3$N.

PETITIONER'S EXHIBIT 1002
US PATENT NO. 6,557,540

Advantages of the K-method over previously used methods of determining tightening torque

- Easily takes into account the different coefficients of friction μ_K and μ_G.

The K-method therefore allows for more reliable design and greater minimum installed tension force (if the example below were calculated using $\mu_{tot} = \mu_K$, the maximum tension force would be impermissibly high, reaching a value just below the yield point. If the calculation were made using $\mu_{tot} = \mu_G$ instead, the tightening torques would be lower and the minimum tension force would be only 68% of 14,800 N).

- In order to express the values listed in Table 3 as μ_{tot} values, more comprehensive tabular information would be required. Table 3 requires only a fraction of this information.
- The K-method is used to precisely determine the tightening torques when tightening threaded fasteners using a torque wrench, and is an advantageous replacement for the tables and somewhat complicated graphs used previously.
- Using yield point or angle-controlled tightening methods, better utilization factors can still be achieved at threaded-fastener connections (see "Tightening of threaded fasteners").

Determining tension forces and tightening torques

The maximum attainable installed tension force $F_{sp\ max}$ is determined using the smallest coefficient of friction in the threads μ_G and Table 5. (Most of the torque applied to the screw shank is used to overcome thread friction, while only the remainder is converted to tension force by the thread pitch; the maximum permissible tension force must not be exceeded even when this residual torque reaches its maximum value and μ_G its minimum value.)

The maximum permissible installed tightening torque $M_{sp\ max}$ is calculated using the K-value for the lowest values for μ_K and μ_G (because the maximum permissible tensioning force must not be exceeded even when maximum tightening torque coincides with the smallest coefficients of friction).

$$M_{sp\ max} = K_{min} \cdot F_{sp\ max} \cdot d$$

The lowest installed tightening torque $M_{sp\ min}$ is a result of the quality of the tightening process and the equipment used. If good power screwdrivers are used or the tightening process is carefully performed by hand using torque wrenches, the nominal torque can usually be achieved within a variation ±10%. The lowest installed tightening torque is then

$$M_{sp\ min} \approx 0.8 \cdot M_{sp\ max}$$

The lowest installed clamping force $F_{sp\ min}$ which then may occur is calculated using the K-value for the maximum values of the two coefficients of friction μ_K and μ_G as follows:

$$F_{sp\ min} = M_{sp\ min}/(K_{max} \cdot d)$$

Example: *An M 10-8.8 bolt or screw (pressed and rolled, phosphated) is used to fasten a ground steel part to an AlMg housing with blind threaded holes; the parts are lightly oiled.*

From Table 3: $\mu_K = 0.16 \ldots 0.22$

$\mu_G = 0.08 \ldots 0.20$ → for $\mu_G = 0.08$ in accordance with Table 3: $F_{sp\ max} = 29{,}500$ N

From Table 4: $K_{min} = 0.176 \mid K_{max} = 0.280$

$M_{sp\ max} = 0.176 \cdot 29500 \cdot 0.010 = 51.9$ N · m

$M_{sp\ min} = 0.8 \cdot M_{sp\ max} = 41.5$ N · m

$F_{sp\ min} = 41.5/(0.280 \cdot 0.010) = 14800$ N

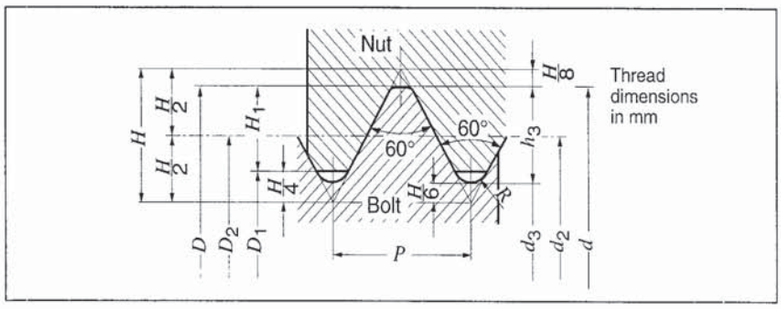
(with d in m)

PETITIONER'S EXHIBIT 1002
US PATENT NO. 6,557,540

Threads (Selection)

ISO metric screw threads

(DIN 13, ISO 965); Nominal dimensions



Metric standard thread

Example of designation: M8 (nominal thread diameter: 8 mm)

Nominal thread dia. $d = D$	Pitch P	Pitch diameter $d_2 = D_2$	Minor diameter d_3	Minor diameter D_1	Thread depth h_3	Thread depth H_1	Tensile stress area A_s in mm²
3	0.5	2.675	2.387	2.459	0.307	0.271	5.03
4	0.7	3.545	3.141	3.242	0.429	0.379	8.78
5	0.8	4.480	4.019	4.134	0.491	0.433	14.2
6	1	5.350	4.773	4.917	0.613	0.541	20.1
8	1.25	7.188	6.466	6.647	0.767	0.677	36.6
10	1.5	9.026	8.160	8.376	0.920	0.812	58.0
12	1.75	10.863	9.853	10.106	1.074	0.947	84.3
14	2	12.701	11.546	11.835	1.227	1.083	115
16	2	14.701	13.546	13.835	1.227	1.083	157
20	2.5	18.376	16.933	17.294	1.534	1.353	245
24	3	22.051	20.319	20.752	1.840	1.624	353

Metric fine thread

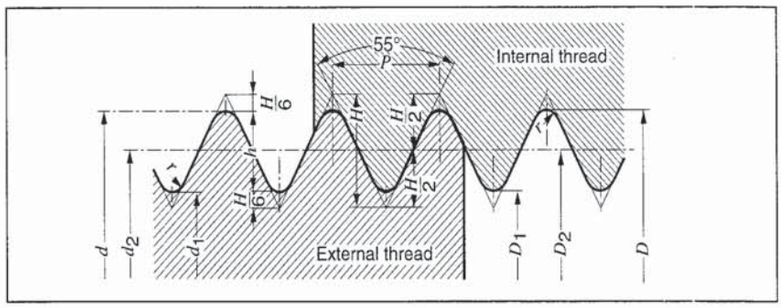
Example of designation: M8 x 1 (Nominal thread diameter: 8 mm; pitch: 1 mm)

Nominal thread dia. $d = D$	Pitch P	Pitch diameter $d_2 = D_2$	Minor diameter d_3	Minor diameter D_1	Thread depth h_3	Thread depth H_1	Tensile stress area A_s in mm²
8	1	7.350	6.773	6.917	0.613	0.541	39.2
10	1.25	9.188	8.466	8.647	0.767	0.677	61.2
10	1	9.350	8.773	8.917	0.613	0.541	64.5
12	1.5	11.026	10.160	10.376	0.920	0.812	88.1
12	1.25	11.188	10.466	10.647	0.767	0.677	92.1
16	1.5	15.026	14.160	14.376	0.920	0.812	167
18	1.5	17.026	16.160	16.376	0.920	0.812	216
20	2	18.701	17.546	17.835	1.227	1.083	258
20	1.5	19.026	18.160	18.376	0.920	0.812	272
22	1.5	21.026	20.160	20.376	0.920	0.812	333
24	2	22.701	21.546	21.835	1.227	1.083	384
24	1.5	23.026	22.160	22.376	0.920	0.812	401

PETITIONER'S EXHIBIT 1002
US PATENT NO. 6,557,540

Pipe threads for non self-sealing joints

(DIN ISO 228-1); Parallel internal threads and external threads; nominal dimensions

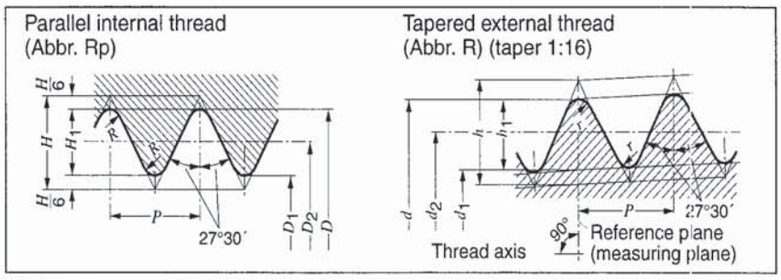


Example of designation: G 1/2 (nominal thread size 1/2 inch)

Nominal thread size	Number of threads per inch	Pitch P mm	Thread depth h mm	Major diameter $d = D$ mm	Pitch diameter $d_2 = D_2$ mm	Minor diameter $d_1 = D_1$ mm
1/4	19	1.337	0.856	13.157	12.301	11.445
3/8	19	1.337	0.856	16.662	15.806	14.950
1/2	14	1.814	1.162	20.955	19.793	18.631
3/4	14	1.814	1.162	26.441	25.279	24.117
1	11	2.309	1.479	33.249	31.770	30.291

Whitworth pipe threads for threaded pipes and fittings

(DIN 2999); Parallel internal threads and taper external threads; nominal dimensions (mm)



Designation		Major diameter	Pitch diameter	Minor diameter	Pitch	Number of threads per inch
External thread	Internal thread	$d = D$	$d_2 = D_2$	$d_1 = D_1$	P	Z
R 1/4	**Rp 1/4**	13.157	12.301	11.445	1.337	19
R 3/8	**Rp 3/8**	16.662	15.806	14.950	1.337	19
R 1/2	**Rp 1/2**	20.955	19.793	18.631	1.814	14
R 3/4	**Rp 3/4**	26.441	25.279	24.117	1.814	14
R 1	**Rp 1**	33.249	31.770	30.291	2.309	11

Areas of application: For joining pipes with parallel internal threads to valves, fittings, threaded flanges, etc. with tapered external threads.

PETITIONER'S EXHIBIT 1002
US PATENT NO. 6,557,540

Joining and bonding techniques

Welding

Automotive components and subassemblies are joined using a wide and highly variegated range of welding and bonding techniques. Resistance-pressure and fusion welding are among the most commonly applied welding methods. This summary concentrates on the resistance-welding procedures in standard production use (processes and symbols based on DIN 1910, Part 5).

Resistance welding

Resistance spot-welding

In resistance spot-welding, locally applied electrical current is used to melt the contact surfaces of the parts to be joined into a soft or fluid state; the parts are then joined together under pressure. The contact-point electrodes which conduct the welding current also convey the electrode force to the parts. The amount of heat required to form the welding joint is determined according to $Q = I^2 \cdot R \cdot t$ (Joule's Law).

The precise amount of heat required is a function of current, resistance and time. The following factors should be coordinated in order to achieve a good weld and adequate spot diameter d_1:

- welding current I,
- electrode force F and
- welding time t.

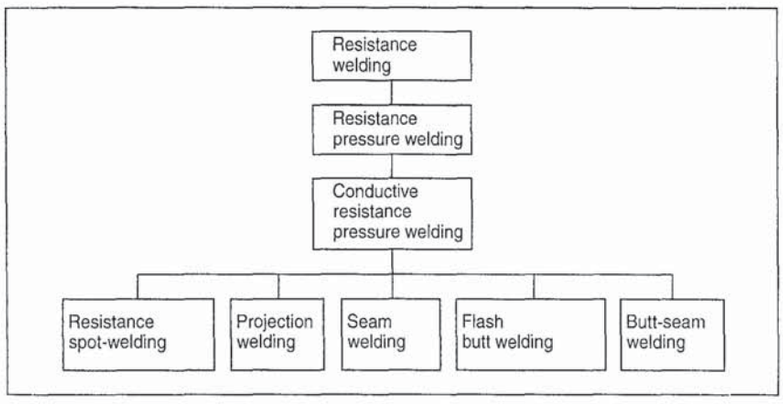
According to the manner in which the current is conducted, a distinction is drawn between:

- bilateral direct resistance spot-welding and
- unilateral indirect resistance spot-welding.

The electrode for a specific spot-welding operation is selected with reference to shape, outside diameter and point diameter. Before welding, the parts must always be completely free of scaling, oxides, paint, grease and oil; they therefore receive appropriate surface treatment prior to welding (where indicated).

Projection welding

Projection welding is a process in which electrodes with a large surface area are employed to conduct the welding current and the electrode force to the workpiece. The projections, which are generally incorporated into the thicker of the workpieces, cause the current to concentrate at the contact surfaces. The electrode force compresses the projections partially or completely during the welding process. A permanent, inseparable joint is produced at the contact points along the welding seam. One or more than one projection can be welded simultaneously, depending on the type of projection (round or annular) and the power available from the welding unit.



PETITIONER'S EXHIBIT 1002
US PATENT NO. 6,557,540

Depending on the number of spots welded, a distinction is drawn between
– single-projection welding and
– multiple-projection welding.

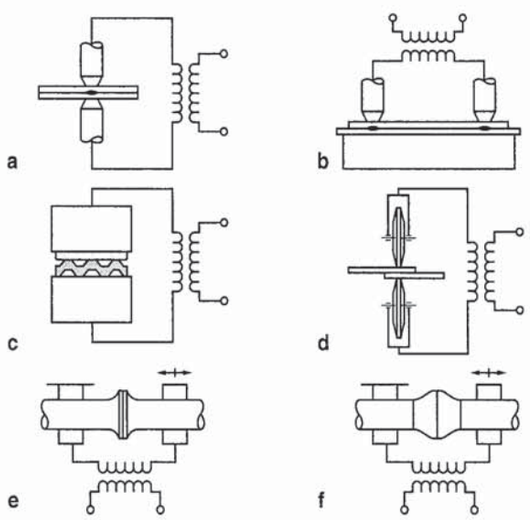
This technique requires high welding currents applied for short periods of time.
Applications:
– welding parts of different thicknesses,
– welding multiple projections in a single operation.

Seam welding
In this process, roller electrodes replace the spot-welding electrodes used in resistance spot-welding. Contact between the roller pair and the workpiece is limited to an extremely small surface area. The roller electrodes conduct the welding current and apply the electrode force. Their rotation is coordinated with the movement of the part.
Applications:
Production of sealed welds or seam spot welds (e.g. fuel tanks).

Flash-butt welding
In flash-butt welding, the butt ends of the workpieces are joined under moderate pressure while the flow of current at the contact surfaces produces localized heat and melting (high current density). The metal's vapor pressure drives molten material from the contact patches (burn-off) while force is applied to form an upset butt weld. The butt ends should be parallel to each other and at right angles to the direction in which the force is applied (or virtually so). Smooth surfaces are not required. A certain amount of extra length must be factored in to compensate for the losses incurred in the flash-welding process.
Result:
A weld with the characteristic projecting seam (burr).

Butt-seam welding
This process employs copper jaws to conduct the welding current to the workpieces being joined. When the welding temperature is reached, the current switches off. Constant pressure is maintained and the workpieces then weld to-

Welding techniques
a) Bilateral resistance spot-welding, b) Unilateral resistance spot-welding, c) Projection welding, d) Seam welding, e) Flash butt welding, f) Butt-seam welding.



PETITIONER'S EXHIBIT 1002
US PATENT NO. 6,557,540

gether (requirement: properly machined butting faces). The result is a burr-free seam. The process does not completely displace contamination that may be present at the butt ends.

Fusion welding
The term "fusion welding" describes a process employing limited local application of heat to melt and join the parts; no pressure is applied.

Shielded (inert gas) arc welding is a type of fusion welding. The electrical arc extending between the electrode and the workpiece serves as the heat source. Meanwhile, a layer of inert gas shields the arc and the melted area from the atmosphere. The type of electrode is the factor which distinguishes between the various techniques:

Tungsten inert-gas welding
In this process, an arc is maintained between the workpiece and a stable, non-melting tungsten electrode. The shielding (inert) gas is argon or helium. Weld material is supplied from the side (as in gas fusion welding).

Gas-shielded metal-arc welding
In this process, an arc is maintained between the melting end of the wire electrode (material feed) and the workpiece. The welding current flows to the wire electrode via sliding contacts in the torch holder. Insert-gas metal-arc welding uses inert gases (slowly reacting and noble gases such as argon, helium, or combinations of the two) as protective gas. Active-gas metal-arc welding, on the other hand, employs reactive gases such as CO_2 and mixed gases containing CO_2, argon and sometimes oxygen, and is frequently referred to as CO_2 welding.

This process is employed for welding non-alloy and mild-alloy steels.
In addition, the following welding techniques are employed in the automobile industry:
- electron-beam welding,
- friction welding,
- arc pressure welding (stud welding),
- stored-energy welding (pulse welding).

Soldering

In soldering, a supplementary material (solder) is melted onto two or more parts of similar or varying metallic composition in order to produce a permanent connection between them. Flux and/or protective gas may also be used. The melting temperature of the solder is below that of the parts being joined. The solder is distributed along the join to produce the connection without the parts themselves being melted.

Soldering processes are classified by working temperature. This is defined as the lowest surface temperature at the connection between the workpieces to be joined at which the solder can be melted and distributed to form a bond.

Soft soldering
Soft soldering is employed to form permanent solder joints at melting temperatures below 450 °C (as with soldering tin). Soft solders which melt at temperatures of 200 °C and below are also known as quick solders.

Hard soldering
Hard soldering (brazing) is used to form permanent joins at melting temperatures above 450 °C (as with copper/zinc, combined copper/zinc and silver alloys, e.g. silver brazing filler). Further data on soldering materials is contained in DIN Sheets 1707, 8512, 8513 and 8516.

Fluxes (non-metallic substances) are applied to remove any film (oxidation) remaining on the surface of the parts after cleaning and to prevent a new film from forming: this makes it possible to apply a consistent coat of solder to the joint surfaces. Data on fluxes can be found in DIN 8511.

The strength of a soldered joint can be equal to that of the base material itself. This phenomenon is due to the fact that the more rigid adjoining materials limit the solder's deformation potential.

The method used for heating provides yet another criterion for the classification of soldering processes. The two standard types are: open-flame soldering and iron soldering.

PETITIONER'S EXHIBIT 1002
US PATENT NO. 6,557,540

Flame soldering
A hand-held burner or a gas-fired unit provides the heat. Depending on the specific soldering operation, either oxy-acetylene burners (familiar from gas welding) or soldering lamps are employed.

Iron soldering
A hand-held or mechanically guided soldering iron provides the heat. Irons can also be used to solder pretinned surfaces.

Other processes include: oven, salt-bath, immersion, resistance, and induction soldering.

Adhesive technologies

Organic or anorganic adhesives are employed to form permanent rigid connections between two metallic or non-metallic materials. The adhesive bonds under pressure, either at room temperature or with moderate heat. The bond is adhesive, in other words physical and chemical bonding forces operate at the molecular level to bond the surfaces. A distinction is drawn between single-component and two-component adhesives, referring to their as-delivered condition.

Single-component adhesives
These are components which contain all the constituents necessary to form a bond.

Two-component adhesives
The second component in an adhesive of this type is a hardener that initiates the cross-linking process. An accelerator may be added to the hardener. Metal adhesives are generally of the two-component type. The hardening (cross-linking) process is polymerization, polycondensation or polyaddition under the influence of temperature and/or time. Spatially interlinked macro-modules are the result. Depending on the hardening temperature, a distinction is drawn between cold adhesives (harden at room temperature, relatively easy to apply, and hot adhesives harden at 100 ... 200 °C).

Adhesive connections should be designed to ensure that the bond is subjected exclusively to tensile shear loads. Overlapping connections are virtually the only application for adhesives. Butt joins subjected to tensile or sliding forces should be avoided.

Metal adhesives can be employed in conjunction with spot welding. The adhesive prevents premature swelling of the sheets between the resistance-welded spots. This method is also suitable for reducing stress peaks at the edges of the weld spots and limited the number of spots required. Constructions of this nature evince enhanced structural integrity, rigidity, and damping when subjected to dynamic loads. Welding is carried out when the adhesive is still soft; otherwise the adhesive would act as an insulator.

The most significant metal adhesives include: epoxy, polyester and acrylic resins, vinyl acetate, and metal cement.

Automotive applications
Adhesive joining has become a standard technique in automotive engineering. The individual areas of application can be classified as follows.
- Body shell: Raised-seam and brace bonding for attached components.
- Painting line: Attachment of stiffeners.
- Assembly line: Attachment of insulating material, appliqués, moldings, mirror-support bracket to windshield.
- Component production: Bonding brake pads, laminated safety glass (LSG), rubber-to-metal connections to absorb vibration.

PETITIONER'S EXHIBIT 1002
US PATENT NO. 6,557,540

Riveting

Riveting is used to produce a permanent fixed connection between two or more components made of identical or dissimilar materials. Depending on the method and application, riveted connections are divided into the following categories:
- permanent rigid connections (interference fits, for example in mechanical and plant engineering),
- permanent, sealed connections (for example in boilers and pressure vessels) and
- extremely tight seals (for example in pipes, vacuum equipment, etc.).

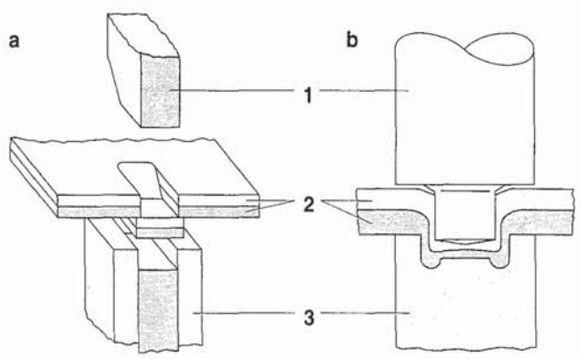
In some areas such as mechanical engineering in general and in tank manufacture, riveting has largely been displaced by welding. A distinction is drawn between cold and hot riveting, depending on the temperature used. Cold riveting is employed for rivet joints up to 10 mm in diameter in steel, copper, copper alloys, aluminum, etc. Rivets with diameters in excess of 10 mm are installed hot.

The most common types of rivet are mushroom head, countersunk, tallow-drop, hollow and tubular. There are also standardized rivets for specialized applications, for example explosive rivets and pop rivets. Pop rivets are hollow and are expanded by a drift or punch. The types of rivet and the corresponding materials are defined in DIN sheets; structural integrity and chemical composition are specified in DIN 17 111. In order to avoid the danger of electrochemical corrosion, the rivet material and the material of the parts being joined should be similar, if possible.

Advantages/disadvantages compared to other joining techniques
- Unlike welding, riveting exerts no effects such as hardening or molecular alteration on the material,
- no distortion of the components,
- suitable for joining dissimilar materials,
- riveting weakens the components,
- butt joints cannot be riveted and
- riveting is generally more expensive than welding when performed outside the factory.

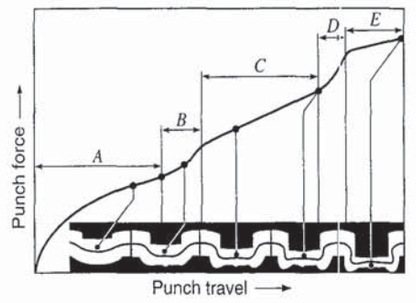
Automotive applications
- Riveting joint pins (window winders, windshield-wiper linkages),
- Riveting reinforcement plates (in the course of repairs).

Pressurized clinching
a) Clinching, b) Tox clinching; 1 Punch, 2 Work, 3 Die.



PETITIONER'S EXHIBIT 1002
US PATENT NO. 6,557,540

Punch force/punch travel curve
A Combined indentation and melding.
B Upsetting and expansion.
C Filling upper contour of mold.
D Filling annular canal.
E Cup extrusion.



Bonding and joining (pressurized clinching)

Pressurized clinching is a mechanical process for penetration assembly of layered materials. It combines cutting, penetration and cold upsetting in a single continuous joining operation without the application of additional heat. The basic principle is one of joining through reshaping. DIN 8593, Part 5, issued in September 1985 contains the first reference to this process as a means of joining sheet-metal panels by deformation.

The past few years have marked the advent of tox clinching as yet another joining process: it resembles penetration clinching, but does not include a cutting process. The tools employed for tox clinching are relatively small. The diameter can be varied to suit specific applications. At present, pressurized clinching can be used to join panels up to 3 mm thick, whereby the total thickness of the two sheets should not exceed 5 mm. The panels being joined can be of the same material (e.g. steel/steel) or dissimilar materials (e.g. steel/non-ferrous metal). In addition, pressurized clinching can be used to join coated sheets and painted parts, as well as components to which adhesives have been applied. Multiple clinching can be used to produce numerous pressure-assembly elements (up to 50) in a single process (one stroke of the press, for example). The typical curve for punch force relative to punch travel can be divided into five characteristic phases (A...E).

Advantages/disadvantages of pressurized clinching
- No need for noise-abatement encapsulation,
- tox clinching does not impair corrosion protection,
- when combined with a cutting operation there is a partial loss of corrosion protection,
- no heat distortion,
- painted, protected (oil, wax) and glued sheets can be clinched,
- different materials can be joined (e.g. steel/plastic)
- energy savings, no power supply required for welding and no cooling water,
- one side of the workpiece evinces a projection similar to that produced by a rivet head, while the other side has a corresponding depression.

Automotive applications
- Windshield wiper brackets,
- Fastening door interior panels,
- Positioning individual components.

PETITIONER'S EXHIBIT 1002
US PATENT NO. 6,557,540

Punch riveting

The punch riveting technique joins solid materials employing stamping and riveting elements (solid or semi-hollow rivets) in a combined cutting and joining operation.

The parts to be joined do not have to be predrilled and stamped, as is the case with other riveting techniques.

Punch riveting with solid rivets

The first stage in punch riveting with solid rivets is to position the work on the die plate.

The top section of the rivet unit, including the blank holder, descends and the rivet die presses the rivet through the parts to be joined in a single stamping operation.

Punch riveting with semi-hollow rivets

The first stage in punch riveting with semi-hollow rivets is to position the work on the (bottom) die plate. The rivet die descends and presses the semi-hollow rivet through the upper sheet into the lower sheet in a single stamping operation. The rivet deforms and the bottom spreads to form a securing element, usually without fully penetrating the lower sheet.

Equipment

Highly rigid hydraulic tools are used in punch riveting. Rivets can be singled from a batch feed or carried in belts with individual holders to the riveting tool.

Materials

The rivets must be harder than the materials to be joined. The most common materials are steel, stainless steel, copper and aluminum with various coatings.

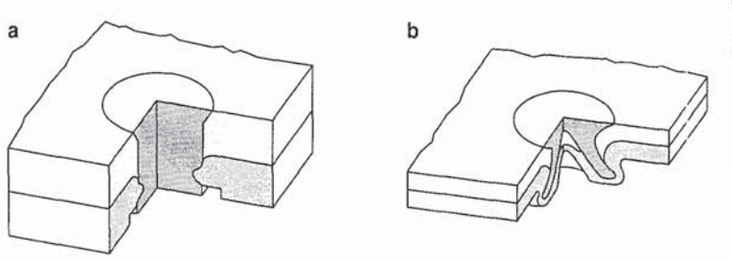
Characteristics

- Used to join similar and dissimilar materials (e.g. steel, plastic or aluminum), parts of various thicknesses and strengths, and painted sheets.
- No preliminary stamping or drilling, no electrical current or vacuum extraction required.
- Approved overall material thicknesses: steel 6.5 mm; aluminum 11 mm.
- Low-heat, low-noise joining process.
- Tools have a long service life (approx. 300,000 rivet applications) with consistent quality.
- Process dependability with monitored process parameters.
- High forces have to be applied.
- Restricted jaw reach.

Applications

Punch riveting with solid rivets: joining metal sheets in automotive engineering, e.g. window winders in passenger cars. Punch riveting with semi-hollow rivets: joining materials at the body-in-white stage in automotive engineering, household appliances, joining metals to composites (heat shields).

Punch-riveted joints
a) Solid rivet, b) Semi-hollow rivet.



PETITIONER'S EXHIBIT 1002
US PATENT NO. 6,557,540

Sheet-metal processing

Deep-drawing technology

Units and symbols

Symbols		Units
D	Section diameter	mm
d_B	Support diameter of hold-down device	mm
d_1	Stamping diameter, 1st draw	mm
d_2	Stamping diameter, 2nd draw	mm
F	Total deep-drawing force	kN
F_B	Hold-down force	kN
F_Z	Deep-draw force	kN
p	Pressure of hold-down device	N/mm²
R_m	Tensile strength	N/mm²
s	Sheet thickness	mm
β_1, β_2	Individual drawing ratio	
β_{max}	Maximum possible drawing ratio	

Drawing methods

The drawing procedure employs a drawing die, punch and sheet-metal retaining device to reshape flat sections, blanks and round plates.

The variables exercising an influence on the deep-drawing of three-dimensional bodywork components are exceedingly complex; rough calculations thus do not provide a suitable basis for their definition. The finite-element method (FEM), in which powerful computers employ numerical procedures from continuum mechanics, is used to calculate deep-drawing processes. Software development has reflected the significance of specific parameters affecting the deep-drawing process, including the influence of friction, of bilateral contact, of material values which vary according to rolling direction, and additional factors.

Deep-draw simulation is of major assistance in designing deep-drawing tools, helping to optimize production times for this equipment.

Deep-drawing process

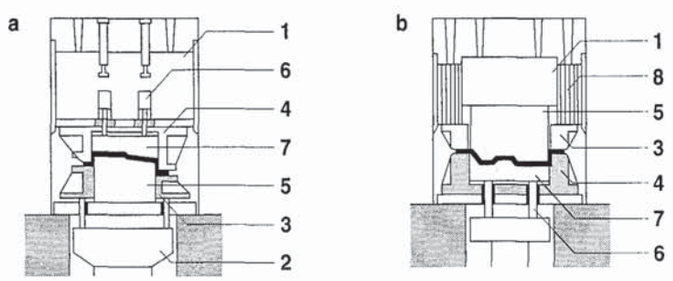
The drawing process reshapes a flat blank into a concave section. A punch, surrounded by a retaining mechanism (holding-down clamp, blank holder), pulls the sheet metal into the matrix. The clamp applies the defined force to the sheet, prevents creases from forming, and permits application of tensile force.

The maximum possible drawing ratio is determined by various factors:
- material strength,
- tool dimensions and sheet thickness,
- retention force,
- friction,
- lubrication,
- material and surface of the workpiece.

Drawing with single-action presses

This category includes all crank presses in which the ram represents the only moving component.

Deep drawing
a) With single-action press, b) With double-action press; 1 Ram, 2 Air cushion, 3 Hold-down device, 4 Matrix, 5 Punch, 6 Air pins, 7 Matrix insert, 8 Hold-down ram.



PETITIONER'S EXHIBIT 1002
US PATENT NO. 6,557,540

Applications: for deep-drawing flat workpieces in simple reshaping operations to produce trimmers, arches, supports.

Drawing on double-action presses

Double-action drawing presses employ separate rams to retain the metal and to pull it. The hold-down ram is actuated mechanically via disk or toggle, or hydraulically.

Applications: for deep-drawn components of complex geometry, including fenders, wheel arches, decklids.

Calculations for the drawing process

$$F_Z = \pi \cdot (d_1 + s) \cdot s \cdot R_m$$

$$F_B = \frac{\pi}{4} \cdot (D^2 - d_B^2) \cdot p$$

$$F = F_Z + F_B$$

$$\beta_1 = D/d_1;\ \beta_2 = d_1/d_2.$$

Example

D = 210 mm; d_B = 160 mm; d_1 = 140 mm; p = 2.5 N/mm²; R_m = 380 N/mm²; s = 1 mm; β_{max} = 1.9.

Result

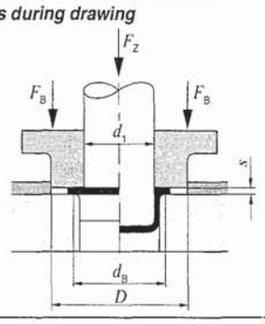
Drawing ratio β_1 = 1.5; Deep-drawing force F_Z = 112.2 kN; Sheet retention force F_B = 36.3 kN; Total deep-drawing force F = 148.5 kN.

The diagram shows the motions of the drawing ram and the hold-down ram in the course of one cycle. The rams have differing strokes. The drawing ram, with its longer stroke, is set in motion first, while the shorter-stroke retention ram starts second, but is first to achieve contact.

Material	β_1 max.	β_2 max.	Pressure of hold-down device p N/mm²
St 12	1.8	1.2	2.5
St 13	1.9	1.25	
St 14	2.0	1.3	
Copper	2.1	1.3	
CuZn 37 w	2.1	1.4	2.0...2.4
CuZn 37 h	1.9	1.2	
CuSn 6 w	1.5	–	
Al 99.5 w	2.1	1.6	
AlMg 1 w	1.85	1.3	1.2...1.5
AlCuMg 1 pl w	2.0	1.5	
AlCuMg 1 pl ka	1.8	1.3	

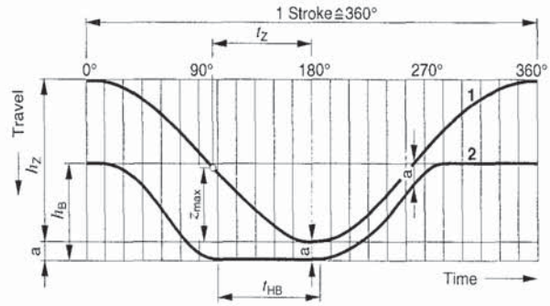
[1]) Valid up to d_1/s = 300; specified for d_1 = 100 mm, s = 1 mm. Different sheet thicknesses and punch diameters result in minor deviations from the figures given. Basic qualities are also used with galvanized surfaces. The figures can vary slightly.

Forces during drawing



Time-distance diagram for a double-action drawing press

1 Curve for drawing ram, 2 Curve for hold-down ram;
h_z Stroke of drawing ram, h_B Stroke of hold-down ram, z_{max} Max. drawing depth,
t_z Duration of drawing process, t_{HB} Holding time of hold-down ram, a Approach of drawing ram



PETITIONER'S EXHIBIT 1002
US PATENT NO. 6,557,540

Laser technology

Deviation mirrors are used to deflect the coherent light beam generated by the laser for concentration in a focusing device. At the focal point the laser beam has a diameter of approx. 0.3...0.5 mm, allowing intensities in excess of 10^6...10^8 W/cm^2 to be achieved. The workpiece melts and vaporizes in milliseconds if the focal point is in its immediate vicinity, an effect which can be exploited in laser-based processing operations. According to the physical condition of the active medium, the device is classified as a solid-state, gas, semiconductor or liquid laser. The following are applied in industrial metal processing:

Solid-state laser (Nd:YAG)
Neodynium (Nd) is an element of the rare-earth group, while YAG stands for yttrium-aluminum-garnet ($Y_5Al_5O_{12}$). The crystal exhibits mechanical and thermal stability equal to that of the ruby.

The Nd:YAG laser emits light in the infrared range of the spectrum, with a wavelength of 1.06 µm. The essential advantage of the Nd:YAG laser lies in the fact that the generated beam can be transmitted through optical fibers, making it possible to dispense with complicated beam-relaying systems. Present laser power ratings are in the range of 400... 1200 W; pulse-mode operation is generally employed. The foremost application for solid-state lasers is in welding parts with high requirements for precision, e.g. in precision mechanics. Welding depths depend on power and welding speed, and are in the range of tenths of a millimeter.

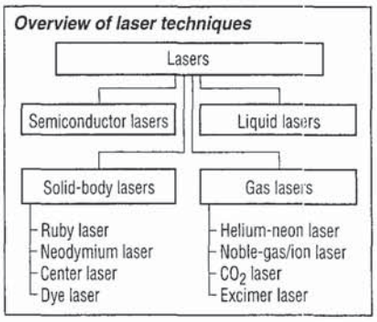
Gas laser (CO_2)
The CO_2 laser is among the most important gas-laser devices. Molecular gas serves as the active medium. Radiation emissions are in the medium infrared band, with wavelengths spread across a number of spectral ranges between 9.2 and 10.9 µm; the mean is 10.6 µm. This type of laser is generally used in continuous operation, with standard laser power ratings of between 2 and 5 kW. Laboratory units with up to 20 kW have already been installed.

Characteristics of the laser cutter
- Clean, burr-free edges,
- high dimensional/manufacturing precision (no subsequent processing necessary),
- minimal thermal and mechanical stresses on the workpiece during the cutting process,
- uncomplicated clamping devices,
- sheet metal of up to 10 mm can be cut (1 kW), rapid cutting (10 m/min with metal 1 mm thick).

Characteristics of laser welding
- High depth/width ratio (e.g. approx. 1 mm seam width at 5 mm seam depth),
- minimal base-material thermal stress results in narrow heat-affected zone (HAZ),
- minimal distortion,
- welding in protective-gas atmosphere,
- joint gaps must be virtually zero,
- welding with filler metals is possible (for bridging gaps and achieving specific effects at the weld),
- specialized clamping and equipment technology is required.

Applications in machine tool and automotive engineering
- Cutting and welding bodywork sheet metal,
- welding (joining) blanks of various thicknesses,
- welding (joining) of rotationally symmetrical parts (transmission components, tappets, automotive components),
- boring and perforation,
- surface hardening, e.g. in treating valve seats, etc.,
- providing surfaces with upgraded finishes, e.g. structural transformation around cylinder liners.

Overview of laser techniques



PETITIONER'S EXHIBIT 1002
US PATENT NO. 6,557,540

Tribology

Purpose and goals

Tribology is defined as "The study of the phenomena and mechanisms of friction, lubrication, and wear of surfaces in relative motion". Industrial application is directed toward gathering information for use in extending the service lives of products and maximizing utilization of resources. The specific activities are as follows:

- Analysis of friction and wear,
- Analysis and evaluation of tribological damage,
- Provision of technical recommendations on materials, lubricants and design (for damage control and in the design of new components and products),
- Quality assurance,
- Assistance in providing optimal performance,
- Service-life assessment,
- Development and selection of new materials and lubricants.

The complexity of the task renders a synergetic approach essential. The disciplines involved include materials science, physics, chemistry and mechanical engineering.

Definitions

Friction (DIN 50281)
Friction is physical resistance to relative motion at two or more surfaces in a state of mutual contact. The most significant physical parameters for describing friction are:
Friction force: The amount of force with which a motion is resisted.
Coefficient of friction (or friction factor): Friction force relative to normal force.
Friction power: Friction force x sliding speed.
Classification of friction:

1. According to condition of friction (type of contact),
2. According to type of motion.

Condition of friction (type of contact)
Gas friction: A gas layer completely separates the base object and the opposed body from one another, thereby assuming the entire load.
Fluid friction (hydrodynamic and hydrostatic friction): A fluid layer completely separates the base object and opposed body from one another, thereby assuming the entire load.
Combination friction: The base object and the opposed body are in mutual contact at surface peaks. The load is shared by the fluid/lubricating film and by the objects in contact.
Dry or boundary friction: The lubricating film no longer performs any support function, but residue from previously absorbed lubricants continues to exercise a tribological effect.
Solid-body friction: Direct contact between the opposed surfaces.

Types of motion
Possible types of motion contact include sliding friction, rolling friction, and combinations of the two.

In many cases the effects which friction produces in machine components are undesirable, as there are negative consequences for energy consumption and/or associated temperature increases and/or changes to the material. In other cases, friction can make a necessary contribution to proper operation. This is the case with self-locking transmission devices, where the lubricant must furnish a specific coefficient of friction, and in some types of clutches in which defined levels of friction are also required.

Tribological concepts (DIN 50323)
Tribology embraces the science and associated technology devoted to the interaction of surfaces in mutually opposed states of motion. It focuses on the entire range of friction, wear and lubrication, and also includes the effects at the contact surfaces of solids as well as those between solids and gases.

Tribo-technology (DIN 50323)
This branch is devoted to the actual technical application of tribology.

Tribological stress (DIN 50320)
The stress which results at a solid body

PETITIONER'S EXHIBIT 1002
US PATENT NO. 6,557,540

from contact with, and the relative motion of, an opposed body in solid, fluid or gaseous form.

Tribological damage
Damage resulting from tribological stress. This contrasts with the concepts of wear and wear damage as defined in DIN 50320, which always include material erosion. Here, the term "tribological damage" extends to embrace both numerous tribologically induced changes to the material's surface, as well as reductions in operational efficacy which according to DIN 50320 are not regarded as wear.

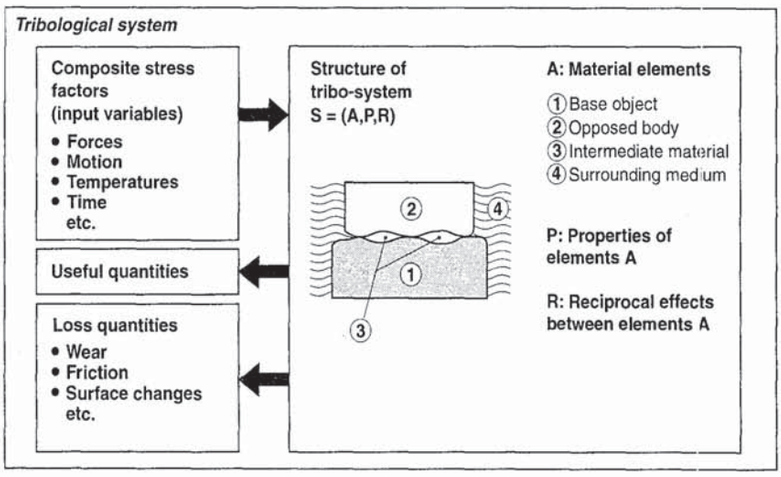
Wear (DIN 50320)
Progressive loss of material from the surface of a solid body, caused by tribological stress. Wear is characterized by the presence of abraded particles, as well as changes in both the material and structure of the surface which is exposed to tribological stress. This type of wear is generally undesirable, and impairs functionality (exception: "running-in" processes). Thus any such procedures which enhance the object's operational value are not considered as wear.

Tribological system

Wear can be regarded as a system characteristic. There exists no specific material value for "wear-resistance" as such, corresponding to, say, tensile strength in materials science. The tribological system for the contact surfaces which are the focus of the present discussion consists of:
- The material "A elements": base object, opposed body, intermediate material and surrounding medium (see illustration),
- The properties P of the elements A,
- The reciprocal influence R between the elements A.

The elements' properties and their reciprocal effects form the structure of the tribological system. As the composite stress factor (comprising forces, motion, temperature) acts upon this structure, it is transformed into useful quantities and loss quantities. The latter include friction and wear.

Because tribological stresses are surface stresses, the previously mentioned P properties must also be viewed as surface characteristics. In technical applications, there frequently exists a substantial discrepancy between the material values measured for the base material and those actually found upon examination of the surfaces. Manufacturing procedures, cleaning processes, and the operating environment can all cause changes in the surface layer, provoking attendant variations in the tribological response of the material.



PETITIONER'S EXHIBIT 1002
US PATENT NO. 6,557,540

Types of wear

Wear processes can be classified according to the type of stress and the materials involved (system structure), a classification from which the following types of wear emerge (DIN 50320):

System structure
Solid body/solid body:
Sliding → Sliding wear,
Rolling → Rolling wear,
Oscillation → Vibration wear.

System structure
Solid body/liquid:
Flow/oscillation → cavitation erosion

Manifestations of wear

The manifestations of wear as defined by DIN 50 320 apply to the surface changes resulting from abrasion, as well as to the type and shape of the resulting particles.

Wear mechanisms

Adhesion
Formation and separation of (atomic) surface bonds.

There is a transfer of material when the separation deviates from the original boundary between the base object and the opposed body.

The adhesion process starts at the molecular level, but can expand until damage on a massive scale occurs (seizing).

Abrasion
Scraping stress and microscopic scraping action, performed by the base object, the opposed body, reaction products or solid particles in the intermediate medium.

Surface fatigue
Alternating tribological loads (e.g. impact, rolling, sliding stress, cavitation) cause mechanical stresses. The resulting fissures lead to material separation (separation of wear particles).

Tribo-chemical reactions
Reaction of the base and/or opposed object with the intermediate material (and surrounding medium), caused by tribological stress.

Wear quantities

Rates of wear are defined by the so-called wear quantites. These provide direct or indirect indices of the variations in the shape or in the mass of a body which are traceable to wear (definitions based on DIN 50 321).

Coefficient of wear
The quantities by which wear is defined can only be indicated as system-specific quantities.

The wear coefficient k facilitates comparison of wear rates at varying surface pressures and speeds:

$$k = W_v/(F \cdot s) \text{ in } mm^3/(N \cdot m)$$

F Force,
W_v Volumetric wear,
s Sliding distance.

Tribological damage analysis

In cases where operation of a component results in damage or changes of a kind which could be expected to affect the component's functional integrity, DIN 50320 indicates that all stresses and characteristics occurring at the points of tribological contact should be investigated (DIN 50320, Appendix A).

The topographical and material analysis of tribological contact (base object, opposed body, intermediate material) provides information on the mechanisms causing the damage and/or wear (adhesion, abrasion, surface fatigue, tribochemical reaction). These investigations also provide data on accompanying phenomena and on changes in the lubricant.

The analysis must be based on the following information:
– surface structure,
– material composition of the surface,
– microstructure,

PETITIONER'S EXHIBIT 1002
US PATENT NO. 6,557,540

-- microhardness,
-- intrinsic tension,
-- material composition and chemical/physical changes in the lubricant.

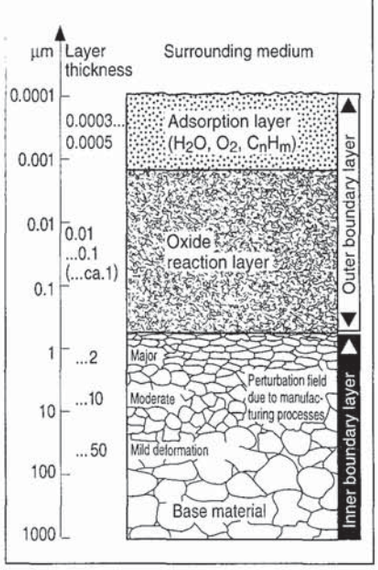
Tribological test procedures

DIN 50 322 divides wear testing into 6 categories:
Category I: Operational testing.
Category II: Test-stand procedure with complete machine.
Category III: Test-stand procedure with assembly or entire unit.
Category IV: Testing with unmodified component or reduced assembly.
Category V: Simulated operational stress with test specimens.
Category VI: Model test with simple test specimens.
The original production assembly is employed for testing according to Categories I through III, while the structure of the system is modified substantially from Category IV onward. It is highly advisable to integrate the tribological examinations of essential and safety-related products into a tribological test series:
- Model testing (e.g. pin and sphere, plate for sliding and vibration wear),
- Component testing,
- Product testing.

Model tests (with simple test specimens), although frequently employed in basic research, are no longer used for examining complex tribological systems. Of the various elements in the sequence of tribological tests, it is examination of the actual product itself that provides the most reliable information. Modern research procedures (such as radio-nuclide testing) make it possible to garner precise data on wear as a function of composite stress.

For radio-nuclide testing (RNT), the parts to be examined are marked radioactively. The abraded particles can then be detected "on-line" by gamma-ray measurement.

Material layers subject to tribological stress at surface



Inhibiting wear

Variations in design, materials and lubricants can all be employed to improve tribological properties.

Design

The design options include:
- Improving the surface topography,
- Reduction of surface pressures by raising the contact-surface ratio,
- Surface reinforcement,
- Improving lubrication efficiency.

Material

The materials options include:
- Skin-layer hardening,
- Skin-layer remelting,
- Surface-layer remelt alloying,
- Thermochemical processes,
- Electrical and chemical plating,
- Resurface welding,
- Thermal spraying,
- Metal coating,
- PVD/CVD layers (physical/chemical vapor deposition, e.g., TiN, TiC),
- Ion-beam treatment (e.g. ion implantation, ion-beam mixing, transition-layer mixing and ion-beam supported coating),

PETITIONER'S EXHIBIT 1002
US PATENT NO. 6,557,540

- Diamond-like carbon coatings (metallic),
- Anti-friction paints,
- Penetration coatings (soft metals prevent high local surface pressures).

There exist a multiplicity of surface treatment and coating processes. The process parameters can frequently be adjusted to focus on specific kinds of wear. The result is a wide potential field of options for applying tribology to assist products in meeting numerous requirements.

Lubricants

In many cases, selection of the appropriate lubricant (P. 230) and optimal lubrication-system design will exercise a dramatic effect on the tribological properties – the potential is frequently greater than that represented by a change in materials. The choice of lubricant is the initial response when dealing with unsatisfactory operating characteristics.

Lubricity

Lubricity testing is based on specially defined wear parameters. The test results provide a relative index of the efficiency of fluids as separating media in defined tribological systems. In evaluations under otherwise identical conditions, a fluid displays a higher lubricity than another when it produces relative reductions in wear between the opposed elements in the tribological system and/or lower generation of friction energy (DIN/ISO 12 156).

It is important to distinguish between lubricity and viscosity.

Descriptions and specific numerical data on lubricity are derived from product, component and model wear testing with specifically defined stress and load parameters. The results are indicated in specific test data for wear.

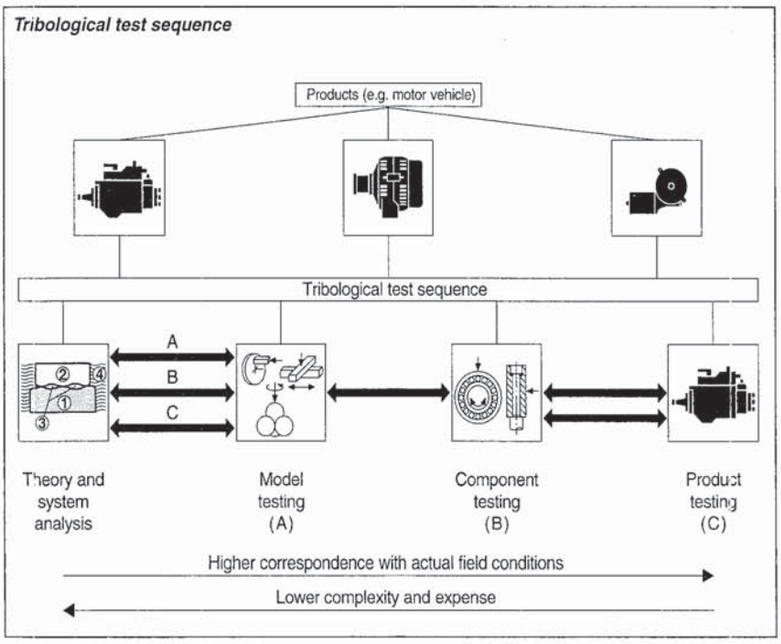
The results of this type of testing are valid only for the object tribological system.

In many products the separating element in the tribological system is also a flow medium, as in hydraulic and fuel-injection systems.

The lubricity level of such a fluid must suffice to ensure reliable operation and a long service life.

Special additives can be employed to enhance lubricity.

Tribological test sequence



PETITIONER'S EXHIBIT 1002
US PATENT NO. 6,557,540

Road-going vehicle requirements

Driveability

The vehicle must be capable of effecting the transition from a stationary to a mobile state. Once in motion, it must be able to ascend gradients and accelerate to the desired cruising speed with a reasonable degree of alacrity. With a given power P, ideal correspondence with these requirements is achieved when force M and the engine speed n can be varied according to the formula $P = M \cdot n$. Under these conditions, the limits on the potential field of operation are defined by $P_{Nominal}$, resulting in an inverse relationship between available force and vehicle speed (limit curve defined by tractive-force hyperbola).

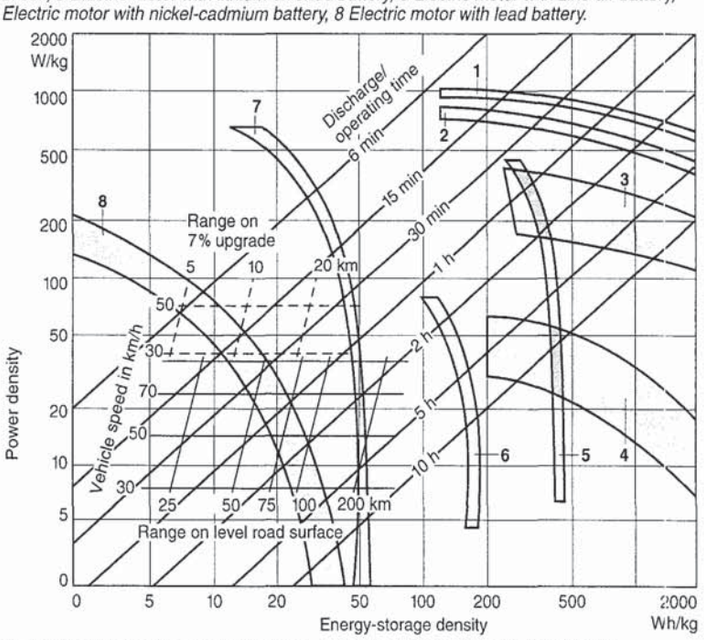
Power density and storage density

Both the power density (W/kg) and the energy-storage density (Wh/kg) of the combined engine/energy-storage system must be high if the size of the vehicle – and with it the mass to be accelerated – are to be maintained at a modest level. Low density factors for power and energy storage would increase vehicle size and mass, with attendant escalations in the power and energy consumption which would be needed to achieve the desired performance (acceleration, speed).

Discharge or operating time of the energy-storage device

The vehicle's operating time – and thus the operating range which can be covered before the energy-storage device must be replenished (renewed/refilled/recharged) – is a function of the energy-storage density, the power requirement, and the vehicle weight; the latter, in turn, is influenced by the power-to-weight ratio of the drive system.

Power and energy-storage densities for various propulsion concepts *(Engine/motor and storage unit).*[1]
1 Gas turbine, 2 Internal-combustion engine, 3 External-combustion engine, 4 Electric motor with fuel cell, 5 Electric motor with lithium-chloride battery, 6 Electric motor with zinc-air battery, 7 Electric motor with nickel-cadmium battery, 8 Electric motor with lead battery.

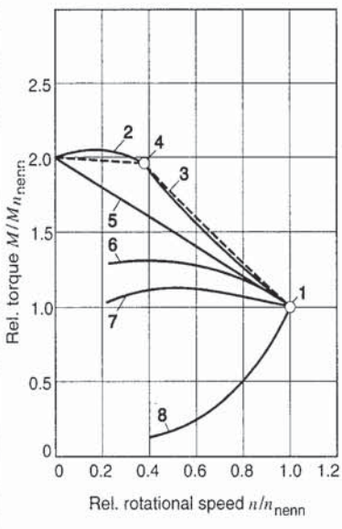


[1]) From "The Automobile and Air Pollution", US Dep. of Commerce (Morsebericht); Mahle "Kolben-Handbuch" (Piston Handbook).

PETITIONER'S EXHIBIT 1002
US PATENT NO. 6,557,540

The drive and energy-storage configuration employed for a specific application determines the relationship between power density/energy-storage density and operating time; it also exerts a decisive influence on the shape of the torque curve. Favorable power-to-weight ratios combine with high energy-storage densities (period of operation per tank of fuel) to make internal-combustion engines particularly suitable for vehicular applications. However, the torque curves provided by the standard piston powerplants (diesel and spark-ignition engines) are less satisfactory. They thus need some form of transmission unit for both the transfer and the conversion of torque. The unit must be capable of transmitting torque in the slip range (for starting off) while incorporating various torque-conversion ratios (for ascending gradients and selecting different speed ranges).

Relative torques for various power units
1 Reference point: Gas-turbine base point, Piston engine n_{max}, 2 Steam engine, 3 Electric motor, 4 Limit curve for max. pressure/max. current, 5 Dual-shaft gas turbine, 6 Gasoline (SI) engine, 7 Diesel engine, 8 Single-shaft gas turbine.



Electric and steam-driven powerplants also need a transmission due to the limitations imposed by the respective maxima for current and steam pressure.

In addition to fulfilling the basic requirements enumerated above, the powerplant and energy-storage system must also meet the following demands:

Economic efficiency, characterized by minimal fuel consumption, low manufacturing and maintenance costs, long service life;

Environmental compatibility, with low emissions levels for both pollutants and noise, sparing use of raw materials;

Flexibility in operation, including good starting from −30 °C to +50 °C, operation unaffected by climate and altitude, good driveoff, acceleration and braking characteristics.

Internal-combustion (IC) engines are thus the most favorable option for independent self-contained vehicles, whereby the priority assigned to the individual factors in the above list will vary according to application. Examples:

Passenger cars: High power density, low exhaust and noise emissions, low manufacturing costs,

Trucks and buses: Maximum economy, long service life, and conformity with all emissions requirements.

Special drive systems, such as those relying exclusively on electric motors, or hybrids (dual-system buses, P. 533 ff.) can represent the best, or indeed only, option for special applications and/or under certain operating conditions.

Basic requirements for fuels

Engines featuring external combustion place the least exacting demands on fuel quality, as their combustion and working gases are not identical and remain isolated from each other. In contrast, the fuel used in internal-combustion engines must burn rapidly and virtually without residue.

PETITIONER'S EXHIBIT 1002
US PATENT NO. 6,557,540

Determining fuel consumption

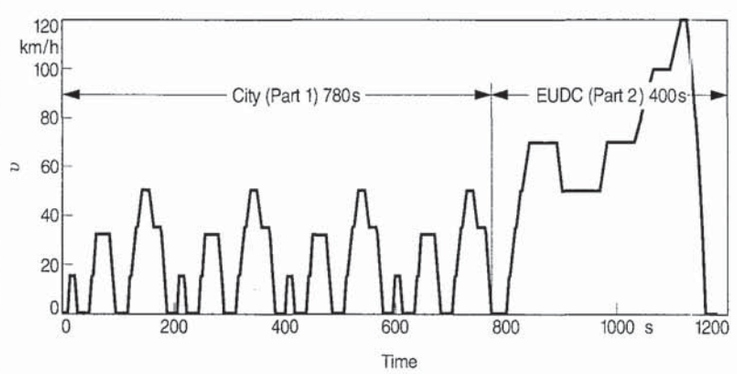
The New European Driving Cycle (NEDC, 93/116/EEC) is a cycle run on a dynamometer to ascertain fuel consumption. It consists of four similarly weighted urban cycles each lasting 195 s and an extra-urban cycle lasting 400 s. The exhaust gas is collected in a sample bag and its components subsequently analyzed. CO, HC and CO_2 are factored into the calculations in accordance with the carbon analysis.

The CO_2 content of the exhaust gas is proportional to the fuel consumption. It can therefore be used as an indicator to gauge the vehicle's fuel consumption (diesel or gasoline, as appropriate).

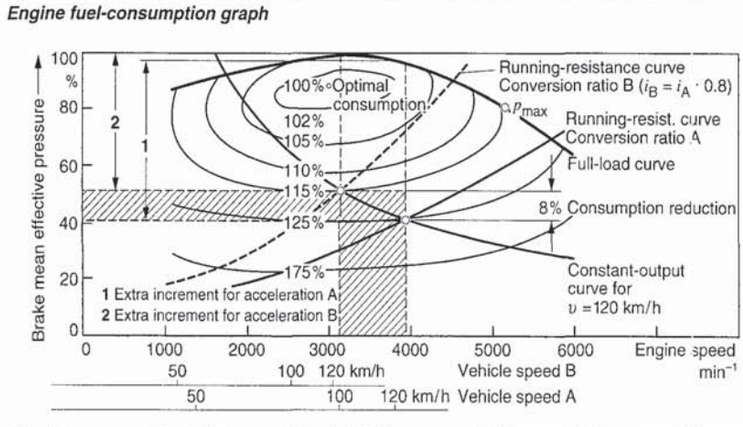
The test mass specified for the vehicle equals the vehicle's empty mass plus a payload of 100 kg. The vehicle mass has to be simulated by finite balanced inertia masses on the dynamometer, so an inertia-mass class is assigned to the vehicle test mass.

Current legislation (EU 2) permits the engine to be started 40 s before testing commences $t = t_0$. This lead-in time will not be allowed under the more stringent EU 3 requirements.

New European Driving Cycle NEDC (93/116/EEC)

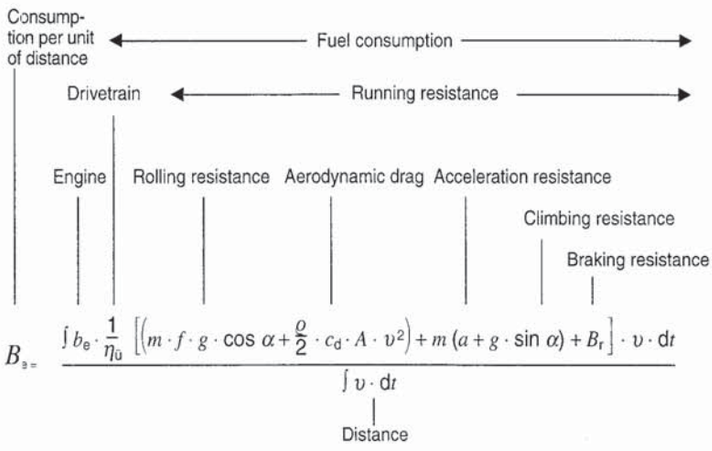


Engine fuel-consumption graph



PETITIONER'S EXHIBIT 1002
US PATENT NO. 6,557,540

Effect of vehicle design on fuel consumption



Symbol		Unit
B_e	Consumption per unit of distance	g/m
$\eta_ü$	Transmission efficiency of drivetrain	–
m	Vehicle mass	kg
f	Coefficient of rolling resistance	–
g	Gravitational acceleration	m/s²
α	Angle of ascent	°
ϱ	Air density	kg/m³
c_d	Drag coefficient	–
A	Frontal area	m²
v	Vehicle speed	m/s
a	Acceleration	m/s²
B_r	Braking resistance	N
t	Time	s
b_e	Specific fuel consumption	g/kWh

The consumption equation distinguishes between three distinct groups of factors:
– Engine,
– Transmission, and
– External resistance factors.

Transmission (gearbox)

The influence of the gearbox is determined by both the power-transmission losses and the transmission (gear) ratios selected for the application. The former should be kept as low as possible; the latter determine the correspondence between vehicle speed and specific points on the engine's fuel-consumption curve.

"Long" (wide-ratio) gearing will generally move a specific operating state onto a point on the curve corresponding to lower fuel consumption (see illustration), albeit at the expense of reduced acceleration.

External resistance factors

Outside resistance to motion can be counteracted by measures such as weight reduction, improved aerocynamics and lower rolling resistance.

On an average production vehicle, 10% reductions in weight, drag and rolling resistance result in fuel-economy improvements of roughly 6%, 3%, and 2%, respectively.

The cited formula distinguishes between acceleration resistance and braking resistance, thereby illustrating with particular clarity the fact that the increased fuel consumption associated with acceleration largely stems from subsequent application of the brakes. If the brakes are not applied, then the vehicle's kinetic energy is exploited to impel it forward (retardation = negative acceleration), with attendant reductions in overall fuel consumption.

PETITIONER'S EXHIBIT 1002
US PATENT NO. 6,557,540

Motor-vehicle dynamics

Dynamics of linear motion

Symbol		Unit
A	Largest cross-section of vehicle[1])	m²
a	Acceleration, braking (deceleration)	m/s²
c_w	Drag coefficient	–
F	Motive force	N
F_{cf}	Centrifugal force	N
F_L	Aerodynamic drag	N
F_{Ro}	Rolling resistance	N
F_{St}	Climbing resistance	N
F_w	Running resistance	N
f	Coefficient of rolling resistance	–
G	Weight = $m \cdot g$	N
G_B	Sum of wheel forces on driven or braked wheels	N
g	Gravitational acceleration = 9.81 m/s² ≈ 10m/s²	m/s²

Symbol		Unit
i	Gear or transmission ratio between engine and drive wheels	–
M	Engine torque	N · m
m	Vehicle mass (weight)	kg
n	Engine speed	min⁻¹
P	Power	W
P_w	Motive power	W
p	Gradient (= 100 tan α)	%
r	Dynamic radius of tire	m
s	Distance traveled	m
t	Time	s
v	Vehicle speed	m/s
v_0	Headwind speed	m/s
W	Work	J
α	Gradient angle	°
μ_r	Coefficient of static friction	–

Additional symbols and units in text.

Total running resistance

The running resistance is calculated as:

$$F_W = F_{Ro} + F_L + F_{St}$$

Running-resistance power

The power which must be transmitted through the drive wheels to overcome running resistance is:

$$P_W = F_W \cdot v$$

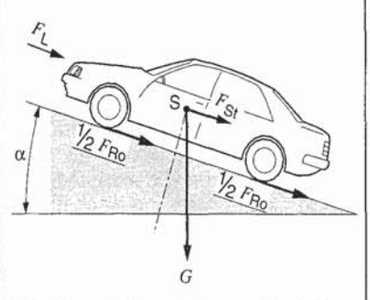
or

$$P_W = \frac{F_W \cdot v}{3600}$$

with P_W in kW, F_W in N, v in km/h.

[1]) On passenger cars $A \approx 0.9 \times$ Track $\times$ Height.

Running resistance



Rolling resistance

The rolling resistance F_{Ro} is the product of deformation processes which occur at the contact patch between tire and road surface.

$$F_{Ro} = f \cdot G = f \cdot m \cdot g$$

An approximate calculation of the rolling resistance can be made using the coefficients provided in the following table and in the diagram on page 339.

The increase in the coefficient of rolling resistance f is directly proportional to the level of deformation, and inversely proportional to the radius of the tire. The coefficient will thus increase in response to

Road surface	Coefficient of rolling resistance f
Pneumatic car tires on	
Large sett pavement	0.015
Small sett pavement	0.015
Concrete, asphalt	0.013
Rolled gravel	0.02
Tarmacadam	0.025
Unpaved road	0.05
Field	0.1...0.35
Pneumatic truck tires on concrete, asphalt	0.006...0.01
Strake wheels in field	0.14...0.24
Track-type tractor in field	0.07...0.12
Wheel on rail	0.001...0.002

PETITIONER'S EXHIBIT 1002
US PATENT NO. 6,557,540

greater loads, higher speeds and lower tire pressure.

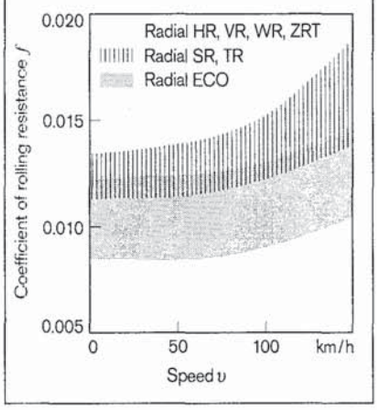
During cornering, the rolling resistance is augmented by the

cornering resistance

$F_K = f_K \cdot G$

The coefficient of cornering resistance f_K is a function of vehicle speed, curve radius, suspension geometry, tires, tire pressure, and the vehicle's response under lateral acceleration.

Rolling resistance of radial car tires on smooth, level road surfaces under normal load and at correct tire pressure



Aerodynamic drag

Aerodynamic drag is calculated as:

$F_L = 0.5 \cdot \varrho \cdot c_d \cdot A \, (\upsilon + \upsilon_0)^2$

With υ in km/h:

$F_L = 0.0386 \cdot \varrho \cdot c_d \cdot A \cdot (\upsilon + \upsilon_0)^2$

Air density ϱ
(at 200 m altitude ϱ = 1.202 kg/m³),
Drag coefficient c_d PP. 37 and 340.

Aerodynamic drag in kW

$P_L = F_L \cdot \upsilon = 0.5 \cdot \varrho \cdot c_d \cdot A \cdot \upsilon \cdot (\upsilon + \upsilon_0)^2$

or

$P_L = 12.9 \cdot 10^{-6} \cdot c_d \cdot A \cdot \upsilon \cdot (\upsilon + \upsilon_0)^2$

with P_L in kW, F_L in N, υ and υ_0 in km/h, A in m², ϱ = 1.202 kg/m³.

Empirical determination of coefficients for aerodynamic drag and rolling resistance

Allow vehicle to coast down in neutral under windless conditions on a level road surface. The time that elapses while the vehicle coasts down by a specific increment of speed is measured from two initial velocities, υ_1 (high speed) and υ_2 (low speed). This information is used to calculate the mean deceleration rates a_1 and a_2. See following table for formulas and example.

The example is based on a vehicle weighing m = 1450 kg with a cross section A = 2.2 m².

The method is suitable for application at vehicle speeds of less than 100 km/h.

	1st Trial (high speed)	2nd Trial (low speed)
Initial velocity Terminal velocity Interval between υ_a and υ_b	υ_{a1} = 60 km/h υ_{b1} = 55 km/h t_1 = 6.5 s	υ_{a2} = 15 km/h υ_{b2} = 10 km/h t_2 = 10.5 s
Mean velocity	$\upsilon_1 = \frac{\upsilon_{a1} + \upsilon_{b1}}{2} = 57.5$ km/h	$\upsilon_2 = \frac{\upsilon_{a2} + \upsilon_{b2}}{2} = 12.5$ km/h
Mean deceleration	$a_1 = \frac{\upsilon_{a1} - \upsilon_{b1}}{t_1} = 0.77 \frac{\text{km/h}}{\text{s}}$	$a_2 = \frac{\upsilon_{a2} - \upsilon_{b2}}{t_2} = 0.48 \frac{\text{km/h}}{\text{s}}$
Drag coefficient	$c_d = \frac{6\,m \cdot (a_1 - a_2)}{A \cdot (\upsilon_1^2 - \upsilon_2^2)} = 0.36$	
Coefficient of rolling resistance	$f = \frac{28.2\,(a_2 \cdot \upsilon_1^2 - a_1 \cdot \upsilon_2^2)}{10^3 \cdot (\upsilon_1^2 - \upsilon_2^2)} = 0.013$	

PETITIONER'S EXHIBIT 1002
US PATENT NO. 6,557,540

Drag coefficient and associated power requirements for various body configurations

		Drag coefficient	Drag power in kW, average values for A = 2 m² at various speeds[1])			
		c_d	40 km/h	80 km/h	120 km/h	160 km/h
	Open convertible	0.5...0.7	1	7.9	27	63
	Station wagon (2-box)	0.5...0.6	0.91	7.2	24	58
	Conventional form (3-box)	0.4...0.55	0.78	6.3	21	50
	Wedge shape, headlamps and bumpers integrated into body, wheels covered, underbody covered, optimized flow of cooling air.	0.3...0.4	0.58	4.6	16	37
	Headlamps and all wheels enclosed within body, underbody covered	0.2...0.25	0.37	3.0	10	24
	Reversed wedge shape (minimal cross-section at tail)	0.23	0.38	3.0	10	24
	Optimum streamlining	0.15...0.20	0.29	2.3	7.8	18
Trucks, truck-trailer combinations		0.8...1.5	–	–	–	–
Motorcycles		0.6...0.7	–	–	–	–
Buses		0.6...0.7	–	–	–	–
Streamlined buses		0.3...0.4	–	–	–	–

[1]) No headwind ($v_0 = 0$).

PETITIONER'S EXHIBIT 1002
US PATENT NO. 6,557,540

Climbing resistance and downgrade force

Climbing resistance (F_{St} with positive operational sign) and downgrade force (F_{St} with negative operational sign) are calculated as:

$$F_{St} = G \cdot \sin \alpha$$
$$= m \cdot g \cdot \sin \alpha$$

or, for a working approximation:

$$F_{St} \approx 0.01 \cdot m \cdot g \cdot p$$

valid for gradients up to $p \leq 20\%$, as $\sin \alpha \approx \tan \alpha$ at small angles (less than 2% error).

Climbing power is calculated as:

$$P_{St} = F_{St} \cdot v$$

with P_{St} in kW, F_{St} in N, v in km/h:

$$P_{St} = \frac{F_{St} \cdot v}{3600} = \frac{m \cdot g \cdot v \cdot \sin \alpha}{3600}$$

or, for a working approximation:

$$P_{St} \approx \frac{m \cdot g \cdot p \cdot v}{360{,}000}$$

The gradient is:

$$p = (h/l) \cdot 100\ \% \text{ or}$$
$$p = (\tan \alpha) \cdot 100\ \%$$

with h as the height of the projected distance l. In English-speaking countries, the *gradient* is calculated as follows:

Conversion:

Gradient 1 in $100/p$

Example: "1 in 2".

Gradient angle α	Incline p %	Incline *Gradient*	Climbing resistance at m = 1000 kg N
45°	100	1 in 1	6500
40°	90		6000
35°	80		5500
30°	70	1 in 1.5	5000
25°	60		4500
20°	50	1 in 2	4000
15°	40	1 in 2.5	3500
10°	30	1 in 3	3000
5°	20	1 in 4	2500
0°	10	1 in 5	2000
		1 in 10	1500
		1 in 20	1000
	0	1 in 50	500
		1 in 100	0

Values at m = 1000 kg					
Climbing resistance F_{St} N	Climbing power P_{St} in kW at various speeds				
	20 km/h	30 km/h	40 km/h	50 km/h	60 km/h
6500	36	54	72	–	–
6000	33	50	67	–	–
5500	31	46	61	–	–
5000	28	42	56	69	–
4500	25	37	50	62	–
4000	22	33	44	56	67
3500	19	29	39	49	58
3000	17	25	33	42	50
2500	14	21	28	35	42
2000	11	17	22	28	33
1500	8.3	12	17	21	25
1000	5.6	8.3	11	14	17
500	2.3	4.2	5.6	6.9	8.3
0	0	0	0	0	0

Example: To climb a hill with a gradient of $p = 18\%$, a vehicle weighing 1500 kg will require approximately $1.5 \cdot 1700$ N = 2550 N motive force and, at v = 40 km/h, roughly $1.5 \cdot 19$ kW = 28.5 kW climbing power.

PETITIONER'S EXHIBIT 1002
US PATENT NO. 6,557,540

Motive force

The higher the engine torque M and overall transmission ratio i between engine and driven wheels, and the lower the power-transmission losses, the higher is the motive force F available at the drive wheels.

$$F = \frac{M \cdot i}{r} \cdot \eta \quad \text{or} \quad F = \frac{P \cdot \eta}{v}$$

η Drivetrain efficiency level
(longitudinally installed engine
$\eta \approx 0.88...0.92$)
(transverse engine $\eta \approx 0.91...0.95$)

The motive force F is partially consumed in overcoming the running resistance F_W. Numerically higher transmission ratios are applied to deal with the substantially increased running resistance encountered on gradients (gearbox).

Vehicle and engine speeds

$$n = \frac{60 \cdot v \cdot i}{2 \cdot \pi \cdot r}$$

or with v in km/h:

$$n = \frac{1000 \cdot v \cdot i}{2 \cdot \pi \cdot 60 \cdot r}$$

Acceleration

The surplus force $F - F_W$ accelerates the vehicle (or retards it when F_W exceeds F).

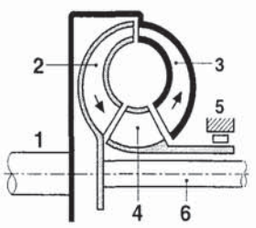
$$a = \frac{F - F_W}{k_m \cdot m} \quad \text{or} \quad a = \frac{P \cdot \eta - P_W}{v \cdot k_m \cdot m}$$

The rotational inertia coefficient k_m, compensates for the apparent increase in vehicle mass due to the rotating masses (wheels, flywheel, crankshaft, etc.).

Motive force and road speed on vehicles with automatic transmissions

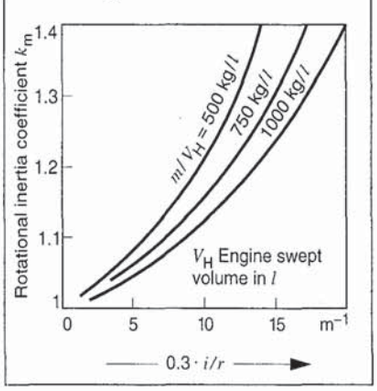
When the formula for motive force is applied to automatic transmissions with hydrodynamic torque converters or hydrodynamic clutches, the engine torque M is replaced by the torque at the converter turbine, while the rotational speed of the converter turbine is used in the formula for engine speed.

Hydrodynamic converter
1 Power, 2 Turbine, 3 Pump, 4 Stator, 5 One-way clutch, 6 Output.

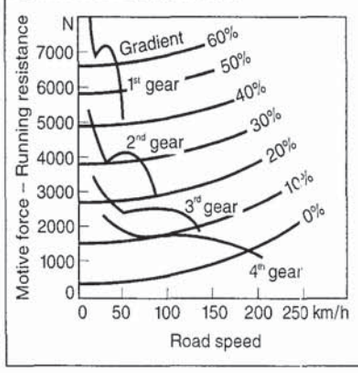


The relationship between $M_{Turb} = f(n_{Turb})$ and the engine characteristic $M_{Mot} = f(n_{Mot})$ is determined using the characteristics of the hydrodynamic converter (P. 635).

Determining the rotational inertia coefficient k_m



Running diagram for car with automatic transmission and hydrodynamic trilok converter under full throttle



PETITIONER'S EXHIBIT 1002
US PATENT NO. 6,557,540

Adhesion to road surface

Coefficients of static friction for pneumatic tires on various surfaces

Vehicle speed km/h	Tire condition	Road condition Dry	Wet: water approx. 0.2 mm	Deep rainfall: water approx. 1 mm deep	Puddles: water approx. 2 mm deep	Iced (black ice)
		Coefficient of static friction μ_{HF}				
50	new	0.85	0.65	0.55	0.5	0.1 and less
	worn[1])	1	0.5	0.4	0.25	
90	new	0.8	0.6	0.3	0.05	
	worn[1])	0.95	0.2	0.1	0.05	
130	new	0.75	0.55	0.2	0	
	worn[1])	0.9	0.2	0.1	0	

The static coefficient of friction (between the tires and the road surface), also known as the tire-road-interface friction coefficient, is determined by the vehicle's speed, the condition of the tires and the state of the road surface (see table above). The figures cited apply for concrete and tarmacadam road surfaces in good condition. The coefficients of sliding friction (with wheel locked) are usually lower than the coefficients of static friction.

Special rubber compounds providing friction coefficients of up to 1.8 are employed in racing tires.

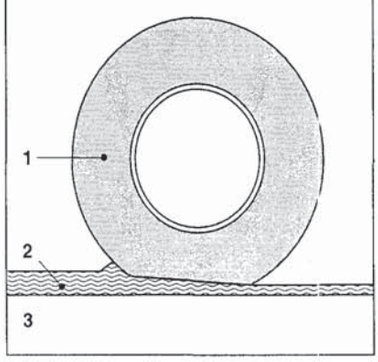
The maxima for acceleration and uphill driving, and for retardation and downhill braking, are provided on page 345.

Aquaplaning

Aquaplaning, has a particularly dramatic influence on the contact between tire and road surface. It describes the state in which a layer of water separates the tire and the (wet) road surface. The phenomenon occurs when a wedge of water forces its way underneath the tire's contact patch and lifts it from the road. The tendency to aquaplan is dependent upon such factors as the depth of the water on the road surface, the vehicle's speed, the tread pattern, the tread wear, and the load pressing the tire against the road surface. Wide tires are particularly susceptible to aquaplaning. It is not possible to steer or brake an aquaplaning vehicle, as its front wheels have ceased to rotate, meaning that neither steering inputs nor braking forces can be transmitted to the road surface.

[1]) Worn to tread depth of ≥1.6 mm (legal minimum in Germany, as per para. 36.2, StVZO (FMVSS/CUR)).

Aquaplaning
1 Tire, 2 Wedge of water, 3 Road surface.



PETITIONER'S EXHIBIT 1002
US PATENT NO. 6,557,540

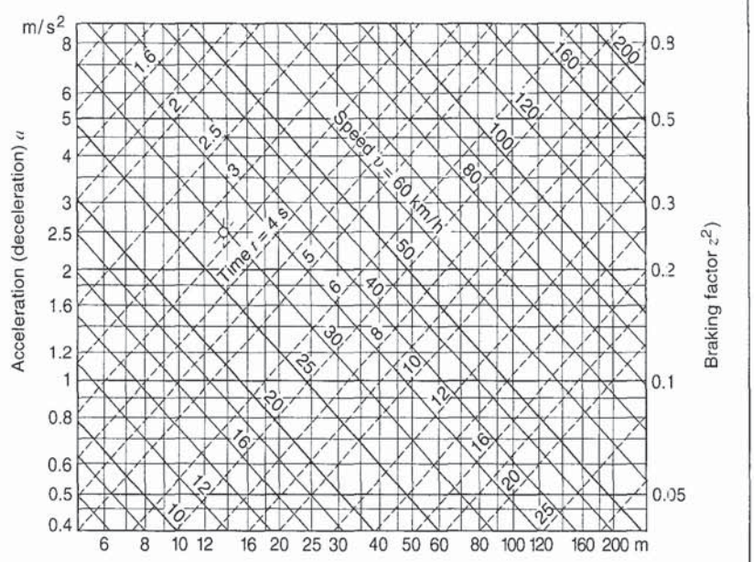
Accelerating and braking

The vehicle is regarded as accelerating or braking (decelerating) at a constant rate when a remains constant. The following equations apply to an initial or final speed of 0:

	Equations for v in m/s	Equations for v in km/h
Acceleration or braking (deceleration) in m/s²	$a = \frac{v^2}{2 \cdot s} = \frac{v}{t} = \frac{2 \cdot s}{t^2}$	$a = \frac{v^2}{26 \cdot s} = \frac{v}{3.6 \cdot t} = \frac{2 \cdot s}{t^2}$
Accelerating or braking time in s	$t = \frac{v}{a} = \frac{2 \cdot s}{v} = \sqrt{\frac{2 \cdot s}{a}}$	$t = \frac{v}{3.6 \cdot a} = \frac{7.2 \cdot s}{v} = \sqrt{\frac{2 \cdot s}{a}}$
Accelerating or braking distance[1] in m	$s = \frac{v^2}{2 \cdot a} = \frac{v \cdot t}{2} = \frac{a \cdot t^2}{2}$	$s = \frac{v^2}{26 \cdot a} = \frac{v \cdot t}{7.2} = \frac{a \cdot t^2}{2}$

Stopping distance, P. 346.
Symbols and units, P. 15.

Constant rates of acceleration and deceleration



Each point on the graph represents a particular relationship between v, a or z[2]), s and t. Two values must be available for all values to be determined.
Given: Vehicle speed v = 30 km/h, braking distance s = 13.5 m.
Determined: Mean deceleration a = 2.5 m/s², retardation z = 0.25, Braking time t = 3.3 s.

---

[1]) If final speed v_2 is not 0, braking distance $s = v_1 \cdot t - at^2/2$ at v_1 in m/s.
[2]) Deceleration rate relative to 1 g.

PETITIONER'S EXHIBIT 1002
US PATENT NO. 6,557,540

Maxima for acceleration and braking (deceleration)

When the motive or braking forces exerted at the vehicle's wheels reach such a magnitude that the tires are just still within their limit of adhesion (maximum adhesion is still present), the relationships between the gradient angle α, coefficient of static friction μ_{HF}[1]) and maximum acceleration or deceleration are defined as follows. The real-world figures are always somewhat lower, as all the vehicle's tires do not simultaneously exploit their maximum adhesion during each acceleration (deceleration). Electronic traction control and antilock braking systems (TCS, ABS, ESP)[2]) maintain the traction level in the vicinity of the coefficient of static friction.

k = Ratio between the load on driven or braked wheels and the total weight. All wheels driven or braked: $k = 1$. At 50% weight distribution $k = 0.5$.
Example: $k = 0.5$; $g = 10$ m/s²,
$\mu_{HF} = 0.6$; $p = 15\%$
$a_{max} = 0.5 \cdot 10 \cdot (0.6 \pm 0.15)$
Braking on upgrade (+): $a_{max} = 3.75$ m/s²,
downgrade braking (–): $a_{max} = 2.25$ m/s²

Work and power

The power required to maintain a consistent rate of acceleration (deceleration) varies according to vehicle speed. Power available for acceleration:

$$P_a = P \cdot \eta - P_W$$

where P = engine output, η = efficiency, and P_W = motive power.

Acceleration and braking (deceleration)

	Level road surface	Inclined road surface α°; $p = 100 \cdot \tan\alpha\,\%$	
Limit acceleration or deceleration a_{max} in m/s²	$a_{max} \le k \cdot g \cdot \mu_r$	$a_{max} \le k \cdot g\,(\mu_r \cos\alpha \pm \sin\alpha)$ approximation[3]): $a_{max} \le k \cdot g\,(\mu_r \pm 0.01 \cdot p)$	+ Upgrade braking or downgrade acceleration – Upgrade acceleration or downgrade braking

Achievable acceleration a_e (P_a in kW, v in km/h, m in kg)

Level road surface	Inclined road surface	
$a_e = \dfrac{3600 \cdot P_a}{k_m \cdot m \cdot v}$	$a_e = \dfrac{3600 \cdot P_a}{k_m \cdot m \cdot v} \pm g \cdot \sin\alpha$	+ Downgrade acceleration – Upgrade acceleration for $g \cdot \sin\alpha$ the approximation[3]) is $g \cdot p/100$

Work and power

	Level road surface	Inclined road surface α°; $p = 100 \cdot \tan\alpha\,\%$	
Acceleration or braking work W in J[4])	$W = k_m \cdot m \cdot a \cdot s$	$W = m \cdot s\,(k_m \cdot a \pm g \cdot \sin\alpha)$ approximation[3]): $W = m \cdot s\,(k_m \cdot a \pm g \cdot p/100)$	+ Downgrade braking or upgrade acceleration – Downgrade acceleration or upgrade braking
Acceleration or braking power at velocity v in W	$P_a = k_m \cdot m \cdot a \cdot v$	$P_a = m \cdot v\,(k_m \cdot a \pm g \cdot \sin\alpha)$ approximation[3]): $P_a = m \cdot v\,(k_m \cdot a \pm g \cdot p/100)$	v in m/s. For v in km/h, use $v/3.6$.

[1]) See P. 343 for numerical values.
[2]) ABS: antilock braking system; P. 659, 693.
TCS: traction control system; P. 606.
ESP: electronic stability program; P. 704.
[3]) Valid to approx. $p = 20\%$ (under 2% error).
[4]) J = N · m = W · s; conversions, P. 16.

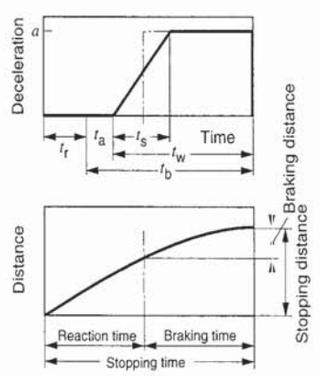
PETITIONER'S EXHIBIT 1002
US PATENT NO. 6,557,540

Stopping distance

This is the distance covered between the moment when a hazard is recognized and the time when the vehicle comes to a complete stop. It is the sum of the distances traveled during the reaction time t_r, the brake response time t_a (at constant vehicle speed υ), and the active braking time t_w. Maximum retardation a is obtained in the pressure-build-up period t_s. Alternately, half of the pressure-buildup period may be considered to be fully decelerated. The periods in which no braking occurs are combined to form the so-called lost time $t_{\upsilon z}$:

$$t_{\upsilon z} = t_r + t_a + t_s/2.$$

Deceleration and stopping distances



The upper limits on retardation are determined by the static coefficient of friction between tires and road surface (P. 343), while the lower extremes are defined by the legally required minima (P. 650).

The difference between the stopping time/distance and the braking time/distance is defined by $t_{\upsilon z}$ or $\upsilon \cdot t_{\upsilon z}$. The brake actuation time given on page 647 includes the times $t_a + t_s/2$.

Reaction time

The reaction time is the period which elapses between recognition of the object, the decision to brake and the time it takes for the foot to hit the brake pedal. The reaction time is not a fixed value: it ranges from 0.3 to 1.7 s, depend ng upon the driver and on external factors (P. 347).

Special tests are necessary to determine individual reaction patterns (such as those performed by the Medical and Psychological Institute for Traffic Safety of the German Inspection, Testing, and Certification Authorities, Stuttgart [TÜV Stuttgart, e.V.]).

	Equations for υ in m/s	Equations for υ in km/h
Stopping time t_h in s	$t_h = t_{\upsilon z} + \frac{\upsilon}{a}$	$t_h = t_{\upsilon z} + \frac{\upsilon}{3.6 \cdot a}$
Stopping distance s_h in m	$s_h = \upsilon \cdot t_{\upsilon z} + \frac{\upsilon^2}{2 \cdot a}$	$s_h = \frac{\upsilon}{3.6} t_{\upsilon z} + \frac{\upsilon^2}{26 \cdot a}$

Personal factors influencing reaction time

	Psycho-physical reaction			Muscular reaction	
Perceived object (i.e. road sign) →	Perceive	Perceive	Decide	Incipient response	Move → Actuated control element (brake pedal)
	Acuity of vision	Perception and understanding	Mental processing	Locomotor system	Personal response time

PETITIONER'S EXHIBIT 1002
US PATENT NO. 6,557,540

Effect of personal and extraneous factors on reaction time

	Reduction down to 0.3 s ←	→ **Extension up** to 1.7 s
A) Personal factors	Trained, reflexive response	Inexperienced, uncoordinated response
	Good frame of mind; optimum performance potential	Poor frame of mind, e.g. fatigue
	Highly skilled driver	Lower level of driving skill
	Youth	Advanced age
	Anticipation	Inattentiveness, distraction
	Physical and mental health	Health disorders in response groups
		Panic, alcohol
B) Extraneous factors Traffic situation	Uncomplicated, easily comprehended, predictable, familiar	Complicated, difficult to comprehend, unpredictable, rarely encountered
Type of perceived object	Explicit, conspicuous	Equivocal, inconspicuous
Location of perceived object	Within field of vision	At edge of field of vision
Nature of control element	Logical layout of mechanic controls	Poor layout of mechanical controls

Brake response and pressure build-up times

The condition of the brakes at the moment at which they are applied (e.g. wet brake disks) is one factor influencing brake response time t_a and pressure build-up time t_s; others are the designs of the actuation and force-transmission mechanism and linkage. Consult ECE R13 for legal regulations concerning t_a and t_s on tightly adjusted brakes. The applicable regulation[1]) for testing braking-system effectiveness uses figures of 0.36 s (vehicle class M_1) and 0.54 s (vehicle classes M_2, M_3, N_1...N_3) in the braking-distance equation $t_a + t_s/2$, see P. 717). The response and pressure build-up times are longer if the brake system is in poor condition. A response delay of 1 s results in a stopping distance of (see table):

[1]) EC Directive 71J320/EEC.

Deceleration a in m/s²	**Vehicle speed prior to braking in km/h**												
	10	30	50	60	70	80	90	100	120	140	160	180	200
	Distance during delay of 1 sec (no braking) in m												
	2.8	8.3	14	17	19	22	25	28	33	39	44	50	56
	Stopping distance in m												
4.4	3.7	16	36	48	62	78	96	115	160	210	270	335	405
5	3.5	15	33	44	57	71	87	105	145	190	240	300	365
5.8	3.4	14	30	40	52	65	79	94	130	170	215	265	320
7	3.3	13	28	36	46	57	70	83	110	145	185	230	275
8	3.3	13	26	34	43	53	64	76	105	135	170	205	250
9	3.2	12	25	32	40	50	60	71	95	125	155	190	225

PETITIONER'S EXHIBIT 1002
US PATENT NO. 6,557,540

Dynamics of lateral motion

Response to crosswinds

Strong crosswinds will deflect a vehicle from its lane, particularly at high speeds. Sudden crosswinds, of the kind encountered when embankments give way to open, unsheltered roads, can evoke yaw-angle changes as well as causing the vehicle to drift off course. On vehicles which are sensitive to crosswind (for reaction time see page 346), these effects are substantial and can occur before the driver has had time to react and take preventive action. It is thus essential that the relevant factors be considered in the vehicle design stage.

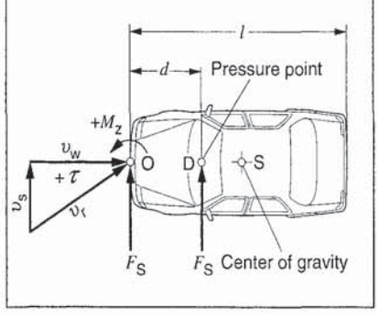
When wind impacts upon the vehicle from an oblique angle, aerodynamic drag is supplemented by a lateral component of the aerodynamic force. This force, which is distributed across the entire body, can be considered as a single force – the crosswind force – directed toward what is known as the pressure point. The actual location of the pressure point is determined by body shape and angle of impact.

The pressure point will usually be found on the front half of the vehicle, whereby it is closer to the center on conventional notchback ("three-box") bodies than on vehicles with a sloping tail section ("fast-backs" and aerodynamic designs). With the latter, the pressure point may even lie forward of the front axle in extreme cases. The pressure point on notchback bodies generally remains in a specific location; on streamlined vehicles it tends to vary according to the angle of impact. All else being equal, the greater lateral forces will occur with the notchback.

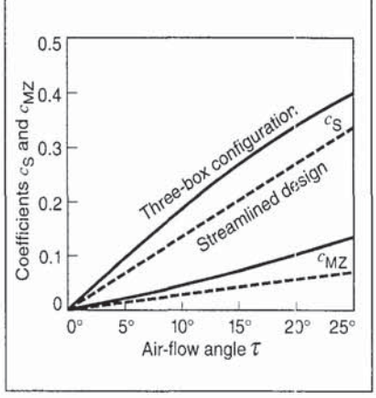
As the above implies, the pressure point will hardly provide a suitable reference point for use in illustrating the effects of crosswinds, because it has no fixed location on the vehicle. At the same time, the center of gravity varies with vehicle load. It is thus useful to select a central location on the forward section of the body as a reference point, a practice which also ensures that the data remain unaffected by the variations in the relative positions of bodywork and suspension.

When the crosswind force is specified for a reference point other than the pressure point, it must be supplemented by the crosswind moment at the pressure point in question. The standard practice in aerodynamics is to replace the forces and moments with dimensionless coefficients which remain independent of air-flow velocity. The graph shows the curves for crosswind force and the yaw coefficients for both a notchback vehicle and a fastback body style. Due to the multiplicity of possible body designs, the present investigation can only provide general refer-

Vehicle exposed to crosswind
$F_S + M_Z$ *impacting at O corresponds to* F_S *acting at D*
v_S *Crosswind velocity*
v_W *Headwind velocity*
v_r *Air-flow velocity*

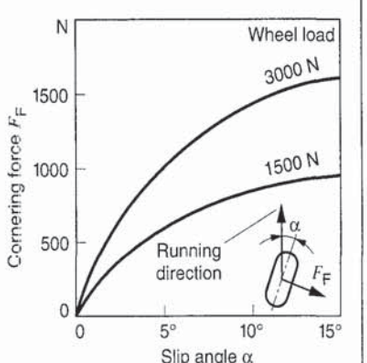


Coefficients of crosswind force c_S and yaw moment c_{MZ} relative to air-flow angle

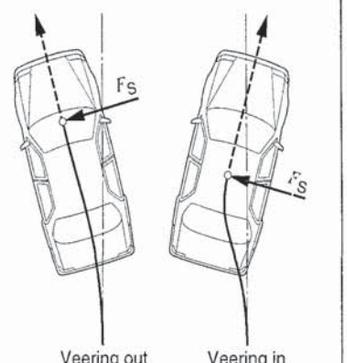


PETITIONER'S EXHIBIT 1002
US PATENT NO. 6,557,540

Cornering force as a function of wheel-slip angle



Crosswind impacting against center of gravity. Vehicle veers in or veers out



ence data; wind-tunnel measurements are essential for obtaining precise information on specific body shapes.

The following equations are applied to derive forces and moments from the coefficients:

Crosswind force $F_S = c_S \cdot \varrho \cdot (v_r^2/2) \cdot A_S$

Yaw moment $M_Z = c_{MZ} \cdot \varrho \cdot (v_r^2/2) \cdot A_S \cdot l$

ϱ Atmospheric density, v_r Resulting air-impact velocity, A_s Projected lateral surface of the vehicle, l Total length of the vehicle (in coherent units), c_S Coefficient of crosswind force, c_{MZ} Coefficient for crosswind-induced yaw.

The distance between the pressure point and the leading edge of the vehicle is calculated using

$$d = M_Z/F_S = l \cdot c_{MZ}/c_S$$

The crosswind force is resisted by the lateral cornering forces at the wheels. The degree of lateral cornering force which a pneumatic tire can provide depends upon numerous factors, such as wheel slip angle, wheel load, tire design and dimensions, tire pressure and the amount of traction afforded by the road surface.

The pneumatic tire's specific response characteristics mean that, at a constant slip angle, higher wheel loads will not evoke proportional increases in cornering forces. In the example (diagram), doubling the wheel load increases the cornering force by a factor of only 1.5...1.7. The slip angle must also be increased if the cornering force is to be doubled. This explains why the axle supporting the greater load assumes a larger slip angle than its less heavily loaded counterpart, assuming that identical ratios of lateral (side) force to tire contact force act on both axles.

When the crosswind force impacts against the center of gravity, the distribution ratio for the required cornering forces between front and rear axles is a function of the wheel-load factors, i.e. the ratio of contact force to lateral force is the same at both axles. When the center of gravity is in the forward section of the vehicle, the crosswind force causes the vehicle to "veer-out" due to the front axle's necessarily greater wheel slip angle; when the center of gravity is at the rear, the vehicle "veers-in". In both cases, the vehicle's center of gravity is deflected downwind from the original path of travel. When the crosswind ceases, the "veering-out" vehicle will continue to deviate from its original path, while the "veering-in" vehicle will return to and indeed go beyond the original line.

The crosswind's impact point, however, will rarely coincide with the center of gravity; the distance forward from the center of the vehicle depends upon the individual body shape. Thus a vehicle which responds to impact at the center of gravity

PETITIONER'S EXHIBIT 1002
US PATENT NO. 6,557,540

by veering inwards, will veer out when exposed to actual crosswinds. Due to the forward displacement of the pressure point, vehicles with a sloping rear section display a greater tendency to veer-out; they are thus more difficult to control than notchback vehicles.

Rear-mounted vertical stabilizer fins can be installed to move the pressure point rearward, toward the center of gravity. However, except in competition vehicles and other special applications, this option has to date rarely been applied.

Placing the pressure point in the immediate vicinity of the vehicle's center of gravity results in improved directional stability. Oversteer vehicles have a minimum tendency to deviate from their path of travel when the pressure point is forward of the center of gravity. On understeer vehicles, the best pressure-point location is just to the rear of the center of gravity.

Crosswind force is generally minimal relative to contact force, and the influence of non-linearity in the ratio of contact force to lateral force is limited when small lateral forces are applied – a vehicle's response to crosswinds is therefore not governed by tire properties alone. Other important factors include compliance in suspension and steering. Thus the suspension designer can also exercise a major influence on the vehicle's crosswind response characteristics.

Oversteer and understeer

Cornering forces can only be generated between a rubber tire and the road surface when the tire rolls at an angle to its longitudinal plane; that is, a certain wheel slip angle is required.

A vehicle is said to understeer when, as lateral acceleration increases, the slip angle at the front axle increases more than it does at the rear axle. The opposite applies for a vehicle which oversteers.

A vehicle will not necessarily display the same self-steering effect at all possible rates of lateral acceleration. Some vehicles always understeer or oversteer, and some display a transition from understeer to oversteer as lateral acceleration increases, while other vehicles respond in precisely the opposite manner.

References:
Barth, R.: "Windkanalmessungen an Fahrzeugmodellen und rechteckigen Körpern mit verschiedenem Seitenverhältnis bei unsymmetrischer Anströmung" (Wind Tunnel Measurements on Vehicle Models and Rectangular Bodies with Different Side Ratios under Asymmetrical Flow). Dissertation, Stuttgart Technical College, 1958.
Barth, R.: "Luftkräfte am Kraftfahrzeug" (Aerodynamic Forces Acting on Motor Vehicles). Deutsche Kraftfahrtforschung und Straßenverkehrstechnik (German Motor Vehicle Research and Traffic Engineering), Vol. 184, Düsseldorf. VDI-Verlag, 1966.
Mitschke, M.: "Dynamik der Kraftfahrzeuge" (Dynamics of Motor Vehicles). Springer-Verlag, 1972.

Cornering behavior

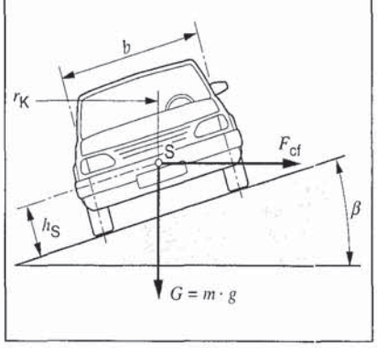
Centrifugal force in curves

$$F_{cf} = \frac{m \cdot v^2}{r_K} \text{ (P. 35)}$$

or, with v specified in km/h and r_K as the radius of the curve in m

$$F_{cf} = \frac{m \cdot v^2}{12.96 \cdot r_K}$$

Centrifugal force when cornering
b Track width in m,
h_S Height of center of gravity in m.



PETITIONER'S EXHIBIT 1002
US PATENT NO. 6,557,540

Critical speeds

The concrete example provided in the table below would apply to a vehicle with a track b = 1.5 m, height of center of gravity h_S = 0.6 m; max. adhesion coefficient μ_r = 0.8, curve radius r_K = 90 m, curve banking β = 20°.

	Flat curve	Banked curve
Speed at which the vehicle exceeds the limit of adhesion (skid)	$v \leq 11.28 \sqrt{\mu_r \cdot r_K}$ km/h	$v \leq 11.28 \sqrt{\frac{(\mu_r + \tan\beta)\, r_K}{1 - \mu_r \cdot \tan\beta}}$ km/h
Example:	≤ 96 km/h	≤ 137 km/h
Speed at which the vehicle tips	$v \geq 11.28 \sqrt{\frac{b \cdot r_K}{2 \cdot h_S}}$ km/h	$v \geq 11.28 \sqrt{\frac{\left(\frac{b}{2 \cdot h_S} + \tan\beta\right) \cdot r_K}{1 - \frac{b}{2 \cdot h_S} \cdot \tan\beta}}$ km/h
Example:	≥ 120 km/h ($\mu_r \geq 1.25$)	≥ 184 km/h ($\mu_r \geq 1.25$)

Body roll in curves

Roll axis

When cornering, the centrifugal force which concentrates around the center of gravity causes the vehicle to tilt away from the path of travel. The magnitude of this rolling motion depends upon the rates of the springs and their response to alternating compression, and upon the lever arm of the centrifugal force (distance between the roll axis and the center of gravity). The roll axis is the body's instantaneous axis of rotation relative to the road surface. Like all rigid bodies, the vehicle body consistently executes a screwing or rotating motion; this motion is supplemented by a lateral displacement along the instantaneous axis.

The higher the roll axis, i.e. the closer it is to a parallel axis through the center of gravity, the greater will be the transverse stability and the less the roll during cornering. However, this generally implies a corresponding upward displacement of the wheels, resulting in a change in track width (with negative effects on operating safety). For this reason, designs are sought which combine a high instantaneous roll center with minimal track change. The goal therefore is to place the instantaneous axes of the wheels as high as possible relative to the body, while simultaneously keeping them as far from the body as possible.

Determining the roll axis

A frequently-applied means for finding the approximate roll axis is based on determining the centers of rotation of an equivalent body motion. This body motion takes place in those two planes through the front and rear axles which are vertical relative to the road. The centers of rotation are those (hypothetical) points in the body which remain stationary during the rotation. The roll axis, in turn, is the line which connects these centers (instantaneous centers). Graphic portrayals of the instantaneous centers are based on a rule according to which the instantaneous centers of rotation of three systems in a state of relative motion lie on a common pole line.

The complexity of the operations required for a more precise definition of the spatial relationships involved in wheel motion makes it advisable to employ computers capable of carrying out calculations in matrix notation (vector algebra, linear geometry, etc.).

References:

E. v. d. Osten-Sacken: "Berechnung allgemein räumlicher, vielgliedriger Gelenkgetriebe"; Dissertation, Aachen Technical College, 1970.

G. Prigge: "Grundsätzliches der Ermittlung der Rollachse von Kraftfahrzeugen mit räumlichen Radführungen"; Dissertation, Braunschweig Technical University, 1972.

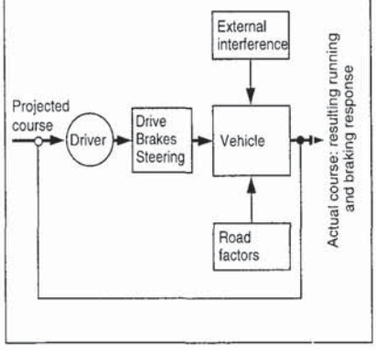
PETITIONER'S EXHIBIT 1002
US PATENT NO. 6,557,540

ISO procedures for evaluating vehicle handling

The science devoted to studying the dynamics of vehicle handling generally defines its subject as the overall behavior of the entire system represented by "driver + vehicle + environment". As the first link in the chain, the driver makes judgements on the vehicle's handling qualities based on the sum of diverse subjective impressions. On the other hand, handling data derived from specific driving maneuvers executed without driver input (open-loop operation) provide an objective description of the vehicle's handling qualities. The driver, who up to the present day still cannot be defined accurately in terms of behavior, is replaced in these tests by a specific, objectively quantifiable interference factor. The resulting vehicular response can then be analyzed and discussed.

Standardized versions of the driving maneuvers in the list (performed on a dry road surface) below have either already been defined by the ISO or are under consideration; they serve as recognized standard procedures for vehicular evaluation [1], [2]:
- Steady-state skidpad [3],
- Transient response [4], [5], [6],
- Braking during cornering [7],
- Crosswind sensitivity,
- Straight-running stability, and
- Reaction to throttle change on skidpad.

"Driver-vehicle-environment" synergism represented as a closed-loop control system

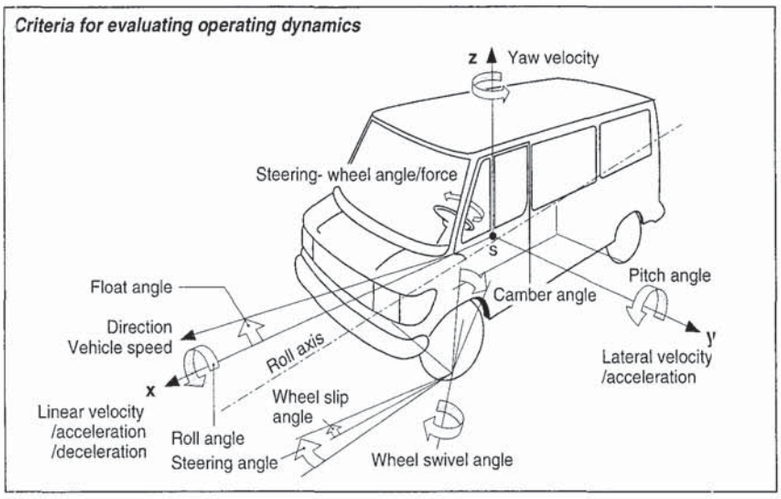


To date, it has still not been possible to arrive at comprehensive objective definitions for the dynamic characteristics associated with closed-loop operation, as adequate data on the precise control characteristics of the human element are still unavailable.

Test quantities

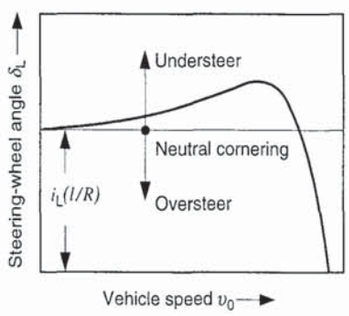
The main criteria employed in evaluating vehicle dynamics are:
- Steering-wheel angle,
- Lateral acceleration,
- Longitudinal acceleration and deceleration,
- Yaw speed,
- Float and roll angles.

Criteria for evaluating operating dynamics



PETITIONER'S EXHIBIT 1002
US PATENT NO. 6,557,540

Definitions of attitude in steady-state cornering (according to Mitschke [10])
i_L Steering ratio, l Wheelbase, R (= const.) Cornering radius, $i_L(l/R)$ Ackermann effect.



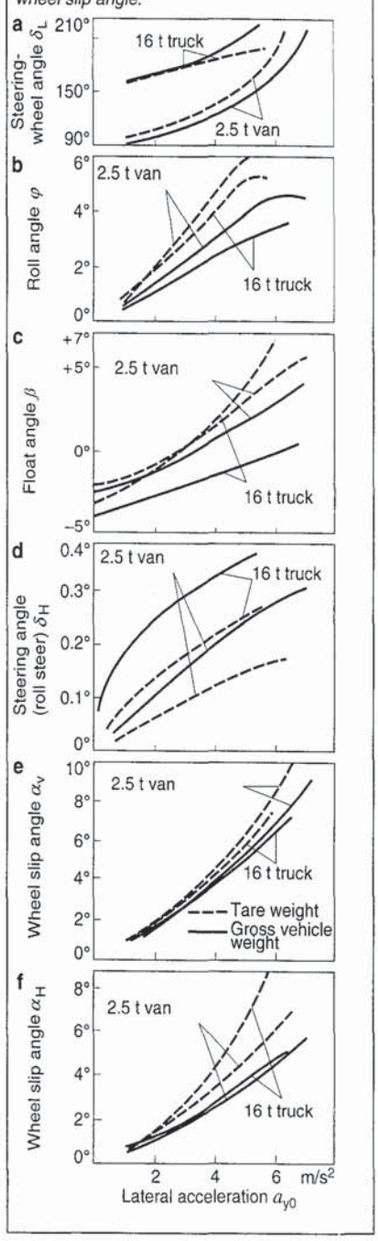
Additional data are employed to verify and confirm the previously derived information on specific points of vehicle handling:
– Linear and lateral velocity,
– Steering angles at front and rear wheels,
– Slip angles at all wheels,
– Camber and pitch angles,
– Steering-wheel force.

Steady-state skidpad

The most important data to be derived from steady-state skidpad testing are the maximum lateral acceleration, and the manner in which individual dynamic parameters respond to the variations in lateral acceleration which occur up to the limit. This information is employed in evaluating the vehicle's self-steering response [2], [3]. Compliance in both the steering system and the suspension is represented in the current standard definition of steering response, which employs the terms "oversteer", "understeer" and "neutral steering". Several dynamic factors and their derivatives are considered in conjunction with lateral acceleration in describing vehicle handling, examples being steering-wheel angle, roll angle and float angle. Other significant vehicle parameters are steering angle and slip angle.

In the following, a light utility van (similar to a passenger car) and a heavy truck are used to provide examples of the results gathered on a dry surface.

Steady-state skidpad *(42 m radius)*
a) Steering-wheel angle, b) Roll angle, c) Float angle, d) Rear-axle steering angle (roll steer), e) Front-wheel slip angle, f) Rear-wheel slip angle.



PETITIONER'S EXHIBIT 1002
US PATENT NO. 6,557,540

Steering-wheel angle
As small utility vehicles are fitted with tires similar to those used in passenger cars, and are also equipped with relatively high-power engines, they achieve high rates of lateral acceleration. Both vehicle types understeer.

Roll angle
The degree of self-steering which prevails at the axles is largely determined by the roll angle. Higher loads result in more pronounced roll angles due to the greater vehicle mass and the attendant increase in effective centrifugal force.

Float angle
The float angle encountered at high rates of lateral acceleration is regarded as an index of controllability, in other words the vehicle's response to driver input. High absolute figures or fluctuations in float angle are regarded as particularly undesirable [8].

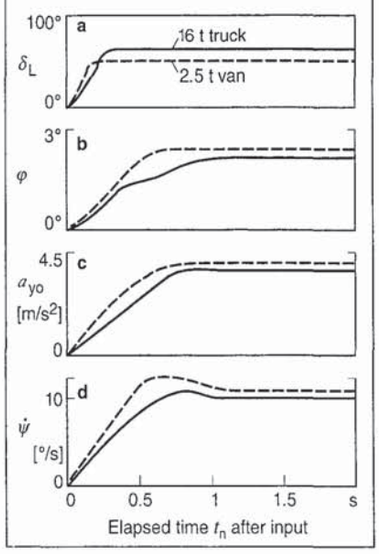
At low rates of lateral acceleration, the float angle is a function of the radius of the driven circle, and the vehicle's center of gravity which varies along with changes in vehicle load.

Rear-axle roll steer
The relationship between the steering angle at the rear axle (roll-steer angle) and lateral acceleration illustrates how the roll-steer angle at the rear axle decreases in response to higher vehicle loads.

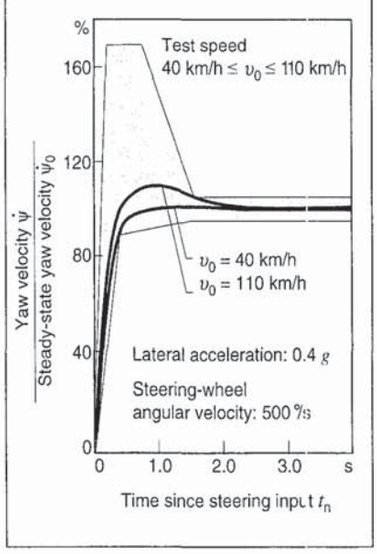
Slip angle
The wheel slip angles at the individual wheels provide information on the vehicle's self-steering characteristics. The wheel slip angles increase in response to higher vehicle loads, a consequence of the tires requiring greater slip angles as their loading increases [2], [9].

Transient response
In addition to self-steering in steady-state testing, yet another significant factor is the vehicle's response during directional changes (e.g. for rapid evasive maneuvers) [2]. Two test methods have become accepted internationally. These are defined according to the type of input stimulus, and illustrate both the time and frequency ranges of the vehicle's response:
– Step-input (sharp change in steering

Sudden steering-angle change *(unloaded, v_0 = 60 km/h)*
a) Steering-wheel angle δ_L, b) Roll angle φ, c) Lateral acceleration a_{y0}, d) Yaw speed $\dot{\psi}$.



ESV limit curves for steady-state yaw speed in "steering-angle jump" test
(2.5 ton van, empty)



PETITIONER'S EXHIBIT 1002
US PATENT NO. 6,557,540

angle),
– Sinusoidal input (sinusoidal steering-angle input).

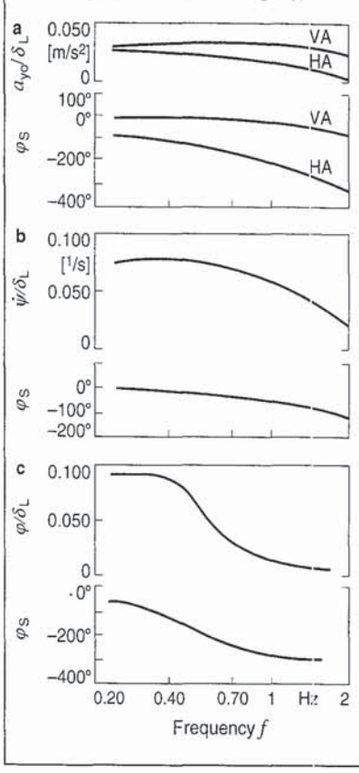
Step input (time response)
Starting with the vehicle traveling in a straight line, the steering wheel is abruptly "pulled" to a specified angle; the vehicle's response serves as the basis for evaluation. The most important quantities to be measured are [5]:
– Steering-wheel angle,
– Yaw speed,
– Vehicle speed, and
– Lateral acceleration.
The light utility van responds to the step input with a more rapid change in lateral acceleration – and thus in yaw – than the heavy truck.

US authorities have defined a transient yaw requirement for Experimental Safety Vehicles (ESV) [11]. Those vehicles which are classified as being similar to passenger cars may exhibit relatively pronounced overswing in the initial input phase (whereby this effect must cease after a certain period).

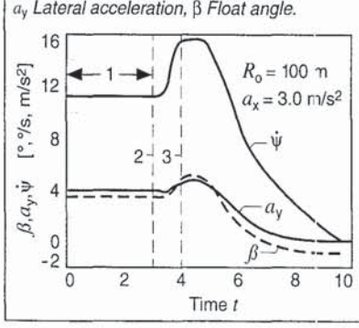
Sinusoidal steering-angle input (frequency curve)
Permanent sinusoidal steering inputs at the steering wheel are also used to measure frequency-response characteristics. This provides yet another basis for evaluating a vehicle's transitional handling response, the intensity and phase of which varies according to the steering frequency. The most important factors for this evaluation are [6]:
– Steering-wheel angle,
– Lateral acceleration,
– Yaw speed, and
– Roll angle.

Braking in a curve
Of all the maneuvers encountered in everyday driving situations, one of the most critical – and thus one of the most important with regard to vehicle design – is braking during cornering. The vehicle's concept must be optimized so that its reaction to this maneuver is characterized by the best possible compromise between steerability, stability and retardation [2], [7]. Testing starts from a specified initial rate of lateral acceleration, and focuses upon

Sinusoidal steering-angle input
(16-ton truck, v_0 = 60 km/h, δ_L = 60°).
Relative to steering-wheel angle:
a) Lateral acceleration a_{y0}/δ_L,
b) Yaw velocity $\dot{\psi}/\delta_L$ and
c) Roll angle φ/δ_L; with phase angle φ_s.



Time curve for braking during cornering
(7.5 ton truck, loaded)
1 Steady-state skidpad, 2 Initial braking, 3 Evaluation point. $\dot{\psi}$ Yaw speed, a_y Lateral acceleration, β Float angle.



PETITIONER'S EXHIBIT 1002
US PATENT NO. 6,557,540

float angle and yaw speed relative to lateral deceleration as the significant factors.

The vehicle, initially in steady-state circulation at a stipulated lateral acceleration, is braked with the rate of deceleration being increased incrementally. In every test, using the time functions, the measurements are taken "1 s after initial braking" for vehicles with hydraulic brakes (a delay of 1.5...2 s after initial braking is applied for heavy-duty commercial vehicles with compressed-air brake systems).

Float angle

Due to the weight transfer away from the rear axle and the tires' response to this phenomenon, higher rates of retardation result in greater float angles. At high rates of deceleration, in the vicinity of the traction limit, the distribution of brake force is the decisive factor for the float angle. The sequence in which the wheels lock exercises a decisive influence on the vehicle's stability.

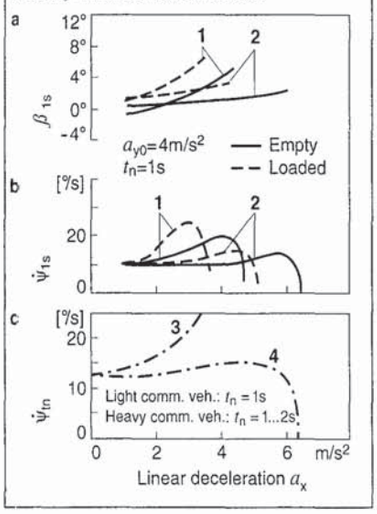
Yaw speed

The yaw speed serves as a reference in determining whether braking performance during cornering is stable or unstable. In the illustration, both vehicles' yaw-speed curves move toward zero as the vehicles progress through phases of increasing deceleration up to full lockup at both axles. This indicates acceptable braking response: The vehicle remains stable.

Typical yaw response when braking during cornering

a) Float angle β_{1s} and b) Yaw speed $\dot{\psi}_{1s}$ 1s after initial braking (t_n), c) Yaw speed at moment t_n.

1 16-ton truck, 2 2.5-ton van, 3 Vehicle starts to skid, 4 Vehicle remains stable.



References:

[1] Rönitz R.; Braess H.H.; Zomotor A. Verfahren und Kriterien des Fahrverhaltens von Personenwagen. (Testing procedure and evaluation of passenger-car driveability). AI 322, 1972, Volume 1.

[2] von Glasner E.C. Einbeziehung der Prüfstandsergebnissen in die Simulation des Fahrverhaltens von Nutzfahrzeugen. (Including test-stand results in driveability simulation for heavy-duty commercial vehicles). Habilitation, Universität Stuttgart, 1987.

[3] ISO. Road Vehicles – Steady-State Circular Test Procedure. ISO, 1982, No. 4138.

[4] ISO. Road Vehicles – Double Lane Change. ISO, 1975, TR 3888.

[5] ISO. Draft Proposal for an International Standard, Road Vehicles – Transient Response Test Procedure (Step/Ramp Input). ISO/TC22/SC9/N 185.

[6] ISO. Draft Proposal for an International Standard, Road Vehicles – Transient Response Test Procedure (Sinusoidal Input). ISO/TC 22/SC9/N219.

[7] ISO. Road Vehicles – Braking in a Turn. Open-Loop Test Procedure. ISO/DIS 7975.

[8] Zomotor A.; Braess H.H.; Rönitz R. Doppelter Fahrspurwechsel, eine Möglichkeit zur Beurteilung des Fahrverhaltens von Kfz? (Double Lane Change, a Method for Evaluating a Vehicle's Driveability?) ATZ 76, 1974, Volume 8.

[9] Mitschke M. Dynamik der Kraftfahrzeuge. (Dynamics of the Motor Vehicle), Springer Verlag, 1st Edition 1972, 2nd Edition 1982 and 1984, and subsequent Editions.

[10] Mitschke M. Fahrtrichtungshaltung – Analyse der Theorien. (Maintaining Direction of Travel – Analysis of the Theories). ATZ 70, 1968, Volume 5.

[11] Mischke A.; Göhring E.; Wolsdorf P.; von Glasner E.C. Contribution to the Development of a Concept of Driving Mechanics for Commercial Vehicles. SAE 83 0643.

PETITIONER'S EXHIBIT 1002
US PATENT NO. 6,557,540

Special operating dynamics for commercial vehicles

Units and symbols

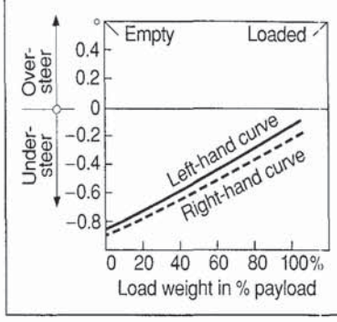
G_V	N	Front-axle load
G_H	N	Rear-axle load
G_G	N	Total weight
G_F	N	Sprung weight
U_V	N	Unsprung weight, front
U_H	N	Unsprung weight, rear
C_{DSt}	N · m/wheel	Torsional spring rate for all stabilizers
$C_{FV,H}$	N/m	Spring rates for axle springs
$C_{RV,H}$	N/m	Spring rates for tires
$S_{FV,H}$	m	Spring track
$S_{RV,H}$	m	Tire track
$m_{V,H}$	m	Instantaneous center height
h_F	m	Height of center of gravity, sprung weight
h_G	m	Height of center of gravity, total vehicle
$C_{QV,H}$	N/m	Lateral stiffness rate of tires
r	m	Radius of curve

Self-steering properties

In the development phase in which the parameters affecting a vehicle's self-steering properties are determined, empirical and test-stand measurements and computer simulations are employed in an optimization process. The major determinants are the geometry and compliance rates of the steering, the frame and the suspension.

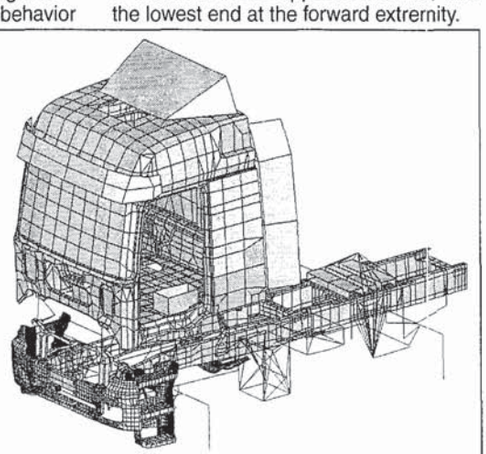
The objects of analysis are those interference factors influencing straight-running stability and cornering behavior which can be traced to the interaction between steering and suspension and which do not stem from driver inputs. The self-steering effect is examined at both the front and rear axles, in steady-state driving on a circular course, during braking and under unilateral spring compression.

Self-steering angle of a 18-ton truck cornering at 3 m/s² lateral acceleration
The self-steering angle is plotted along Y.



When the springs are compressed on one side, a solid axle supported on leaf springs will tend to rotate about the vehicle's vertical axis. The degree of spring tilt exercises a major effect on this type of roll-steer effect. Neutral behavior or mild understeer, desirable from the safety point of view, are enhanced by tilting the front spring upward at the front and downward toward the rear, while the rear spring is mounted in the opposite manner, with the lowest end at the forward extremity.

Finite element model of a semitrailer unit for determining self-steering properties
Includes kinematic patterns for steering and suspension as well as the entire frame of the semitrailer tractor.



PETITIONER'S EXHIBIT 1002
US PATENT NO. 6,557,540

The wheel loads at the truck's rear axle vary dramatically, depending upon whether it is empty or loaded. This leads to the vehicle responding to reductions in load with more pronounced understeer.

On three-axle 6 x 4 vehicles, the non-steered tandem axle unit represents a constraining force around the vehicle's vertical axis, thus enhancing straight-line stability. For low speeds, the additional cornering force required at the front and rear axles is determined as follows:

Cornering forces resulting from constraint
$F_{S1} = F_{S2} - F_{S3}$ with
$F_{S2} = c_{p2} \cdot n_2 \cdot \alpha_2$
$F_{S3} = c_{p3} \cdot n_3 \cdot \alpha_3$

Slip angle

$$\alpha_2 = \frac{1}{r} \cdot \frac{c_{p3} \cdot n_3 \cdot b \cdot (a+b)}{c_{p3} \cdot n_3 \cdot (a+b) + c_{p2} \cdot n_2 \cdot a}$$

$$\alpha_3 = (b/r) - \alpha_2$$

c_p Coefficient of cornering stability from tire performance curve,
n Number of tires per axle, other designations as in illustration.

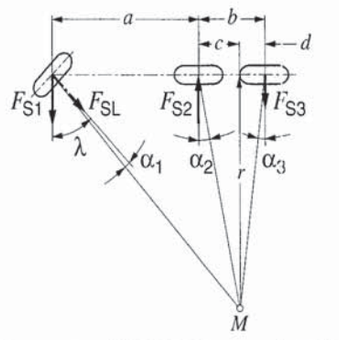
Tipping resistance

As the vehicle's total height increases, there is also an increasing tendency in a curve for it to tip over to the side before it starts to slide. Simulations of the tipping process for precise determination of the tip limit take into account both the elasticities and displacements of the center of gravity.

Achievable rates of lateral acceleration at the tip limit:

Van	$b = 6$ m/s²,
Truck	$b = 5$ m/s²,
Double-decker bus	$b = 3$ m/s².

Cornering forces F_s and slip angle α on a 3-axle vehicle with non-steered tandem axle



Width requirement

The width requirement of motor vehicles and truck-trailer combinations is greater during cornering than when the vehicle moves in a straight line. With respect to selected driving maneuvers, it is necessary to determine the radius described by the vehicle's outer extremities during cornering, both in order to ascertain its suitability for certain applications (e.g. narrow transit routes

Tipping resistance

Approximation formula for critical velocities v_{tip} on a 2-axle truck (in km/h):

$$v_{tip} = 7.98 \cdot \sqrt{\frac{r \cdot (G_V \cdot S_{RV} + G_H \cdot S_{RH})}{G_G \cdot h_G + \frac{G_V^2}{C_{QV}} + \frac{G_H^2}{C_{QH}} + \frac{G_F^2 \cdot h_m^2}{C_D - G_F \cdot h_m}}}$$

with $C_D = \frac{C_{DF} \cdot C_{DR} \cdot i^2}{C_{DF} + C_{DR} \cdot i^2}$; $i = \frac{h_m}{h_m + m}$;

$$h_m = h_m - m; \quad m = \frac{(G_V - U_V) \cdot m_v + (G_H - U_H) m_H}{G_F}$$

$$C_{DF} = 1/2 \cdot (C_{FV} \cdot S_{FV}^2 + C_{FH} \cdot S_{FH}^2) + C_{DSt}$$

$$C_{DR} = 1/2 \cdot (C_{RV} \cdot S_{RV}^2 + C_{RH} \cdot S_{RH}^2)$$

PETITIONER'S EXHIBIT 1002
US PATENT NO. 6,557,540

through constricted areas) and to confirm compliance with legal regulations. Evaluation is conducted with reference to the tractrix principle using electronic programs.

Handling characteristics

Objective analyses of vehicle handling are based on various maneuvers such as steady-state circulation on the skidpad, steering-angle jumps, wag frequency response, and braking in a curve.

The dynamic lateral response of truck-trailer combinations generally differs from that of rigid vehicles. Particularly significant are the distribution of loads between truck and trailer, and the design and geometry of the mechanical coupling device within a given combination.

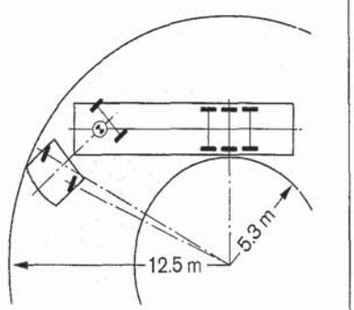
Rotary oscillation, with the vehicle's masses turning against the tires (as compliance element) around a vertical axis, impairs straight-running stability. This phenomenon is induced by

- Rapid steering corrections associated with evasive maneuvers,
- Crosswinds, and
- Pronounced slope to the side of the road, obstacles on one side, lane grooves.

Oscillation amplitudes associated with this pendulum motion must subside rapidly if vehicle stability is to be maintained.

Below is a graphic depiction of the yaw-speed progressions for various types of truck-trailer combination. The worst case is represented by a combination, in which the towing vehicle is empty, while the center-axle trailer is loaded. Here, the curve indicates an excessive increase in resonance. This type of combination demands a high degree of driver skill and circumspection.

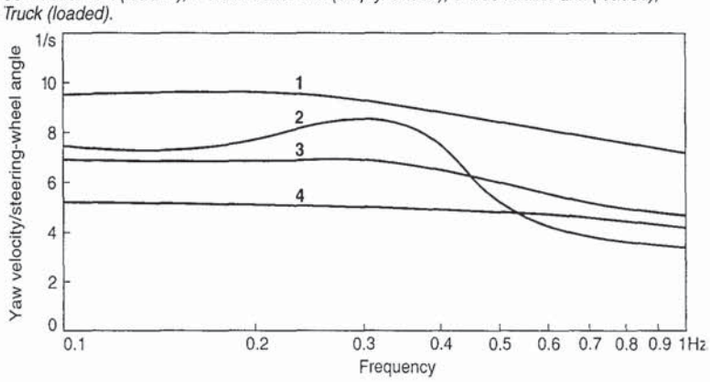
Tractor-semitrailer combination in the circular area as stipulated by the German Road Traffic Regulations (StVZO)



With semitrailer units, braking maneuvers undertaken under extreme conditions can induce jackknifing.

This process is initiated when, on a slippery road surface, loss of lateral-force is induced by excess braking force being applied at the tractor's rear axle, or due to excess yaw moment under μ-split conditions. Installation of an antilock braking system (ABS) represents the most effective means of preventing jackknifing. This measure is mandatory for towing vehicles >18 metric tons since 1 October, 1991.

Yaw-speed frequency progression
1 Semitrailer unit (loaded), 2 Truck-trailer unit (empty/loaded), 3 Truck-trailer unit (loaded), 4 Truck (loaded).



PETITIONER'S EXHIBIT 1002
US PATENT NO. 6,557,540

Requirements for agricultural tractors

Units and symbols

Symbol		Unit
F	Weight (wheel load) of a wheel	N
F_R	Rolling resistance	N
F_{Rh}	Rolling resistance, rear axle	N
F_{Rv}	Rolling resistance, front axle	N
F_{St}	Climbing resistance	N
F_T	Traction (motive) force of a wheel	N
F_{Th}	Traction (motive) force, rear	N
F_{Tv}	Traction (motive) force, front	N
F_w	Soil (ground) resistance	N
F_Z	Drawbar pull of tractor	N
$F_{Zerf.}$	Drawbar-pull requirement of implement	N
P_e	Net engine power	kW
$P_{Getr.}$	Transmission power losses	kW
P_N	Rated engine power	kW
P_R	Auto-motive power requirement	kW
P_S	Slip power losses	kW
P_{St}	Hill-climbing power requirement	kW
P_Z	Drawbar power	kW
v	Vehicle speed	km/h
v_o	Peripheral velocity of a driving wheel	km/h
$\eta_{Getr.}$	Transmission/gearbox efficiency	–
η_L	Tractive efficiency at tractor wheels	–
η_T	Tractive efficiency of a single wheel	–
η_Z	Tractive efficiency of an agricultural tractor	–
λ	Engine utilization ratio	–
$\varkappa$	Coefficient of traction force	–
ϱ	Rolling resistance	–
σ	Wheel slip	%

Applications

Agricultural tractors are employed for field work and for general transport and farmyard duties. Depending upon the type of unit, power from the engine can be transmitted through an auxiliary PTO shaft or hydraulic lines, as well as via the drive wheels. The engine outputs for farm tractors used in the Federal Republic of Germany range up to approximately 250 kW, with weights of over 120 kN.

Higher engine outputs exaggerate the problems associated with supporting the weight at the ground on large-volume tires of adequate capacity, as well as the difficulties encountered in transforming the engine's power into tractive power at acceptable tractor speeds.

Essential requirements of a tractor

- High drawbar pull, high tractive efficiency.
- The engine must combine high torque increase and low specific fuel consumption with as constant a power characteristic as possible.
- Depending upon application and the distances involved, vehicle speeds (rated speeds) up to 25, 32, 40, 50 km/h, with > 60 km/h for special-purpose tractors; multiple conversion ratios with appropriate gear spacing (especially important up to 12 km/h), suitable for shifting under load if possible.
- Power take-off (PTO) shaft and hydraulic connections for powering auxiliary equipment. Option of installing and/or powering equipment at the front of the tractor.
- Facilities for monitoring and operating auxiliary equipment from the driver's seat, e.g. with hydraulic control levers (P. 824).
- Clear and logical layout of control levers in ergonomically correct arrangement.
- On field tractors, provision for adjusting track to suit crop-row spacing.
- Driver protection against vibration, dust, noise, climatic influences and accident.
- Universal applicability.

Drawbar pull and drawbar power of a tractor in field work

The effective drawbar pull is essentially determined by the tractor's weight, the type of drive (rear-wheel or 4-wheel drive) and the operating characteristics of its tires. The operational response of the tractor's drive tires is determined by such factors as type of soil and ground conditions (moisture and porosity), tire dimensions, carcass and tread design, and tire pressure. Due to these particular operating characteristics, the farm tractor in field work develops its maximum drawbar pull only when tire slip is high, whereas the maximum drawbar power is achieved at relatively low levels of slip and drawbar pull. With the engine developing 90% of its maximum output, the drawbar pull of an AWD tractor v ceed 60% of the rated engine pc under extremely favorable condit The effective engine output is:

$$P_e = P_Z + P_R + P_S + P_{Getr.}$$
$$(+ P_{St} \text{ on gradients})$$

The drawbar power is calculate

$$P_Z = F_Z \cdot v$$

With rear-wheel drive, the powe to propel the tractor itself is:

$$P_R = F_{Rv} \cdot v + F_{Rh} \cdot v_o$$

The slip power losses are defin

$$P_S = F_T \cdot (v_o - v) = F_T \cdot \sigma \cdot v_o$$

The power losses in the transmi are determined with the equatic

$$P_{Getr.} = P_e \cdot (1 - \eta_{Getr.})$$

Efficiency levels:
With rear-wheel drive:

$$\eta_L = \frac{F_{Th} - F_{Rv}}{F_{Th} + F_{Rh}} \cdot (1 - \sigma)$$

With all-wheel drive (AWD):

$$\eta_L = \frac{F_{Th} + F_{Tv}}{F_{Th} + F_{Tv} + F_{Rh} + F_{Rv}} \cdot (1 -$$

For single wheel:

$$\eta_T = \frac{F_T}{F_T + F_R} \cdot (1 - \sigma) = \frac{\varkappa}{\varkappa + \varrho} ($$

For the tractor:

$$\eta_Z = \eta_{Getr.} \cdot \eta_L = P_Z / P_e$$

The coefficients are calculated a

$$\varkappa = F_T / F$$
$$\varrho = F_R / F$$
$$\lambda = P_e / P_N$$
$$\sigma = (v_o - v) / v_o$$

Drawbar-pull requirements of auxiliary equipment and traile

At a constant speed on a flat su drawbar-pull requirement depe on the rolling resistance F_R (equipment) or on soil resistanc the force needed to move a to

Examples of the power requi 1 meter swath on moderate gro

Implement	
Tiller on loose soil	
Vibrating harrow	
Circular harrow	

PETITIONER'S EXHIBIT 1002
US PATENT NO. 6,557,540

drawbar pull of an AWD tractor will not exceed 60 % of the rated engine power, even under extremely favorable conditions.
The effective engine output is:

$$P_e = P_Z + P_R + P_S + P_{Getr.}$$
$$(+ P_{St} \text{ on gradients})$$

The drawbar power is calculated as:

$$P_Z = F_Z \cdot v$$

With rear-wheel drive, the power required to propel the tractor itself is:

$$P_R = F_{Rv} \cdot v + F_{Rh} \cdot v_o$$

The slip power losses are defined as:

$$P_S = F_T \cdot (v_o - v) = F_T \cdot \sigma \cdot v_o$$

The power losses in the transmission unit are determined with the equation:

$$P_{Getr.} = P_e \cdot (1 - \eta_{Getr.})$$

Efficiency levels:
With rear-wheel drive:

$$\eta_L = \frac{F_{Th} - F_{Rv}}{F_{Th} + F_{Rh}} \cdot (1 - \sigma)$$

With all-wheel drive (AWD):

$$\eta_L = \frac{F_{Th} + F_{Tv}}{F_{Th} + F_{Tv} + F_{Rh} + F_{Rv}} \cdot (1 - \sigma)$$

For single wheel:

$$\eta_T = \frac{F_T}{F_T + F_R} \cdot (1 - \sigma) = \frac{\varkappa}{\varkappa + \varrho} (1 - \sigma)$$

For the tractor:

$$\eta_Z = \eta_{Getr.} \cdot \eta_L = P_Z / P_e$$

The coefficients are calculated as follows:

$$\varkappa = F_T / F$$
$$\varrho = F_R / F$$
$$\lambda = P_e / P_N$$
$$\sigma = (v_o - v) / v_o$$

Drawbar-pull requirements of auxiliary equipment and trailers
At a constant speed on a flat surface, the drawbar-pull requirement depends either on the rolling resistance F_R (e.g. farm equipment) or on soil resistance F_W (e.g. the force needed to move a tool through the soil) or on both at the same time (e.g. beet lifter). Rolling resistance is calculated using the coefficient of rolling resistance and the sum of the weights supported at the wheels, giving:

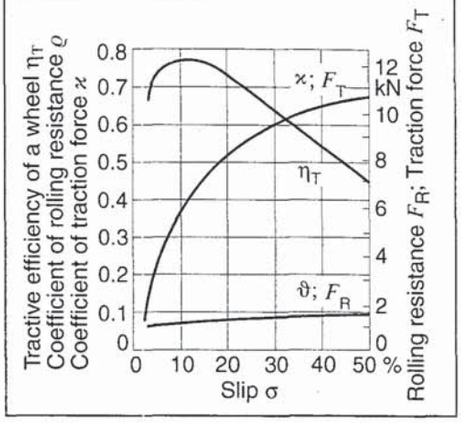
$$F_R = \varrho \cdot \Sigma F$$

For pneumatic tires on asphalt: $\varrho \leq 0.03$
For pneumatic tires on field:

$$\varrho = 0.04...0.35$$

Soil resistance is determined by the type and condition of the soil, number and type of implements, working depth and vehicle speed. General reference figures for plowing would be a specific ground resistance of 400...600 N/dm² on moderate soils, with 600...1000 N/dm² on hard (clay) soils. On moderate ground at speeds of between 6 and 9 km/h, the soil resistance per meter of working width of a cultivator is 5500...7800 N for a working depth of 13...15 cm, and 11,000...12,500 N for a depth of 22...25 cm.

Operating characteristics of a tractor drive wheel
Tire: 16.9/14-30 AS; Wheel load: 1582 daN; Tire pressure: 1.1 bar; Ground: loamy clay, wheat stubble, treated with disk harrow, moisture: 17.3...20.8 %.



Examples of the power required by PTO-driven agricultural equipment working a 1 meter swath on moderate ground.

Implement	Required engine power kW	Working depth cm	Vehicle speed km/h
Tiller on loose soil	10.5...25	8	3...7
Vibrating harrow	8...22	8	3.5...6.5
Circular harrow	0...15	8	3.5...6.5

PETITIONER'S EXHIBIT 1002
US PATENT NO. 6,557,540

Environmental stresses on automotive equipment

Climatic factors

Climatic stress factors acting upon automotive components encompass the effects of the natural environment, i.e. the macroclimate, and influences stemming from the vehicle itself (such as fuel vapor) and the microclimate within a component (such as the heat generated in electrical devices).

Temperature and temperature variations
The range extends from extremely low temperatures (storage, transport) all the way to the high temperatures associated with operation of the internal-combustion engine.

Atmospheric humidity and variations
This range embraces everything from arid desert climates to tropical environments, and can even extend beyond these under certain conditions (as occur for instance when water is sprayed against a hot engine block). Humid heat (high temperatures combined with high atmospheric humidity) is especially demanding. Alternating humidity results in surface condensation, which causes atmospheric corrosion.

Corrosive atmospheres
Salt spray encountered when the vehicle is operated on salt-treated roads and in coastal areas promotes electrochemical and atmospheric corrosion. Industrial atmospheres in concentrated manufacturing regions lead to acid corrosion on metallic surfaces. When they are present in sufficient concentrations, today's increasing amounts of atmospheric pollutants (SO_2, H_2S, Cl_2 and NO_x) promote the formation of contaminant layers on contact surfaces, with the result that resistance increases.

Water
Stresses of varying intensities result from rain, spray, splash, and hose water as encountered when driving in rain, during car and engine washes, and – in exceptional cases – during submersion.

Aggressive chemical fluids
The product in question must be able to resist the chemical fluids encountered in the course of normal operation and maintenance at its particular operating location. Within the engine compartment, such chemicals include fuel (and fuel vapor), engine oil and engine detergents. Certain components are confronted by additional substances, for example, brake-system components and the brake fluid used to operate them.

Sand and dust
Malfunctions result from the friction due to sand and dust on adjacent moving surfaces. In addition, under the influence of moisture, certain types of dust layers can cause current tracking in electrical circuits.

Solar radiation
The sun's rays cause plastics and elastomers to age (a factor to be taken into account in the design of external, exposed components).

Atmospheric pressure
Fluctuations in atmospheric pressure affect the operation and reliability of differential-pressure components, such as diaphragms, etc.

Laboratory simulation of stress

Climatic and environmental conditions are simulated both according to standardized test procedures (DIN IEC 68 – Environmental testing procedures for electronic components and equipment) and in special field-testing programs designed specifically for individual cases. The goal is to achieve the greatest possible approximation of the stresses encountered in actual practice ("test tailoring").

Temperature, temperature variation and atmospheric humidity
Simulation is carried out in temperature and climate chambers as well as in climate-controlled rooms which afford access to test personnel.

The dry heat test allows evaluation of a component's suitability for storage and operation at high temperatures. Testing is not restricted to ascertaining the effects of

PETITIONER'S EXHIBIT 1002
US PATENT NO. 6,557,540

heat upon operation; it also monitors influences on material characteristics. Depending upon the particular application (component mounted on body, engine, or exhaust system), the degree of heat can cover an extremely wide range. The stress time can be up to several hundred hours.

Testing the product's operation under cold conditions devotes particular attention to starting behavior and changes in materials characteristics at low temperatures. The testing range extends down to – 40 °C for operation, and to – 55 °C for storage. At less than 100 hours, the actual testing times are shorter than those employed for dry heat.

A further test simulates temperature fluctuation between the extremes encountered in actual operation; the temperature gradient and the dwell time also contribute to determining the degree of stress. The dwell time must be at least long enough to ensure that the sample achieves thermal equilibrium. The different levels of thermal expansion mean that the temperature variations induce both material aging and mechanical stresses within the component. The selection of appropriate test parameters makes it possible to achieve substantial time-compression factors.

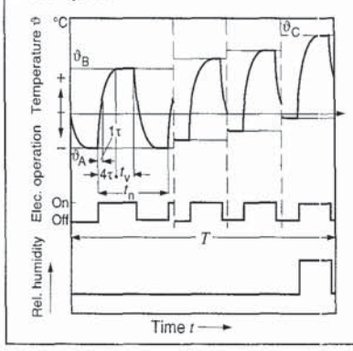
Atmospheric humidity testing under steady-state damp heat (e.g., +40 °C/ 93 % relative humidity) is employed in the evaluation of a product's suitability for operation and storage at relatively high humidity levels (tropical climates).

Corrosive atmospheres

Salt fog is produced by diffusing a 5 % NaCl solution at a room temperature of 35 °C. Depending upon the intended installation location, the test times can extend to several hundred hours. Cyclic salt fog is a combination test comprising the following: "salt fog, dry heat and damp heat". It yields a closer correlation with field results. The industrial-climate test comprises up to 6 cyclical alternations between an 8-hour dwell period at 40 °C/100 % relative humidity at 0.67 % SO_2 and 16 hours at room temperature. The pollutant test with SO_2, H_2S, NO_X and CL_2 is performed either for single gases or as a multisubstance test. Testing is carried out at 25 °C/75 % relative humidity

Test schedule for simulating combined stresses

t_v Dwell time, t_n Temperature-variation cycle, T Test cycle.



with concentrations in the ppm and ppb ranges, and lasts up to 21 days.

Water spray

A pivoting sprayer is used to simulate water spray. Water pressure, spray angle and the pivot angle can all be adjusted for different stress severity levels. The water-spray test employs high-pressure jets and standard steam-cleaners of the type used for cleaning engines.

Aggressive chemical fluids

The sample is wetted with the fluid in question for a defined period. This is followed by 24-hour storage at elevated temperature. This test can be repeated numerous times, according to the particular application.

Sand and dust

Dust simulation is carried using a device which maintains a dust density of 5 g per m^3 in moving air. A mixture of lime and fly ash is one of the substances employed.

Combined tests

Combined temperature, temperature variation and humidity tests on an operating electrical product ensure a high degree of convergence with the aging effects to be anticipated under extreme operating conditions. The advantage of this test is its high level of conformity with actual practice. The disadvantage is the test duration, which is generally well in excess of that required for the corresponding individual investigations.

PETITIONER'S EXHIBIT 1002
US PATENT NO. 6,557,540

Internal-combustion engines

Operating concepts and classifications

The internal-combustion (IC) engine is the most frequently employed power source for motor vehicles. Internal-combustion engines generate power by converting chemical energy bound in the fuel into heat, and the heat thus produced into mechanical work. The conversion of chemical energy into heat is accomplished through combustion, while the subsequent conversion of this thermal energy into mechanical work is performed by allowing the heat energy to increase the pressure within a medium which then performs work as it expands.

Liquids, which supply an increase in working pressure via a change of phase (vaporization), or gases, whose working pressure can be increased through compression, are used as working media.

The fuels – largely hydrocarbons – require oxygen in order to burn; the required oxygen is usually supplied as a constituent of the intake air. If fuel combustion occurs in the cylinder itself, the process is called internal combustion. Here the combustion gas itself is used as the working medium. If combustion takes place outside the cylinder, the process is called external combustion.

Continuous mechanical work is possible only in a cyclic process (piston engine) or a continuous process (gas turbine) of heat absorption, expansion (production of work) and return of the working medium to its initial condition (combustion cycle).

If the working medium is altered as it absorbs heat, e.g. when a portion of its constituents serve as an oxidant, restoration of its initial condition is possible only through replacement.

This is called an open cycle, and is characterized by cyclic gas exchange (expulsion of the combustion gases and induction of the fresh charge). Internal combustion therefore always requires an open cycle.

In external combustion, the actual working medium remains chemically unchanged, and can thus be returned to its initial condition by suitable measures (cooling, condensation). This enables the

Table 1. Classification of the internal-combustion engine

Type of process		**Open process**				**Closed process**	
		Internal combustion				External combustion	
		Combustion gas ≙ working medium				Combustion gas ≠ working medium	
						Phase change in working medium	
						No	Yes
Type of combustion		Cyclic combustion			Continuous combustion		
Type of ignition		Auto-ignition	Externally supplied ignition				
Type of machine	Engine ≙ machine enclosing a working chamber	Diesel	Hybrid	Otto	Rohs	Stirling	Steam
	Turbine ≙ gas turbine	–	–	–	Gas	Hot steam	Steam
Type of mixture		Heterogeneous (in the combustion chamber)		Homogenous	Heterogeneous (in a continuous flame)		

PETITIONER'S EXHIBIT 1002
US PATENT NO. 6,557,540

use of a closed process.

In addition to the main process characteristics (open/closed) and the type of combustion (cyclic/continuous), the various combustion processes for internal-combustion engines can also be defined according to their air-fuel mixture formation and ignition arrangements.

In external air-fuel mixture formation, the mixture is formed outside the combustion chamber. In this type of mixture formation a largely homogenous air-fuel mixture is present when combustion is initiated, so it is also referred to as homogeneous mixture formation.

In internal air-fuel mixture formation the fuel is introduced directly into the combustion chamber. The later internal combustion occurs, the more heterogeneous the air-fuel mixture will be at the time combustion is initiated. Internal mixture formation is therefore also called heterogeneous mixture formation. External ignition designs rely on an electric spark or a glow plug to initiate combustion. In auto-ignition, the mixture ignites as it warms to or beyond its ignition temperature during compression, or when fuel is injected into air whose boundary conditions permit evaporation and ignition.

Cycles

The *p-V* diagram

A basic precondition for continuous conversion of thermal energy into kinetic energy is a modification in the condition of the working medium; it is also desirable that as much of the working medium as possible be returned to its initial condition.

For technical applications the focus can rest on changes in pressure and the corresponding volumetric variations which can be plotted on a pressure vs. volume work diagram, or *p-V* diagram for short.

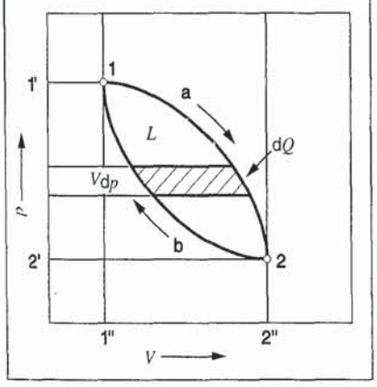
As the figure shows, the addition of heat and the change in condition of the working medium that accompany the progress of the process in the 1→2 phase must consume less energy than that required for the 2→1 phase. Once this condition is satisfied the result is an area corresponding to the process work potential: $L = \oint V dp$.

The *T-S* diagram

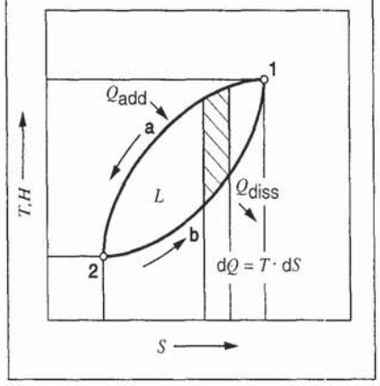
The temperature entropy, or *T-S* diagram, is used to provide a similar graphic representation of the bidirectional thermal energy transfers in this cyclic process.

In the *T-S* diagram heat quantities can be represented as areas in the same manner that work is represented as an area in the *p-V* diagram. With known specific working-medium heats, the *T-S* diagram can be transformed into the *H-S* dia-

A thermodynamic cycle illustrated using the p-V diagram



A thermodynamic cycle illustrated using the T-S or H-S diagram



PETITIONER'S EXHIBIT 1002
US PATENT NO. 6,557,540

gram, known as the enthalpy-entropy diagram, in accordance with the equation $dH = c_p \cdot dT$.

The cycle illustrated in the p-V diagram on page 367 shows the amount of heat added along "a"

$$Q_{add} = \int_2^1 T_a \, dS$$

and the amount of heat dissipated along "b"

$$Q_{diss} = \int_2^1 T_b \, dS, \text{ where}$$

$$Q_{add} - Q_{diss} = L = \oint V dp$$

(difference between the amount of heat supplied and the amount of heat discharged) which corresponds to the available amount of mechanical work. The diagram also shows that a thermal efficiency $\eta_{th} = (Q_{add} - Q_{diss})/Q_{add}$ can be defined based on the equality of mechanical work and the difference between the heat quantities. It also illustrates the theoretical cycle providing the maximum amount of technical work, as found in the area between two specified temperatures for the working medium.

The Carnot cycle

This cycle, described in 1824 by Carnot, consists of two isothermal [1]) and two isentropic [2]) changes in condition, which yield the maximum area in the T-S diagram between T_{max} and T_{min}. Because the Carnot cycle represents maximum process efficiency between the defined temperature limits, it is the theoretical optimum for converting heat into work:

$$\eta_{thCarnot} = (T_{max} - T_{min})/T_{max}$$

Internal-combustion engines operate according to other cycles, however, because isothermal compression, i.e. a pressure increase in the working medium without an increase in temperature, and isothermal expansion are not technically feasible.

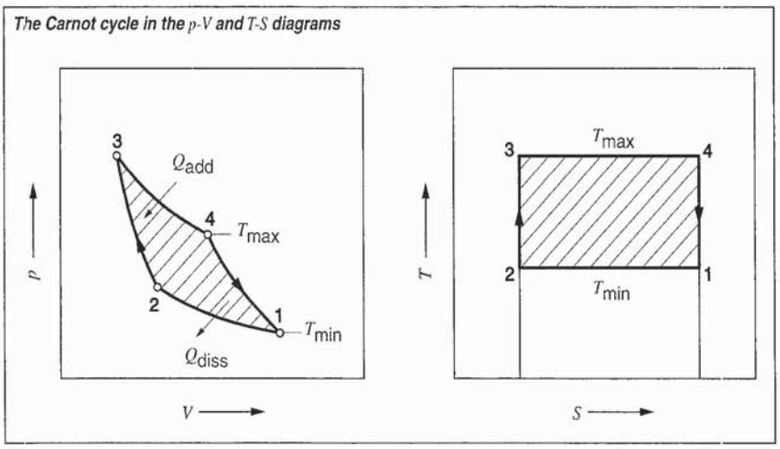
Theoretical treatment today involves the following ideal combustion cycles:
the constant-volume cycle for all piston engines with periodic combustion and generation of work, and
the constant-pressure cycle for all turbine engines with continuous combustion and generation of work.

Both cycles will be dealt with in more detail in the discussion of the corresponding machines.

---

[1]) Isothermal change in condition: temperature does not change.
[2]) Isentropic change in condition: adiabatic (heat is neither added nor dissipated) and frictionless (reversible).
[3]) Isochoric change in condition: volume does not change; see P. 369.

The Carnot cycle in the p-V and T-S diagrams



PETITIONER'S EXHIBIT 1002
US PATENT NO. 6,557,540

Reciprocating-piston engines with internal combustion

Operating concept

All reciprocating-piston engines operate by compressing air or an air-fuel mixture in the working cylinder prior to igniting the mixture, or by injecting fuel into the hot compressed air to initiate combustion. The crankshaft assembly converts the work generated in this process into torque available at the end of the crankshaft.

The p-V diagram reflects the actual power-generation process in the engine as a function of piston travel. It shows the mean effective pressures p_{mi} within the cylinder during a complete working cycle. Easier to produce are other diagrams such as the pressure vs. time (p-t) and the pressure vs. crankshaft angle (p-α) diagrams. The surfaces defined in these two diagrams do not directly indicate the amount of work generated, but they do provide a clear picture of essential data such as firing point and peak combustion pressure. The product of the mean effective pressure in the cylinder and the displacement yields the piston work, and the number of working cycles per unit of time indicates the piston power or the internal power (power index) for the engine. Here it will be noted that the power generated by a reciprocating-piston internal-combustion engine increases as min^{-1} rises (see equations on P. 416 to P. 423).

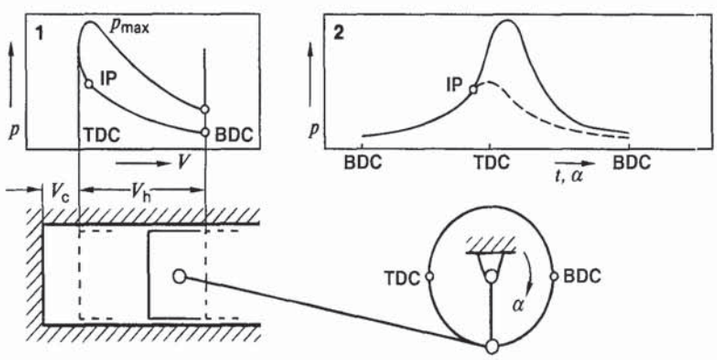
Ideal combustion cycle for piston engines with internal combustion

For reciprocating-piston engines with internal combustion, the ideal thermodynamic combustion process is the "constant-volume process", consisting of isentropic compression, isochoric[3]) heat supply, isentropic expansion and isochoric reversion of the ideal working gas to its initial condition. This cycle is only possible if the following conditions are met:

- No heat or gas losses, no residual gas,
- Ideal gas with constant specific heats c_p, c_v and $\varkappa = c_p/c_v = 1.4$,
- Infinitely rapid heat supply and discharge,
- No flow losses.

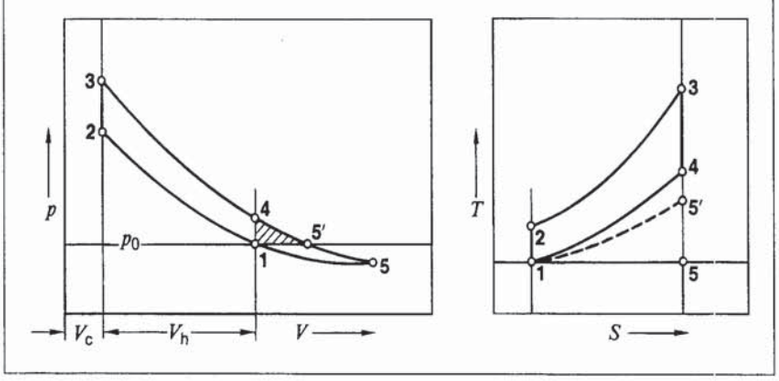
Because the crankshaft assembly restricts expansion to finite levels, the

The engine power cycle
1 In the p-V diagram, 2 in the p-t and p-α diagrams.



PETITIONER'S EXHIBIT 1002
US PATENT NO. 6,557,540

Ideal constant-volume combustion cycle as shown in the p-V and T-S diagrams



4–5–1 surface in the diagrams is not directly available for use. Section 4–5'–1, lying above the atmospheric pressure line, becomes available when an exhaust-gas turbine is connected downstream.

The efficiency of the ideal constant-volume combustion cycle is calculated in the same manner as all thermal efficiencies:

$$\eta_{th} = \eta_v = (Q_{add} - Q_{diss})/Q_{add}$$

with $Q_{add} = Q_{23} = m \cdot c_v \cdot (T_3 - T_2)$ and
$Q_{diss} = Q_{41} = m \cdot c_v \cdot (T_4 - T_1)$

Using the same $\varkappa$ for compression and expansion:

$$\eta_{th} = 1 - Q_{diss}/Q_{add} = 1 - \frac{T_4 - T_1}{T_3 - T_2} = 1 - T_1/T_2$$

if $T_1/T_2 = \varepsilon^{\varkappa-1}$ then
$\eta_{th} = 1 - \varepsilon^{1-\varkappa}$,

where the compression ratio is defined as $\varepsilon = (V_c + V_h)/V_c$ with a displacement of V_h and a compression volume of V_c.

Real internal-combustion engines do not operate according to ideal cycles, but rather with real gas, and are therefore subject to fluid, thermodynamic and mechanical losses.

Efficiency sequence (DIN 1940)
The overall efficiency η_e includes the sum of all losses, and can thus be defined as the ratio of effective mechanical work to the mechanical work equivalent of the supplied fuel:

$\eta_e = W_e/W_B$ where

W_e is the effective work available at the clutch and
W_B is the work equivalent of the supplied fuel.

In order to better distinguish among the different losses, a further distinction can be made:

the fuel conversion factor η_B provides an index of combustion quality:

$$\eta_B = (W_B - W_{Bo})/W_B, \text{ where}$$

W_B is the work equivalent of the supplied fuel,
W_{Bo} is the work equivalent of the unburned fuel.

There are no operating conditions in which complete combustion takes place.

A portion of the supplied fuel does not burn (hydrocarbon constituents in the exhaust gas), or fails to combust completely (CO in exhaust).

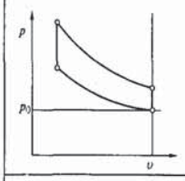
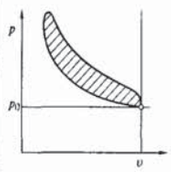
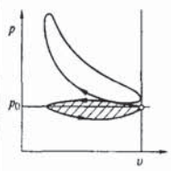
η_B is often defined as "1" for small diesel engines at operating temperature and for comparisons.

The efficiency index η_i is the ratio of indicated high-pressure work to the calorific content of the supplied fuel $\eta_i = W_i/W_B$.

The efficiency of cycle factor η_g includes all internal losses occurring in both high-pressure and low-pressure processes. These stem from:

PETITIONER'S EXHIBIT 1002
US PATENT NO. 6,557,540

Table 2. Graphic representations and definitions of the individual and overall efficiencies of the reciprocating-piston engine

Pressure vs. volume diagram	Designation	Conditions	Definition	Efficiencies
	Theoretical reference constant-volume cycle	Ideal gas, constant specific heats, infinitely rapid heat addition and dissipation, etc.	$\eta_{th} = 1-\varepsilon^{1-\kappa}$ Theoretical or thermal efficiency	η_{th}
	Real high-pressure working cycle	Wall heat losses, real gas, finitely rapid heat addition and dissipation, variable specific heats	η_{gHP} Efficiency factor of the high-pressure cycle	η_g
	Real charge cycle (4-stroke)	Flow losses, heating of the mixture or the air, etc.	η_{gLW} Charge exchange efficiency	η_i
Mechanical losses	Losses due to friction, cooling, auxiliary units	Real engine	η_m	η_m η_m η_e

Real working gas, residual gas, wall heat losses, gas losses and pumping losses. For this reason, η_g is more appropriately broken down into η_{gHD} for the high-pressure portion and η_{gLW} for gas-exchange processes. The efficiency of cycle factor therefore indicates how closely engine performance approaches the theoretical ideal combustion cycle:

$$\eta_g = \eta_{gHD} \cdot \eta_{gLW} = W_i/W_{th} \text{ where}$$

W_i is the indicated work and
W_{th} is the work generated in the ideal-combustion cycle.

Mechanical efficiency η_m defines the relationship between mechanical losses – especially friction losses in the crankshaft assembly and induction/exhaust systems, and in oil and water pumps, fuel pump, alternator, etc. – and the work index:

$$\eta_m = W_e/W_i \text{ where}$$

W_e is the effective work available at the clutch and
W_i is the work index.

The efficiency chain therefore appears as follows:

$$\eta_e = \eta_B \cdot \eta_{th} \cdot \eta_{gHD} \cdot \eta_{gLW} \cdot \eta_m$$

(see Table 2).

PETITIONER'S EXHIBIT 1002
US PATENT NO. 6,557,540

The spark-ignition (Otto) engine

The spark-ignition engine (or SI engine) is a piston engine with external or internal air-fuel mixture formation. External mixture formation generally produces homogenous mixtures, whereas an internally formed mixture is largely heterogeneous at the instant of ignition. The time of mixture formation is a major factor influencing the degree of homogenization achievable by internal mixture formation.

In both cases, the mixture is compressed to approximately 20...30 bar (ε = 8...12) on the compression stroke, to generate a final compression temperature of 400...500 °C. This is still below the auto-ignition threshold of the mixture, which then has to be ignited by a spark shortly before the piston reaches TDC.

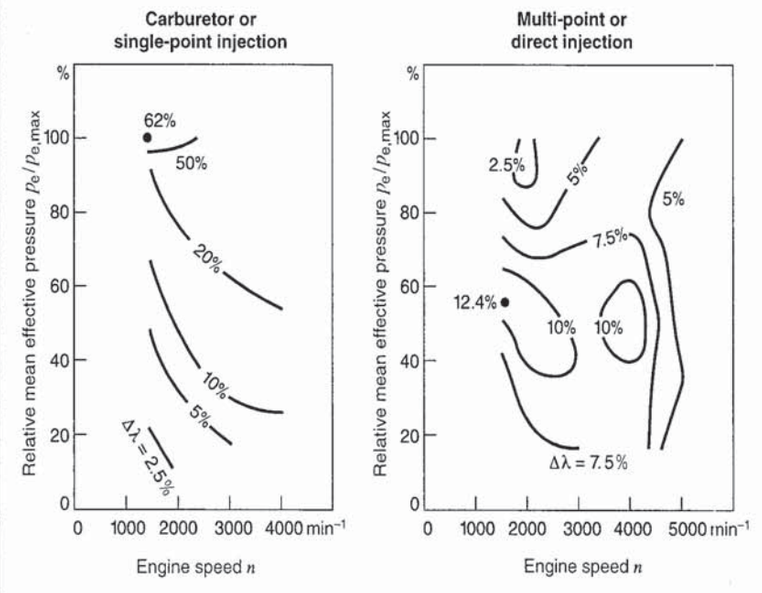
Since reliable ignition of homogenous air-fuel mixtures is only possible within a narrowly defined window of the air-fuel ratio (excess-air factor λ = 0.6...1.6), and flame velocity drops steeply as the excess-air factor λ increases, SI engines with homogenous mixture formation have to operate in a λ range 0.8...1.4 (best overall efficiency is achieved at $1.2 < \lambda < 1.3$). The λ range is further restricted to 0.98...1.02 for engines with three-way catalytic converters.

On account of this narrow λ range, load has to be controlled by the quantity of mixture entering the cylinders (quantity control): this is achieved by throttling the amount of air-fuel mixture entering the cylinders under part-load operating conditions (throttle control).

Optimization of the overall efficiency of SI engines has given rise to increasing development effort directed at engines with internal heterogeneous mixture formation.

Homogenous and heterogeneous mixture formation are alike in that economic efficiency and untreated emissions depend on the combustion process which takes place after ignition. Combustion, in turn, can be influenced to a very large extent by the flows and turbulences that can

Mixture-preparation
Differences in the air-fuel (A/F) ratio in the individual cylinders as a function of load and engine speed.



PETITIONER'S EXHIBIT 1002
US PATENT NO. 6,557,540

be produced in the combustion chamber by the geometry of the intake duct and the combustion chamber.

Homogenous mixture formation

The homogenous mixtures present at the time when ignition commences cause the fuel to vaporize fully, because only gas or gas/vapor mixtures can achieve homogeneity.

If some factor (such as low temperature during a cold start) inhibits complete vaporization of the fuel, sufficient additional fuel must be provided to ensure that the volatile, vaporizable constituent can produce an adequately rich – and therefore combustible – air-fuel mixture (cold-start enrichment).

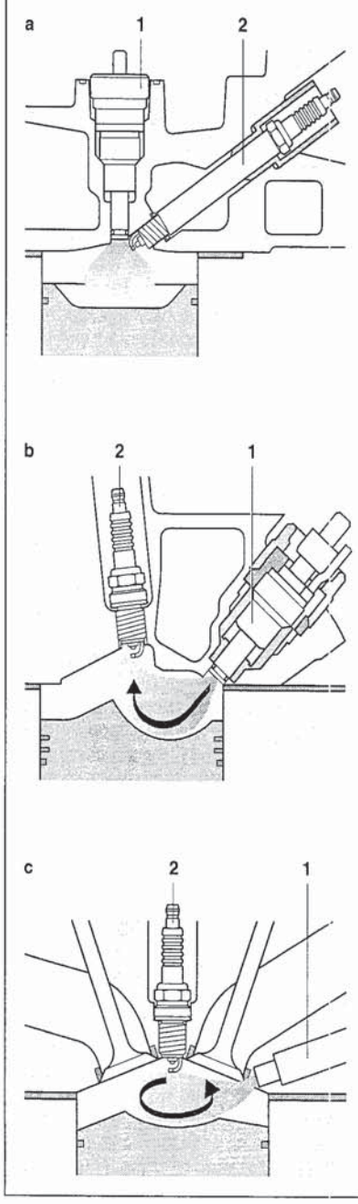
In addition to mixture homogenization, the mixture-formation system is also responsible for load regulation (throttle regulation) and for ensuring the minimization of deviations in the A/F ratio from cylinder to cylinder and from working cycle to working cycle.

Heterogeneous mixture formation

The aim pursued in heterogeneous internal mixture formation is that of operating the engine without throttle control across the entire operating map. Internal cooling is a side-effect of direct injection, so engines of this type can operate at higher compression ratios. The conjunction of these two factors, no throttle control and higher compression, means that the degree of efficiency is higher than that attainable with a homogenous mixture. Load is controlled by means of the mass of injected fuel. Development in mixture-formation systems gave fresh impetus to the "hybrid" or "stratified-charge" techniques that were the subject of much research from about 1970 onward. The definitive breakthrough came with the high-speed fuel injectors that allowed flexibility in injection timing and could achieve the high injection pressures required.

GDI (Gasoline Direct Injection) was the generic term applied to worldwide development in "jet-directed", "wall-directed" or "air-directed" mixture-formation systems (see illustration). The positions of spark plug and injector have a major influence on mixture formation, but flows in the

Mixture-formation systems for gasoline direct injection GDI *(assisted by swirl or tumble in each case)*
a) Jet-directed, b) Wall-directed, c) Air-directed.
1 Fuel injector, 2 Spark plug.



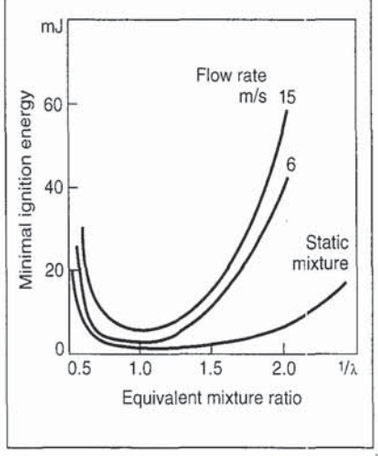
PETITIONER'S EXHIBIT 1002
US PATENT NO. 6,557,540

combustion chamber are another, supporting factor. Swirl (induced by spiral or tangential channels) is primarily rotation about an axis paralleling that of the cylinder, whereas the axis of tumble, which is induced by fill channels, is normal to the cylinder's axis.

Precision positioning of the spark plug and the jet from the fuel injector is essential for jet-directed spray injection. The spark plug is under severe strain, because it is struck directly by the jet of liquid fuel. Wall-directed and air-directed configurations direct the mixture to the plug by means of the motion of the charge, so requirements in this respect are not as high.

Heterogeneous mixture formation entails excess air (unthrottled operation), so lean-burn catalytic converters have to be developed in order to reduce nitrogen-oxide emissions.

Minimal ignition energy for propane/air mixtures



Ignition

The ignition system must reliably ignite the compressed mixture at a precisely defined instant, even under dynamic operating conditions with the attendant substantial fluctuations in mixture flow patterns and air-fuel ratios. Reliable ignition can be promoted by selecting spark-plug locations with good mixture access in combination with efficient mixture swirl patterns; these are especially important considerations for lean operation and at very low throttle apertures. Similar improvements can also be achieved by positioning the spark plug in small auxiliary "ignition chambers".

Ignition-energy requirements depend on the mixture's air-fuel (A/F) ratio. An ignition energy of 0.2 mJ is required for gasoline/air mixtures in the stoichiometric range, while up to 3 mJ may be required to ignite richer or leaner mixtures.

The ignition voltage required increases with the gas pressure at the instant of ignition. Increasing the electrode gap is one way of improving ignition reliability, but at the expense of higher ignition voltage and accelerated electrode wear.

The energy content of the mixture ignited by the spark must be sufficient to ignite the neighboring mixture. This defines the leanest possible mixture and the earliest possible instant of ignition. In engines with a compression ratio $\varepsilon \approx 8...12$, this range is approximately 40...50 °crankshaft before TDC.

Combustion process

The initial thermal reaction which occurs between the provision of the ignition energy by the spark and the exothermal reaction of the air-fuel mixture is the ignition phase. This phase is roughly constant over time, with mixture composition as the only influencing factor. As a result, increasing engine speeds are accompanied by proportionately higher ignition delays – referred to piston travel (°crankshaft) – which change together with excess-air factor (lambda) λ.

The moment of ignition, therefore, has to be advanced as engine speed increases and excess-air factor λ rises. Ignition advance, however, is limited by the fall-off in the mixture's energy density in the vicinity of the electrodes (see above). When this physical limit is reached, designers can resort to twin spark-plug configurations or pre-chamber ignition to improve the situation.

The heat-release transient is determined by the rate of combustion, which in turn is defined by the speed of flame propagation and the area of the flame front. The speed of flame propagation depends

PETITIONER'S EXHIBIT 1002
US PATENT NO. 6,557,540

on diffusion processes at the flame front and reaches a peak of approximately 20...40 $m \cdot s^{-1}$ in gasoline-air mixtures with approx. 10% air deficiency ($\lambda = 0.9$). It is influenced by the excess-air factor λ and the temperature of the mixture.

The area of the flame front can be influenced by the geometry of the combustion chamber and the position of the spark plug. Folding of the flame front due to turbulence and induced flows (such as swirl and tumble) is a significant factor in this respect. The flows induced primarily by the induction process and to a lesser extent by combustion-chamber geometry in conjunction with the compression squish fold the flame front and thus accelerate the process of energy conversion. Tumble, swirl and squish increase with engine speed and consequently, folding of the flame front also becomes more pronounced. This explains why the rate of heat release increases with speed despite the fact that by definition, the rate of flame propagation must remain constant.

Although it can factor in ultra-low-turbulence processes or in tests in low-flow pressure chambers, the turbulence created by flame propagation itself is of no significance in the combustion process as it takes place in modern SI engines.

The rising pressure due to local flame propagation causes an increase in temperature throughout the mixture, including that not yet reached by the flame and known as the "end gas". On account of local heat radiation and heat conduction, however, the temperature in the flame front is higher than in the rest of the mixture. This ensures regular flame propagation. The anomaly known as combustion knock or pre-ignition, due to simultaneous combustion of the end gas, occurs when the increase in pressure causes the temperature of the end gas to exceed its ignition limits.

Low fuel consumption and high efficiency are promoted by high combustion speeds (brief duration), combined with the optimal thermal release pattern relative to piston travel. Maximum heat release should occur shortly (approx. 5...10 °crankshaft) after top dead center. If most of the heat is released too early, wall heat losses and mechanical losses (high peak pressure) are increased. Late heat release leads to sacrifices in thermal efficiency (efficiency of cycle factor) and high exhaust-gas temperatures.

The ignition timing must be selected for optimum thermal generation curves in accordance with the:

- Air-fuel mixture ratio (λ, T),
- Effects of engine parameters (particularly load and speed) on combustion-chamber turbulence,
- Constant-duration ignition and flame propagation processes, meaning that variations in ignition timing are required as engine speed increases.

Problems and limits of combustion

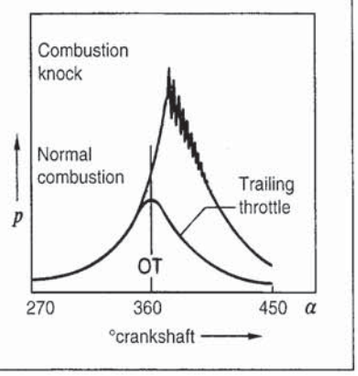
In actual practice, reliable flame initiation and propagation in engines with external mixture formation and spark ignition prohibit the use of mixtures leaner than $\lambda > 1.3$, although these would be desirable for improving the levels of theoretical (polytropic exponent) and gas-exchange (low throttle losses) efficiency, along with useful reductions in wall-heat and dissociation losses (reduction in combustion temperature). Appropriate tests are undertaken with GDI engines (Gasoline Direct Injection).

Although higher compression ratios provide enhanced part-load efficiency, they also increase the risk of combustion knock (pre-ignition) under full load. Pre-ignition occurs when the entire charge of end gas reaches ignition temperature and burns instantaneously without regular flame propagation. The end gas is highly compressed and its energy density is therefore very high, so pre-ignition suddenly releases very large amounts of heat. The high local temperatures caused in this way place extreme loads on the engine components and can also damage them. The high-energy cycles also result in extreme pressure peaks. Within the combustion chamber these pressure peaks propagate at the speed of sound and can cause damage to the piston, cylinder head, and cylinder-head gasket at critical points.

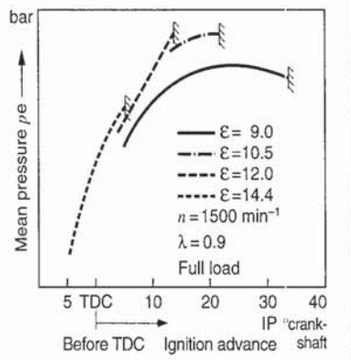
The risk of combustion knock can be reduced by using fuel additives or by richer mixtures (supplementary internal cooling).

PETITIONER'S EXHIBIT 1002
US PATENT NO. 6,557,540

Combustion knock with normal combustion and trailing throttle in the p-α diagram



Potential mean effective pressure at pre-ignition limit as a function of compression ratio and timing



The current expedient of avoiding pre-ignition by retarding the ignition timing raises problems of its own, especially when used on high-compression engines. Because the ignition curve (mean pressure relative to ignition point) becomes increasingly steeper as compression increases, the resulting sacrifices in mean effective pressure are accompanied by extreme exhaust-gas temperatures. Reliable detection and avoidance of pre-ignition are thus vitally important in the ε = 11...13 compression range.

Load control

In unthrottled GDI engines with heterogeneous mixture, load is controlled by means of the quantity of fuel injected. Spark-ignition engines with homogenous mixture formation, on the other hand, afford little latitude for operation with lean mixtures, so load control has to be implemented by adjusting the mass flow of mixture. In carburetor engines, which have lost virtually all their significance in automotive engineering, this can be achieved by throttling the mixture mass flow. In engines with intake-manifold injection, throttle control to reduce the density of the intake air is the conventional approach. This arrangement, however, increases charge-cycle losses, so development is concentrating on alternative methods of load control. Mass flow can be influenced, for example, by prematurely closing the intake valves and thus shortening the effective intake periods. This complicated means of load control, however, requires fully variable valve timing and can cause fuel condensation as the result of expansion when the intake valves are closed. This drawback can be countered with "feedback control", an arrangement in which the intake valves are not closed until the requisite mass of mixture has just had time to fill the cylinder.

Another way of reducing or even eliminating throttle losses is exhaust-gas recirculation with the intake valves open. Load can be varied across a wide range by modulating the exhaust-gas recirculation rate.

Regulating charge-air pressure is a method of accomplishing load control over wide regions of the characteristic map with supercharged spark-ignition engines.

PETITIONER'S EXHIBIT 1002
US PATENT NO. 6,557,540

Power output and economy

The efficiency index for engines with external mixture formation and spark ignition falls primarily in the lower portion of the map (see illustration). This is owing to combustion inefficiency (insufficient turbulence, inadequate charge density) along with an inefficient gas-exchange process.

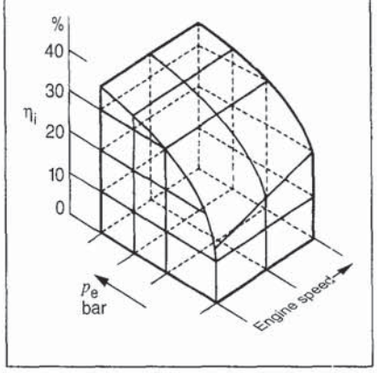
Effective efficiency is further reduced by the low mechanical efficiency characteristic of this region of the map.

All measures for avoiding these lower sections of the map therefore contribute to improving the engine's overall efficiency.

Selective interruption of the fuel supply to individual cylinders allows the remaining cylinders to operate at higher efficiency levels with improved combustion and gas exchange. Valve deactivation provides further reductions in power loss by allowing the intake and exhaust valves for the deactivated cylinders to remain closed. Cylinder shut-off entails immobilizing the mechanical power-transmission components of the idle cylinders for further increases in mechanical efficiency.

The measures cited above vary in terms of sophistication, but engine speed reduction also enhances general efficiency while promoting effective gas exchange; simultaneous reductions in mean frictional pressure also improve mechanical efficiency.

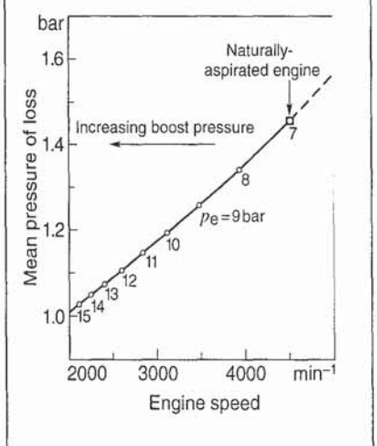
Curves of indicated efficiency vs. load factor and engine speed for a spark-ignition engine with throttle control



The diesel engine

A diesel engine is a reciprocating-piston engine with internal (and thus heterogeneous) mixture formation and auto-ignition. During the compression stroke intake air is compressed to 30...55 bar in naturally aspirated engines or 80...110 bar in supercharged engines, so that its temperature increases to 700...900 °C. This temperature is sufficient to induce auto-ignition in the fuel injected into the cylinders shortly before the end of the compression stroke, as the piston approaches TDC. In heterogeneous processes the mixture formation is decisive in determining the quality of the combustion which then follows, and the efficiency with which the inducted combustion air is utilized, and thus in defining the available mean effective pressure levels.

Relationship between engine speed and mean pressure of friction loss
5-liter gasoline engine, P_e = 130 kW = constant at increasing engine load, p_e Mean pressure.



PETITIONER'S EXHIBIT 1002
US PATENT NO. 6,557,540

Mixture formation

In heterogeneous mixtures, the air-fuel ratio λ extends from pure air ($\lambda = \infty$) in the spray periphery to pure fuel ($\lambda = 0$) in the spray core.

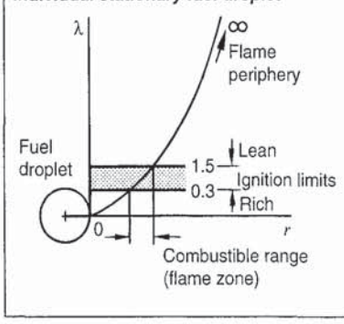
The figure provides a schematic illustration of the λ distribution and the associated flame zone for a single stationary droplet. Because this zone always occurs for every drop of injected mixture, load control with heterogeneous mixture formation can be performed by regulating the fuel supply. This is termed mixture-quality control.

As with homogenous mixtures, combustion takes place in the relatively narrow range between $0.3 < \lambda < 1.5$. The mass transport necessary for generating these combustible mixtures relies on diffusion and turbulence; these are produced by the mixture formation energy sources described below as well as by the combustion process itself.

Kinetic energy of the fuel spray

The spray's kinetic energy varies according to the pressure differential at the nozzle orifice. Along with the spray pattern (as determined by the nozzle geometry) and the fuel's exit velocity it determines the configuration of the space in which the air and fuel interact as well as the range of droplet sizes in the chamber. The spray energy is influenced by the delivery rate of the fuel-injection pump and the dimensions of the metering orifice in the injector nozzle.

Curve of the air-fuel (A/F) ratio λ in an individual stationary fuel droplet



Thermal energy

Thermal energy from the combustion-chamber walls and the compressed air vaporize the injected fuel (as a film layer on the walls and as droplets).

Combustion-chamber shape

The shape of the combustion chamber and the action of the piston can be utilized to create turbulence (squish), or to distribute liquid fuel or the fuel-air vapor jet.

Controlled air patterns (swirling action)

If the direction of fuel flow is roughly perpendicular to the direction of the vortex and droplet vaporization is taking place, a movement imparted to the combustion air inside the combustion chamber, usually in the form of solid-particle rotating flow, promotes the flow of air toward the fuel stream, and removes the combusted gases from the stream.

As the wall film evaporates, the air's swirling motion absorbs the vapor layer and provides thermal insulation between the combusted and fresh gases, while the microturbulence patterns superimposed upon the solid-particle vortex ensure rapid mixture of air and fuel. The air's controlled solid-particle swirl can be induced using special induction tract geometries or by shifting a portion of the cylinder charge into a rotationally symmetric auxiliary chamber (by transporting it through a side passage).

Partial combustion in a swirl chamber

When fuel is partially combusted in an auxiliary chamber its pressure rises above that in the main combustion chamber. This increase then propels the partially oxidized combustion gases and vaporized fuel through one or more passages into the main combustion chamber, where they are thoroughly mixed with the remaining combustion air.

The diesel combustion process makes use of at least one (but usually an appropriate combination) of these mixture formation methods.

PETITIONER'S EXHIBIT 1002
US PATENT NO. 6,557,540

Direct injection
This term refers to all designs with a single unified combustion chamber.

Low-swirl or static-charge spray-injection combustion
This combustion process operates virtually without swirl of the air mass in the cylinder, or even with none at all, and relies on the energy in the injection jets to ensure mixture formation. It was formerly used in large medium- and slow-speed diesels operating with high excess-air factors on account of thermal design considerations.

The combustion chamber is a wide, usually ω-shaped recess centered in the piston crown. Fuel is injected through a central, vertical multi-hole nozzle with 5...8 orifices.

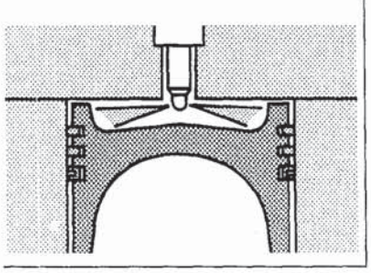
Higher excess-air factors and higher injection-jet energies (resulting from higher injection pressures) are two consequences of the increasingly lower emission limits for NO_X and particulates in the exhaust gas. At the same time, all modern commercial-vehicle engines with displacements down to approximately 1 *l* per cylinder are turbocharged and are fitted with governors to restrict their speed ranges for the sake of improved fuel consumption. These are the reasons why this method has become commonplace for commercial-vehicle engines, particularly since the retarded start of injection for the sake of further reductions in NO_X emissions goes hand in hand with higher thermal loads in the engines themselves.

Swirl-assisted multiple-orifice nozzle combustion process
The mixture-forming energy of the injection jets alone is not enough for sufficiently uniform and rapid mixture preparation in high-revving diesels with wide operating-speed ranges and small swept volumes (in other words, the engines most frequently found in passenger cars and vans). Supportive motion of the air inside the combustion chamber is required. This is achieved by installing pistons with considerably shallower recesses. These recesses are constricted at the top n order to create highly turbulent squish from the piston gap in the vicinity of the injection-jet contact points and to accelerate the swirl of the air charge induced by the design of the inlet elements (swirl inlet ducts). The total swirl velocity of the in-cylinder air mass achieved in this way is selected to ensure that the air-fuel mixture formed over the injection period from the injection jet issuing from the nozzle, and the air swirl rotating about an axis normal to this jet, completely fills and utilizes the downflow region of the combustion chamber until the next injection jet is received.

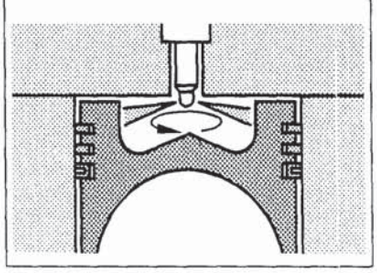
Consequently, this method employs nozzles with a significantly smaller number of orifices, namely 4...6. In this case, too, the nozzle is positioned as close as possible to an imaginary line extending though the center of the piston recess.

If the air-fuel mixture fails to completely fill the combustion-chamber segment, both air utilization and power output will suffer. On the other hand, if there is an

Combustion-chamber shape and nozzle location for the static-charge spray-injection process without air swirl



Combustion-chamber shape and nozzle location for multiple-orifice process with air swirl



PETITIONER'S EXHIBIT 1002
US PATENT NO. 6,557,540

overlap and the mixture extends beyond this space between the individual injection events, the resulting excessive local fuel concentration leads to air deficiencies and increased formation of soot.

M System

In the MAN wall-distribution combustion system (M system) most of the fuel is sprayed against the wall of the combustion chamber. This process supplements the energy in the injection spray by exploiting the heat from the combustion-chamber wall and the swirling action of the air to form the mixture. The single-orifice nozzle, projecting into the narrow piston-crown chamber at an angle, sprays the fuel into the swirl and against the combustion-chamber wall. Here the fuel forms a film which vaporizes and forms a very homogenous mixture with the swirling combustion-chamber air as it passes. This process combines excellent air utilization with low exhaust-gas opacity (soot emissions).

The fuel film evaporates more slowly from the combustion-chamber wall than the droplets in the compressed air, so combustion processes of this nature are no longer of practical value in terms of the requirements applicable to fuel consumption and gas-phase emissions.

Divided-chamber (two-chamber) combustion systems

Divided-chamber combustion systems are well-suited to small, high-speed diesel engines, usually installed in passenger cars. Here, very stringent requirements are placed on mixture formation speed and air utilization (potential λ). At the same time, economic considerations dictate that the use of the expensive injection equipment required to generate high injection energy be avoided.

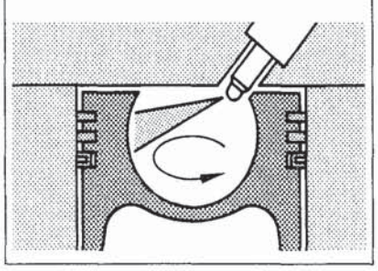
In addition, swirl-type intake passages present difficulties with regard to volumetric efficiency.

The divided-chamber method combines rich mixtures in the auxiliary chamber with relatively lean charges in the main chamber to achieve extremely low NO_x and HC emissions.

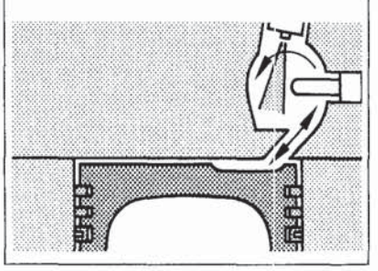
Swirl-chamber system

This process features an almost spherical auxiliary chamber, comprising approx. 50 % of the total compression volume, located at the edge of the main combustion chamber. The connection between the auxiliary and main chambers is furnished by a passage which enters the main chamber at an angle directed toward the center of the piston. The swirl chamber houses the injector and the glow plug (starting aid). The compression stroke generates an intense air vortex in the swirl chamber. As in the M process, the fuel is injected eccentrically to converge with the swirl pattern and land against the chamber's wall. Critical factors are the design of the swirl chamber (for instance, with supplementary mixture vaporization surfaces where the injection spray contacts the wall) and the locations of the injector and the glow plug; these factors define the quality of the combustion process. This process combines very high engine speeds (> 5000 min^{-1}), with good air utilization and low particulate emissions.

Combustion-chamber shape and nozzle location in the MAN M system



Combustion-chamber shape and nozzle location for the swirl-chamber system



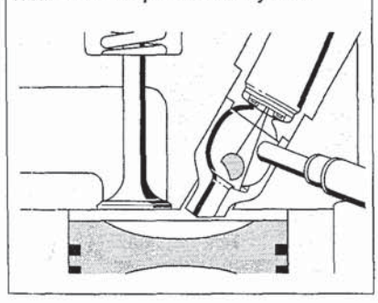
PETITIONER'S EXHIBIT 1002
US PATENT NO. 6,557,540

Prechamber system

The prechamber system features an auxiliary chamber (prechamber) which is centrally located relative to the main combustion chamber, with 35...40 % of the compression volume. Here too, the injection nozzle and glow plug (starting aid) are located in the prechamber. It communicates with the main combustion chamber through several orifices to allow the combustion gases to mix as completely as possible with the main combustion air. One optimized prechamber concept utilizes the deflection surface below the injector nozzle to simultaneously induce rapid mixture formation and a controlled turbulence pattern (on some designs) in the prechamber. The turbulent flow meets the injection spray, which is also aimed into the swirl at an angle. The entire system, including the downstream glow plug, provides combustion with very low emissions and major reductions in particulates. The process is distinguished by a high air-utilization factor, and is also suitable for high engine speeds.

On account of the inherently high fuel consumption, prechamber combustion is becoming less and less viable for passenger-car applications. Common rail injection (P. 551) and refined turbocharging techniques for small engines have rendered direct injection increasingly commonplace in passenger-car diesel engines.

Combustion-chamber shape and nozzle location for the prechamber system



Combustion process

The start of injection (and thus the start of mixture formation) and the initiation of the exothermal reaction (start of ignition) are separated by a certain period of time, called ignition lag. The actual delay is defined by:

- the ignitability of the fuel (cetane number),
- the compression end pressure (compression ratio, boost factor),
- the compression end temperature (compression ratio, component temperatures, intercooling), and
- the fuel-management system.

The combustion process, which begins with the start of ignition, can be subdivided into three phases. In the "premixed flame" phase, the fuel injected prior to the start of ignition and mixed with the air combusts. The fuel injected once ignition has started combusts in a "diffusion flame". That portion of the combusted fuel which burns as a very rapid premixed flame is primarily responsible for the pressure rise, and thus is the primary cause of both combustion noise and oxides of nitrogen. The slower-burning diffusion flame is the main source of particulates and unburned hydrocarbons.

The third, post-injection, phase is when the soot formed primarily during the second phase is oxidized. This phase is becoming increasingly significant in modern combustion processes.

The heat release of a diesel engine depends on the combustion process itself, but also to a very large extent on the start of injection, the injection rate, and the maximum injection pressure. In direct-injection diesel engines, the number of orifices in the nozzle is another crucial factor. The injection system, moreover, requires a pre-injection capability (pilot injection) in order to reduce combustion noise and ensure that injection for the main injection phase commences as early as possible. This reduces fuel consumption for given levels of nitrogen-oxide emissions.

The diagram illustrates the thermal-release patterns which are characteristic of the various injection methods. The dual-stage combustion available with the di-

PETITIONER'S EXHIBIT 1002
US PATENT NO. 6,557,540

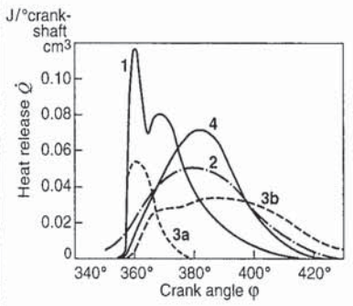
vided-chamber process provides yet another means of influencing the combustion process by allowing selection of different diameters for the passage between the auxiliary and main chambers.

Problems and limits of combustion

Because the fuel injected into diesel engines must ignite through auto-ignition, highly volatile fuel is required (cetane number CN ≈ 45...50). Since at low starting speeds compression does not begin until after intake-valve closure (that is, significantly after BDC), the effective compression ratio, and with it the compression temperature, are greatly reduced. This means that despite high compression ratios, ignition problems can occur during starting, particularly when the engine is cold.

In addition, cold engine components tend to absorb thermal energy from the compressed air (polytropic exponent: $1.1 < n < 1.2$). The equation $T_1 = T_0 \cdot \varepsilon^{n-1}$ indicates that a reduction in the effective compression or the polytropic exponent causes a reduction in the final compression temperature. At the same time, mixture formation is unsatisfactory at low engine speeds (low injection pressure, large fuel droplets) and air movement is inadequate. Extended vaporization times (injection begins sooner) and an increase in the injected fuel quantity – to significantly higher levels than the full-load quantity (providing more low-boiling fuel) can only partially solve the starting problem, because the higher-boiling fuel constituents leave the engine in the form of white or blue smoke. Thus starting aids designed to increase the temperature, such as glow plugs or flame starting systems, are essential, especially in small engines.

Thermal-release curves
1 Air-distributed direct fuel injection (naturally-aspirated engine tuned for maximum economy), 2 Wall-distribution direct injection (designed for minimal noise), 3 Divided-chamber process in auxiliary chamber (3a) and main chamber (3b), 4 Minimum emissions static-charge spray injection (intercooled turbocharged engine).



Because a significant portion of the mixture-formation process occurs during combustion in heterogeneous processes, it is important to avoid local concentrations of excessively rich mixture in the diffusion flame, as the result would be an increase in soot emissions, even with extremely lean overall mixtures. The air-fuel ratio limits at the officially mandated tolerance level for smoke provide an index of air-utilization efficiency. Divided-chamber engines reach the smoke limit with excess air of 5...15%, while the comparable figure is 10...80% for direct-injection diesels. It should be noted that large-volume diesel engines must also be run with significant levels of excess air owing to thermal component load.

Soot is an inevitable byproduct of heterogeneous combustion, so a sootless diesel engine must inevitably remain a conditional development and will require significant improvement in soot oxidation.

It has, however, proven possible to reduce the particulate emissions from modern diesel engines to below the visibility threshold using a variety of measures. These include raising injection pressures at the nozzle, and the transition to optimized spray injection processes featuring larger combustion recesses in the piston, multiple injector orifices, exhaust-gas turbocharging, and charge-air cooling. The planned limits for particulates, however, dictate the need for the development of particulate filters employing the requisite regenerative systems.

Due to the abrupt combustion in that portion of the fuel that vaporizes and mixes with air during the ignition-lag period, the auto-ignition process may be characterized by "hard", loud combustion during operation under those conditions where this fuel comprises a large propor-

PETITIONER'S EXHIBIT 1002
US PATENT NO. 6,557,540

tion of the total. These conditions include idle, low part-throttle on turbocharged engines, and high-load operation on high-speed naturally-aspirated powerplants.

The situation can be improved by decreasing the ignition lag (preheating the intake air, turbocharging or increasing compression) and/or by reducing the injected fuel quantity during the ignition-lag period. On direct-injection engines, this reduction is usually obtained by applying pilot injection, whereas on divided-chamber engines a special injector configuration is employed (throttling pintle nozzle).

Not to be confused with the "hard" combustion inherent to the design is the "knock" to which turbulence-chamber arrangements with pintle nozzles are particularly susceptible, and which occurs primarily in the medium- and low-load areas of the diesel's operating curve. This phenomenon is traceable to inadequacies in the mixture-formation system (poor injector "chatter" or soot at the injectors), and is characterized by a pulsating metallic sound.

The diesel engine must be designed for operation with high peak pressures, and its materials and their dimensions must be selected accordingly. The reasons include:

- High compression ratios required for reliable starting and noise reductions,
- Combustion process with maximum ignition propagation for fuel economy, and
- Increasingly frequent use of turbochargers featuring higher charge pressures.

Owing to the fact that diesel engines must also operate with excess air (lean) at full throttle, they generally have lower specific outputs than their spark-ignition counterparts.

Hybrid processes

Hybrid engines share characteristics with both diesel and spark-ignition engines.

Charge stratification

In stratified-charge SI engines the mixture directly adjacent to the spark plug is enriched to ensure reliable ignition, while the rest of the combustion process proceeds in an extremely lean mixture. The objective is to combine the part-throttle economy comparable to that of a diesel with (especially important) low NO_x and CO emissions.

Research on open-chamber combustion systems with many characteristics similar to those of diesel systems (mixture quality control, high-pressure injection, etc.) is focusing on employing internal mixture formation (Texaco TCCS, Ford PROCO, Ricardo, MAN-FM, KHD-AD) to generate an ignitable mixture at the spark plug while using progressively leaner mixtures (down to pure air) in the remainder of the combustion chamber.

Processes which use internal mixture formation have an air-utilization factor comparable to that of diesel engines.

Divided-chamber combustion systems tend to resemble spark-ignition engines in their basic layout (throttle control, mixture induction, etc.). In these the spark plug is located within a small auxiliary chamber – the ignition chamber – corresponding to roughly 5...25 % of the total compression volume. One or several passages connect this primary ignition chamber with the main combustion chamber.

The auxiliary combustion chamber features an additional injector which injects a portion of the fuel directly (VW, Porsche-SKS), or a supplementary valve to supply fuel-air mixture to the ignition chamber (Honda-CVCC).

A disadvantage of these processes is their more complex design and the higher HC emissions stemming from lower exhaust-gas temperatures and the attendant reductions in secondary combustion activity in the exhaust tract.

PETITIONER'S EXHIBIT 1002
US PATENT NO. 6,557,540

Multifuel engines

In multifuel engines, the ignitability and knock resistance of the fuel can be relatively insignificant; these engines must be able to burn fuels of varying qualities without sustaining damage. Because fuels used with multifuel engines can have a very low knock-resistance rating, external mixture formation would be accompanied by the danger of combustion knock or preignition. For this reason, multifuel engines always use internal mixture formation and retarded injection timing (similar to the diesel engine). The injection pump for multifuel operation has an annular lubrication channel in the pumping element to lubricate the plungers with engine oil from the forced-feed lubrication system. This lubrication channel also prevents fuel from entering the pump's camshaft chamber. Because the low ignition quality of the fuels makes auto-ignition difficult or even impossible, multifuel engines operate with extremely high compression ratios (Mercedes-Benz, MTU: ε = 25:1). As an alternative they may be equipped with an auxiliary ignition source such as spark plugs or glow plugs (MAN-FM). At ε = 14...15, the compression ratio in these engines with externally-supplied ignition lies between that of spark-ignition and diesel engines.

A special type of ignition is the ignition spray process used in alcohol and gas engines (KHD, MWM), in which supplementary diesel fuel – corresponding to 5...10 % of the full-throttle supply of diesel fuel – is sprayed directly into the combustion chamber to ensure ignition. In this process, the main energy source can be supplied via external or internal mixture formation.

Whereas stratified charging with new mixture-formation systems is a focus of attention within the framework of ongoing development of GDI engines, multifuel engines are of virtually no significance at this time.

Gas exchange

In combustion engines employing open processes, the gas-exchange (exhaust and refill) system must serve two decisive functions:

1. Replacement is employed to return the gas medium to its initial (start of cycle) condition, and
2. The oxygen required to burn the fuel is provided in the form of fresh air.

The parameters defined in DIN 1940 can be used to evaluate the gas-exchange process. For overall air flow (air expenditure $\lambda_a = m_g/m_{th}$) the entire charge transferred during the work cycle m_g is defined with reference to the theoretical maximum for the specific displacement. In contrast, the volumetric efficiency $\lambda_{a1} = m_z/m_{th}$ is based exclusively on the fresh charge m_z actually present or remaining in the cylinder. The difference between m_z and the total charge transfer m_g consists of the proportion of the gas that flows directly into the exhaust tract in the overlap phase, making it unavailable for subsequent combustion. The retention rate

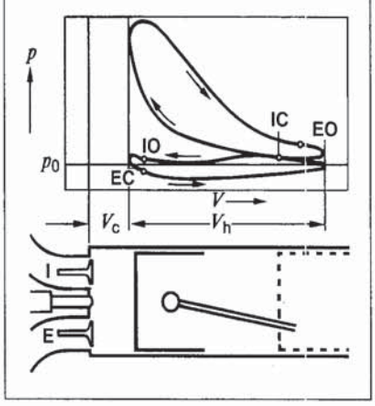
$\lambda_z = m_z/m_g$

is an index of the residual charge in the cylinder. The scavenge efficiency

$\lambda_S = m_z/(m_z+m_r)$

indicates the volume of the fresh charge m_z relative to the existing total charge, consisting of the fresh charge and the

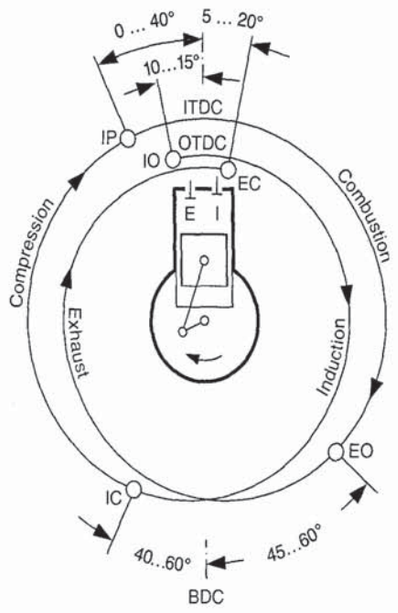
Representation of the four-stroke gas exchange process in the p-V diagram



PETITIONER'S EXHIBIT 1002
US PATENT NO. 6,557,540

4-stroke gas-exchange process

E Exhaust,
EO Exhaust opens,
EC Exhaust closes,
I Intake,
IO Intake opens,
IC Intake closes,
TDC Top dead center,
OTDC Overlap TDC,
ITDC Ignition TDC,
BDC Bottom dead center,
IP Ignition point.



residual gas m_r. Here, the parameter m_r indicates the amount of residual gas from earlier working cycles remaining in the cylinder after the exhaust process.

In a 2-stroke cycle, the gas is exchanged with every rotation of the crankshaft at the end of the expansion in the area around bottom dead center. In a 4-stroke cycle, separate intake and exhaust strokes provide a supplementary gas-exchange cycle.

4-stroke process

Valve timing – and thus gas exchange – are regulated by a control shaft (camshaft) rotating at half the frequency of the crankshaft by which it is driven. The camshaft opens the gas-exchange valves by depressing them against the valve springs to discharge the exhaust gas and to draw in the fresh gas (exhaust and intake valves respectively). Just before piston bottom dead center (BDC), the exhaust valve opens and approx. 50 % of the combustion gases leave the combustion chamber under a supercritical pressure ratio during this predischarge phase. As it moves upward during the exhaust stroke, the piston sweeps nearly all of the combustion gases from the combustion chamber.

Shortly ahead of piston top dead center (TDC) and before the exhaust valve has closed, the intake valve opens. This crankshaft top dead center position is called the gas-exchange TDC or overlap TDC (because the intake and exhaust processes overlap at this point) in order to distinguish it from the ignition TDC. Shortly after gas-exchange TDC, the ex-

PETITIONER'S EXHIBIT 1002
US PATENT NO. 6,557,540

haust valve closes and, with the intake valve still open, the piston draws in fresh air on its downward stroke. This second stroke of the gas-exchange process, the intake stroke, continues until shortly after BDC. The subsequent two strokes in the 4-stroke process are compression and combustion (expansion).

On throttle-controlled gasoline engines, during the valve overlap period exhaust gases flow directly from the combustion chamber into the intake passage, or from the exhaust passage back into the combustion chamber and from there into the intake passage. This tendency is especially pronounced at low throttle openings with high manifold vacuum. This "internal" exhaust-gas recirculation can have negative effects on idle quality, but it is impossible to avoid entirely, as a compromise has to be found between adequate high-speed valve lift and a satisfactory idle.

Early exhaust valve timing allows a high degree of blowdown, and thus guarantees low residual-gas compression as the piston sweeps through its upward stroke, although at the price of a reduction in the work index for the combustion gases.

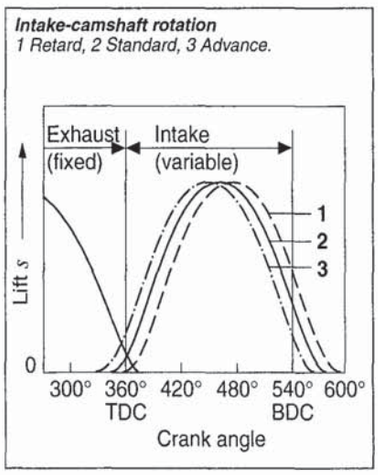
The "intake valve closes" (IC) timing exercises a decisive effect on the relationship between air expenditure and engine speed.

When the intake valve closes early (IC) the maximum charge efficiency occurs at low engine speeds, while late closing shifts the efficiency peak toward the upper end of the min^{-1} spectrum.

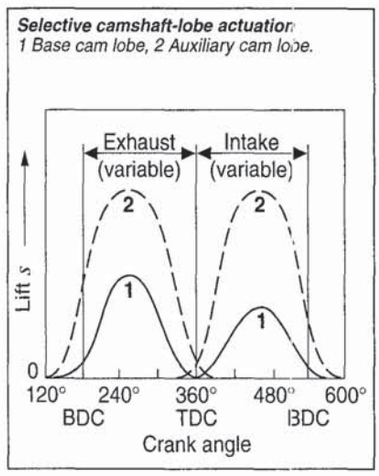
Obviously, fixed valve timing will always represent a compromise between two different design objectives: Maximum brake mean effective pressure – and thus torque – at the most desirable points on the curve, and the highest possible peak output. The higher the min^{-1} at which maximum power occurs, and the wider the range of engine operating speeds, the less satisfactory will be the ultimate compromise. Large variations in the valves' effective flow opening relative to stroke (i.e. in designs featuring more than two valves) will intensify this tendency.

At the same time, the demands for minimal exhaust emissions and maximum fuel economy mean that low idle speeds and high low-end torque (despite and along with high specific outputs for reasons of power-unit weight) are becoming increasingly important. These imperatives have led to the application of variable valve timing (especially for intake valves), whereby the most significant concepts (with attention focused on high-speed gasoline engines in series production) have been the following:

Variable camshaft timing by rotation: A hydraulic control mechanism rotates the intake camshaft to vary the valve timing for "intake opens" and "intake closes" as a



Intake-camshaft rotation
1 Retard, 2 Standard, 3 Advance.



Selective camshaft-lobe actuation
1 Base cam lobe, 2 Auxiliary cam lobe.

PETITIONER'S EXHIBIT 1002
US PATENT NO. 6,557,540

function of engine speed (Alfa-Romeo, Mercedes-Benz).

The camshaft is set for delayed closing of the intake valve at idle and at high engine speeds. This results in a certain amount of valve overlap at overlap top dead center (OTDC) for stability at idle and enhanced output at high min^{-1}. The camshaft is rotated to close the intake valve early (IC) under full load in midrange operation, furnishing higher volumetric efficiency with correspondingly high levels of torque.

Selective camshaft-lobe actuation: The timing of the intake and exhaust valves is varied by alternating between separate lobes featuring two different lift profiles (Honda).

The first lobe features a profile tailored for optimum intake and exhaust timing and valve lift in the lower and middle engine-speed ranges. At high min^{-1}, a rocker arm that pivots freely at low speeds is coupled to the standard rocker arm; this rocker arm rides on a second cam lobe to provide greater lift and extended opening times.

Infinitely-variable valve lift and timing: Continuous modification of valve timing as a function of engine speed (Fiat).

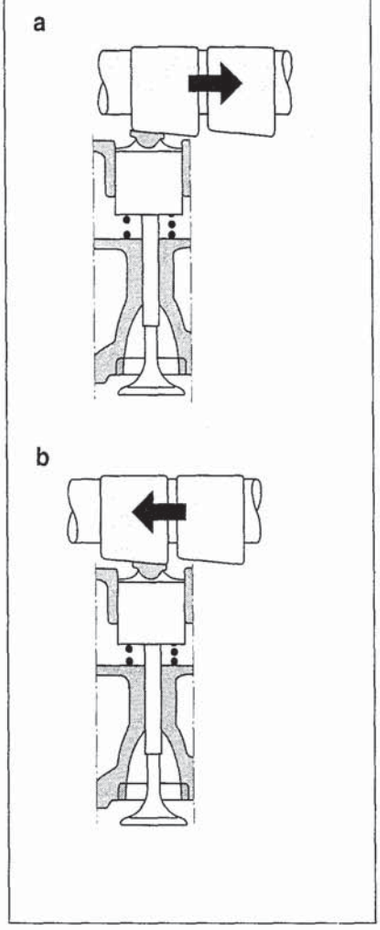
This is the optimum concept, but it is also the most difficult to implement. It employs cam lobes with a curved three-dimensional profile and lateral camshaft shift to achieve substantial increases in torque over the engine's entire min^{-1} range.

High-speed solenoid injectors (injection valves) have opened the way for development of electro-hydraulically actuated valve timing systems. Work is also under way on valve timing arrangements with solenoid actuation. At this time, however, solutions of this nature have not progressed as far as series production.

Evaluating gas-exchange components

The intake and exhaust tracts can be evaluated using stationary flow testing with flow numbers or passage efficiency levels. It is useful to evaluate the exhaust valves in the lower lift range with reference to supercritical pressures of the kind occurring in the blowdown phase.

Infinitely-variable valve lift and timing
a) Minimum lift, b) Maximum lift.



Alongside assessment of the flow number, analysis of in-cylinder flow is becoming increasingly significant. These studies can also be based on stationary flow testing and the derived parameters for swirl and tumble. Increasing use is being made of 3D computer models which, unlike the available measuring techniques, can furnish local information about flow conditions. Highly developed engine models are widely used today in the theoretical assessment of the overall gas cycle.

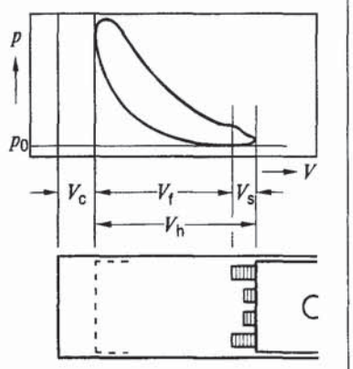
PETITIONER'S EXHIBIT 1002
US PATENT NO. 6,557,540

Advantages of the 4-stroke process:
Very good volumetric efficiency over the entire engine-speed range, low sensitivity to pressure losses in the exhaust system, along with relatively good control of the charging-efficiency curve through selection of appropriate valve timing and intake system designs.

Disadvantages of the 4-stroke process:
Valve control is highly complex. The power density is reduced because only every second shaft rotation is used to generate work.

2-stroke process
To maintain gas exchange without an additional crankshaft rotation, the gases are exchanged in the two-stroke process at the end of expansion and at the beginning of the compression stroke. The intake and exhaust timing are usually controlled by the piston as it sweeps past intake and exhaust ports in the cylinder housing near BDC. This configuration, however, requires symmetrical control times and involves the problem of short-circuit scavenging. In addition, 15...25 % of the piston stroke cannot produce work because only charge volume V_f and not displacement volume V_h can be exploited for power generation. Because the two-stroke process lacks separate intake and exhaust strokes, the cylinder must be filled and scavenged using positive pressure, necessitating the use of scavenging pumps. In an especially simple and very frequently-used design, the bottom surface of the piston works in conjunction with a crankcase featuring a minimal dead volume to form a scavenging pump. The illustrations show a 2-stroke engine with crankcase scavenging or crankcase precompression along with the associated control processes. The processes which take place on the scavenging pump side are shown in the inner circle, while those occurring on the cylinder side are shown in the outer circle. Satisfactory cylinder scavenging is available using crossflow scavenging, loop scavenging and uniflow scavenging.

Graphical representation of the 2-stroke gas-exchange process in the p-V diagram



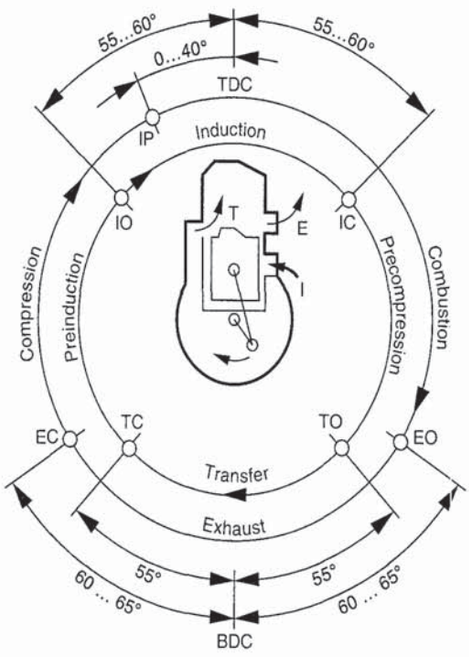
Advantages of the 2-stroke process:
Simple engine design, low weight, low manufacturing costs, better torsional force pattern.

Disadvantages of the 2-stroke process:
Higher fuel consumption and higher HC emissions (cylinder scavenging is problematic), lower mean effective pressures (poorer volumetric efficiency), higher thermal loads (no gas-exchange stroke), poor idle (higher percentage of residual gas).

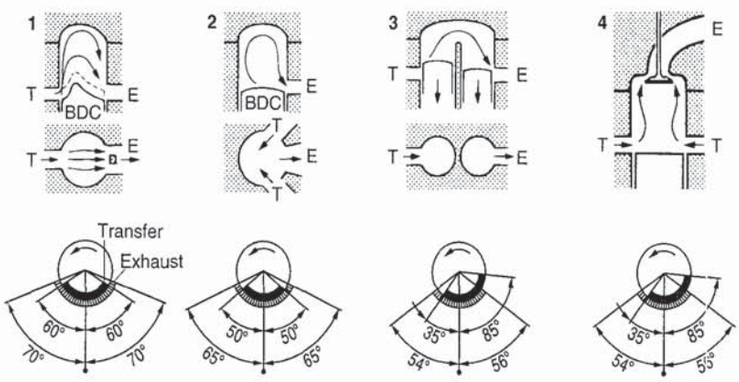
PETITIONER'S EXHIBIT 1002
US PATENT NO. 6,557,540

2-stroke gas-exchange process with crankcase compression

E Exhaust,
EO Exhaust opens,
EC Exhaust closes,
I Intake,
IO Intake opens,
IC Intake closes,
T Transfer passage, closes,
TO Transfer passage
TC Transfer passage opens,
TDC Top dead center,
BDC Bottom dead center,
IP Ignition point.



2-stroke scavenging.
1 Cross scavenging, 2 Loop scavenging, 3 and 4 Uniflow scavenging.



PETITIONER'S EXHIBIT 1002
US PATENT NO. 6,557,540

Supercharging processes

The power of an engine is proportional to the processed air mass m_z. Because this air throughput, in turn, is proportional to air density, the power of an engine, given a specific displacement and engine speed, can be increased by precompressing the air before it enters the cylinders, i. e. by supercharging.

The supercharging ratio indicates the density rise as compared to a naturally-aspirated engine. One determining factor is the system used (potential pressure ratio). The maximum ratio for a given pressure increase is obtained when the temperature of the compressed air (boost air) is not increased or is returned to its initial level by intercooling.

In the spark-ignition engine, the supercharging ratio is restricted by the pre-ignition threshold. In the diesel engine maximum permissible peak pressures are the limiting factor. In order to avoid these problems, supercharged engines usually have lower compression ratios than their naturally aspirated counterparts.

Dynamic supercharging

The simplest type of supercharging exploits the dynamic properties of the intake air.

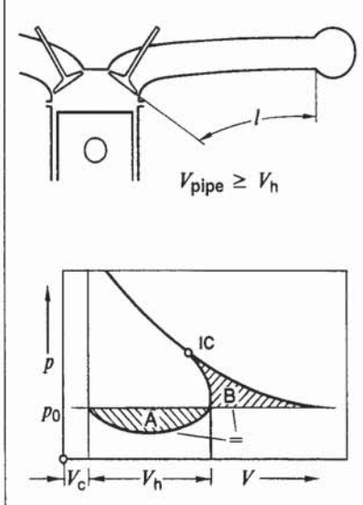
Ram-pipe supercharging

Each cylinder has a special intake manifold of a specific length, usually connected to a common plenum chamber. The energy balance is characterized by the fact that the intake work of the piston is converted into kinetic energy in the column of gas upstream from the intake valve, and this kinetic energy, in turn, is converted into charge compression work.

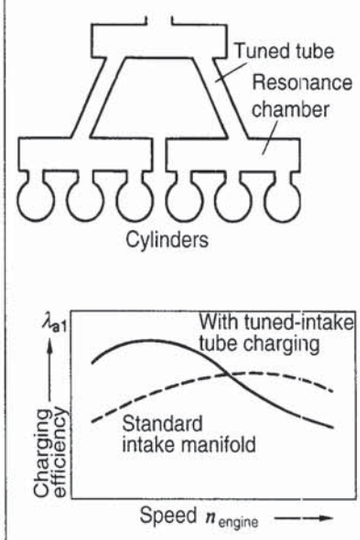
Tuned-intake-tube charging

In tuned-intake charging, short ducts connect groups of cylinders with the same ignition intervals to resonance chambers. These resonance chambers are connected to the atmosphere or a common chamber by tuned tubes, and act as Helmholtz resonators.

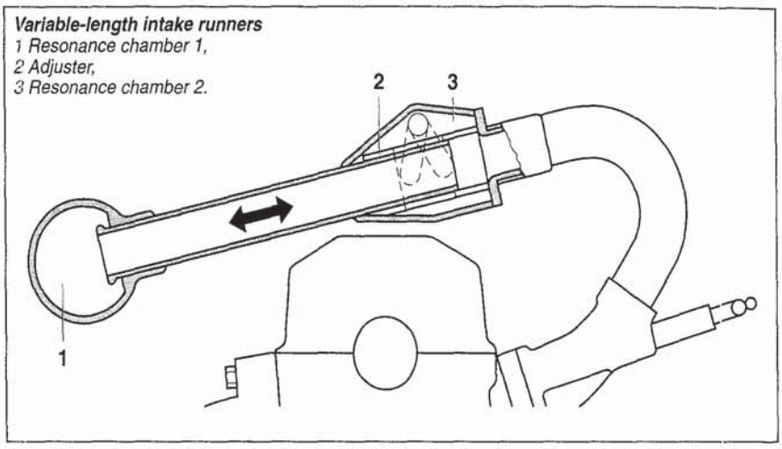
Ram-pipe supercharging
Configuration and energy balance.
Induction work A of the piston corresponds to compression work B.



Tuned-intake-tube charging
Configuration and charging-efficiency curve.



PETITIONER'S EXHIBIT 1002
US PATENT NO. 6,557,540



Variable-length intake runners
1 Resonance chamber 1,
2 Adjuster,
3 Resonance chamber 2.

Variable-geometry intake manifold

Several manufacturers (BMW, Citroën, Opel, Ford) have already introduced systems employing the principles of dynamic boost (including combination designs). These systems enhance charge efficiency, above all at low min^{-1}.

Switch-over in the variable-geometry system uses flaps or similar devices to connect or isolate the different groups of cylinders as a function of engine speed.

At low min^{-1} the variable-length intake runners operate in conjunction with an initial resonance chamber. The length of the intake runners is adjusted continually as engine speed increases, the entire process culminating with the opening of a second resonance chamber.

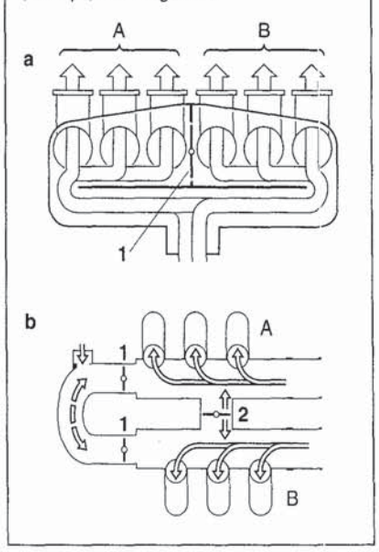
Mechanical supercharging

In mechanical supercharging, the supercharger is powered directly by the engine, which usually drives the supercharger at a fixed transmission ratio. Mechanical or electromagnetic clutches are often used to control supercharger activation.

A clear illustration of the relationship between the engine and the supercharger is provided by the diagram for pressure vs. volumetric flow rate, in which the pressure ratio π_c of the supercharger is plotted against volumetric flow rate $\dot{V}$.

The curves for unthrottled 4-stroke engines (diesel) are particularly descriptive because they contain sloped straight lines (engine mass flow characteristics) which represent increasing engine air-throughput values as the pressure ratio $\pi_c \triangleq p_2/p_1$ increases at constant engine speed.

The diagram shows pressure ratios which result at corresponding constant supercharger speeds for a positive-displacement supercharger and a hydrokinetic compressor.



Variable-geometry intake manifold
a) Two-stage operation.
b) Three-stage operation.
A, B Cylinder groups;
1, 2 Flaps, min^{-1}-regulated

PETITIONER'S EXHIBIT 1002
US PATENT NO. 6,557,540

Only superchargers whose delivery rates vary linearly with their rotational speeds are suitable for vehicle engines. These are positive-displacement superchargers of piston or rotating-vane design or Roots blowers (see P. 440). Hydrokinetic flow compressors are not suitable.

Advantages of mechanical supercharging:
Relatively simple superchargers on "cold" side of engine. Engine exhaust gas is not involved. Supercharger responds immediately to load changes.

Disadvantages of mechanical supercharging:
The supercharger must be engine-powered, causing increased fuel consumption.

Exhaust-gas turbocharging
In exhaust-gas turbocharging, the energy for the turbocharger is extracted from the engine's exhaust gases. Although the process exploits energy that remains unused (owing to crankshaft assembly expansion limits) by naturally-aspirated engines, exhaust back-pressure increases as the gases furnish the power required to turn the compressor.

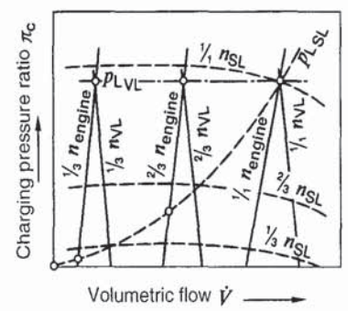
Current turbocharged engines employ an exhaust-driven turbine to convert the energy in the exhaust gas into mechanical energy, making it possible for the turbocharger to compress the induction gas.

The exhaust-gas turbocharger is a combined exhaust-driven turbine and flow compressor (see P. 442).

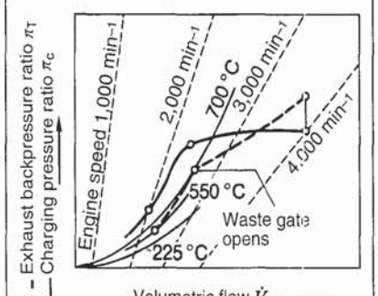
Exhaust-gas turbochargers are usually designed to generate a high boost pressure even at low engine speeds. Conversely, however, boost pressure at the high end of the engine min^{-1} range can increase to levels that could place excessive load on the engine. Engines with wide speed ranges in particular therefore require a waste gate bypassing the turbine, although this means a loss of exhaust-gas energy. Much more satisfactory results can be achieved with a compromise between high charge pressure at low min^{-1} and avoidance of engine overload at the high end of the min^{-1} range by employing Variable Turbine Geometry (VTG). The blading of a VTG turbine adjusts to suit the flow cross-section and thus the gas pressure at the turbine by variation of the flow cross-section.

Advantages of exhaust-gas turbocharging:
Considerable increase in power output per liter from a given configuration; improved torque curve within the effective engine-speed range; significant improvement in fuel consumption figures relative to naturally-aspirated engines with the same output power; improvement in exhaust-gas emissions.

Pressure vs. volumetric flow-rate map of mechanically driven positive-displacement supercharger and turbocharger
VL *Positive-displacement supercharger,*
SL *Hydrokinetic flow compressor.*



Pressure vs. volumetric flow-rate map of an exhaust-gas turbocharger showing boost pressure and exhaust backpressure curves



PETITIONER'S EXHIBIT 1002
US PATENT NO. 6,557,540

Disadvantages of exhaust-gas turbocharging:
Installation of the turbocharger in the hot exhaust-gas tract requiring materials resistant to high temperatures; complexity and space requirements for turbocharger and intercooler; low base torque at low engine speed; throttle response is extremely sensitive to the efficient matching of the turbocharger to the engine.

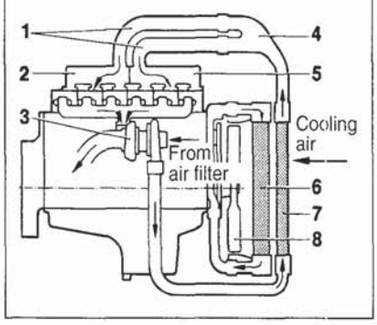
Pressure-wave supercharging
The pressure-wave supercharger uses direct energy exchange between exhaust gas and the intake air to increase the latter's density. This is accomplished by utilizing the differing speeds of the gas particles and pressure waves on the one side, and the reflection properties of these pressure waves on the other (see P. 446).

The pressure-wave supercharger consists of a cell rotor with an air casing on one side and an exhaust casing on the other. These incorporate specific timing edges and gas-pocket configurations.

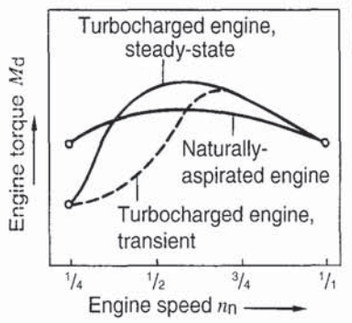
Advantages of pressure-wave supercharging:
Rapid throttle response because energy exchange between exhaust gas and boost air takes place at the speed of sound; high compression at low engine speeds.

Disadvantages of pressure-wave supercharging:
Restrictions on installation flexibility owing to the belt drive and gas lines; increased quantities of exhaust gas and scavenge air; loud operation; extremely sensitive to increased resistance on the low-pressure side.

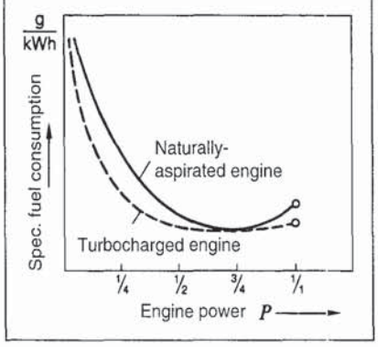
Truck diesel engine with exhaust-gas turbocharging, tuned-intake-tube supercharging and intercooler
1 Tuned tubes, 2 Resonance chamber for cylinders 4 – 5 – 6, 3 Turbocharger, 4 Balance chamber, 5 Resonance chamber for cylinders 1 – 2 – 3, 6 Radiator, 7 Intercooler, 8 Fan



Static and transient torque curves for turbocharged and naturally-aspirated engines



Specific part-load fuel consumption curves for atmospheric-induction and turbocharged engines of the same power



PETITIONER'S EXHIBIT 1002
US PATENT NO. 6,557,540

Power transfer in reciprocating-piston engines

Engine types

Single-piston-power unit
The working chamber is formed by cylinder head, cylinder liner, and piston.

In-line engine (1)
Cylinders arranged consecutively in a single plane.

V-engine (2)
The cylinders are arranged in two planes in a V configuration.

Radial engine (3)
The cylinders are arranged radially in one or more planes.

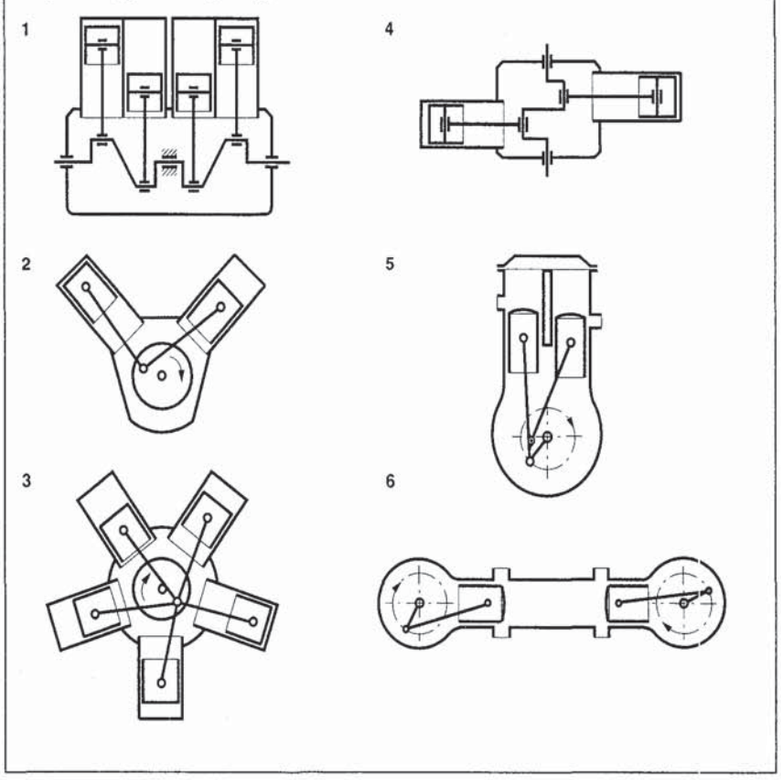
Opposed-cylinder (boxer) engine (4)
The cylinders are horizontally opposed.

Multi-piston-power unit
More than one (usually two) working pistons share a common combustion chamber.

U-engine (5)
The pistons move in the same direction.

Opposed-piston engine (6)
The pistons move in opposite directions.

Reciprocating-piston engine types



PETITIONER'S EXHIBIT 1002
US PATENT NO. 6,557,540

Direction of rotation
(DIN 73021)[1])

Clockwise rotation: as viewed looking at the end of the engine opposite the power-output end. Abbreviation: cw.

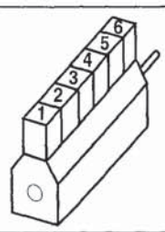
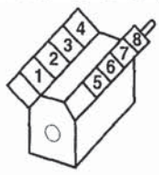
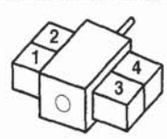
Counterclockwise rotation: as viewed looking at the end of the engine opposite the power-output end. Abbreviation: ccw.

Numbering the cylinders
(DIN 73021)[1])

The cylinders are numbered consecutively 1, 2, 3, etc. in the order in which they would be intersected by an imaginary reference plane. As viewed looking at the end of the engine opposite the power-output end. This plane is located horizontally to the left when numbering begins; the numerical assignments then proceed clockwise around the longitudinal axis of the engine (see figures below). If there is more than one cylinder in a reference plane, the cylinder nearest the observer is assigned the number 1, with consecutive numbers being assigned to the following cylinders. Cylinder 1 is to be identified by the number 1.

Firing order

The firing order is the sequence in which combustion is initiated in the cylinders. Engine design configuration, uniformity in ignition intervals, ease of crankshaft manufacture, optimal crankshaft load patterns, etc., all play a role in defining the firing order.

Design	Number of cylinders	Normal firing order (examples)
 Power output	4	1 3 4 2 or 1 2 4 3
	5	1 2 4 5 3
	6	1 5 3 6 2 4 or 1 2 4 6 5 3 or 1 4 2 6 3 5 or 1 4 5 6 3 2
	8	1 6 2 5 8 3 7 4 or 1 3 6 8 4 2 7 5 or 1 4 7 3 8 5 2 6 or 1 3 2 5 8 6 7 4
 Power output	4	1 3 2 4
	6	1 2 5 6 4 3 or 1 4 5 6 2 3
	8	1 6 3 5 4 7 2 8 or 1 5 4 8 6 3 7 2 or 1 8 3 6 4 5 2 7
 Power output	4	1 4 3 2

[1]) Applies to motor-vehicle engines only. For internal-combustion engines for general and marine use, the reverse direction (as viewed looking at the power-output end) is standardized (ISO 1204 and 1205, DIN 6265).

PETITIONER'S EXHIBIT 1002
US PATENT NO. 6,557,540

Crankshaft-assembly operation and dynamic properties

The purpose of the piston, connecting rod and crankshaft assembly in the reciprocating-piston engine is to transform the gas forces generated during combustion within the working cylinder into a piston stroke, which the crankshaft then converts into useful torque available at the power-output end of the engine. The cyclic principle of operation leads to unequal gas forces, and the acceleration and deceleration of the reciprocating power-transfer components generate inertial forces. It is usual to distinguish between internal and external effects of the gas-pressure and inertial forces.

The external effects, consisting of free forces or moments, impart movement to the engine. This is then transmitted to the engine supports in the form of vibration.

In this context, the smooth running of an engine is understood to mean freedom from low-frequency vibration, while quiet running means freedom from high-frequency, audible vibration.

The internal forces induce periodically variable loads in block, piston, connecting rod, crankshaft assembly and force-transfer components. These factors must be included in calculations for defining their dimensions and fatigue resistance.

Crankshaft assembly and gas force

The crankshaft assembly of a single-cylinder powerplant comprises the piston, connecting rod (conrod) and crankshaft. These components react to gas forces by generating mass inertial forces of their own.

The gas force F_G which acts on the piston can be subdivided into the side forces F_N applied by the piston to the cylinder wall and supported by it, and the connecting-rod force F_S. The connecting-rod force, in turn, causes the tangential force F_T to be applied at the crankshaft journal. This force together with the crank radius generates the shaft torque and the radial force F_R.

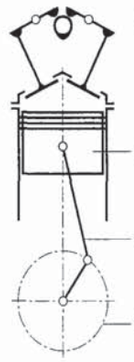
These forces can be calculated as a function of the gas force using the crank angle α, the pivoting angle of the connecting rod β and the stroke/connecting rod ratio λ:

Connecting-rod force: $F_S = F_G/\cos\beta$
Piston side force: $F_N = F_G \cdot \tan\beta$
Radial force: $F_R = F_G \cdot \cos(\alpha+\beta)/\cos\beta$
Tangential force: $F_T = F_G \cdot \sin(\alpha+\beta)/\cos\beta$
where $\lambda = r/l$; $\sin\beta = \lambda \cdot \sin\alpha$;

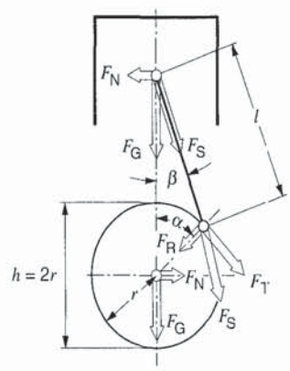
$$\cos\beta = \sqrt{1-\lambda^2 \cdot \sin^2\alpha}$$

All of these relationships can be represented in the form of a Fourier series, which can be useful in vibration calculations.

Piston and crankshaft assembly of the reciprocating-piston engine *(concept)*
1 Valve gear,
2 Piston,
3 Connecting rod,
4 Crankshaft



Gas-force components shown on a basic crankshaft assembly



PETITIONER'S EXHIBIT 1002
US PATENT NO. 6,557,540

Inertial forces and moments of inertia

The mass inertial properties of the piston, connecting rod and crankshaft assembly are a composite of the forces of the rotating masses of the crankshaft around their axis (x-axis) and the reciprocating masses in the cylinder direction (z-axis for in-line engines). With multiple-cylinder machines, free moments of inertia occur owing to different points of application for gas and inertial forces. The inertial properties of a single-cylinder engine can be determined using the piston mass m_K (exclusively oscillating mass), the crankshaft mass m_W (exclusively rotating mass) and the corresponding connecting-rod mass components (usually assumed to consist of oscillating and rotating rod masses amounting to one third and two thirds of the total mass respectively):

Oscillating mass

$$m_o = m_{Pl}/3 + m_K$$

Rotating mass

$$m_r = 2\,m_{Pl}/3 + m_W$$

The rotating inertial force acting on the crankshaft is as follows:

$$F_r = m_r \cdot r \cdot \omega^2$$

Oscillating inertial force:

$$F_o = m_o \cdot r \cdot \omega^2 \cdot (\cos\alpha + \lambda \cdot \cos 2\alpha + \ldots)$$

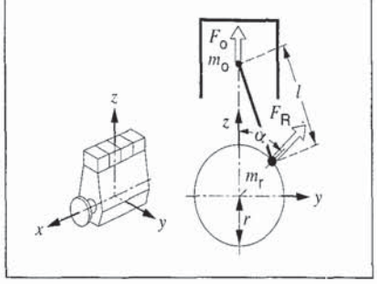
(1st Order; 2nd Order)

The following approximations also apply:

$$F_y = r \cdot \omega^2 \cdot m_r \cdot \sin\alpha$$

$$F_z = r \cdot \omega^2 \cdot [m_r \cdot \cos\alpha + m_o \cdot (\cos\alpha + \lambda \cdot \cos 2\alpha)]$$

Reference coordinates and inertial forces *(single-cylinder engine)*



where $\lambda = r/l$

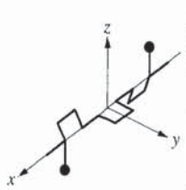
The inertial-force components are designated as inertial forces of the 1st, 2nd or 4th order, depending upon their rotational frequencies relative to engine speed.

In general, only the 1st and 2nd order components are significant; higher orders can be disregarded.

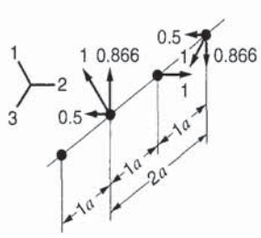
In the case of multiple-cylinder engines, free moments of inertia are present when all of the complete crankshaft assembly's inertial forces combine to produce a force couple at the crankshaft. The crankshaft assembly must therefore be regarded as a three-dimensional configuration when determining the free moments of inertia, while the inertial forces can be determined using a two-dimensional system.

Moments of inertia of a crankshaft with three throws *(example)*

Practical configuration



Moments of inertia, 1st order



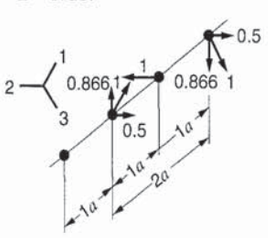
$$\frac{M_1}{(m_r + m_0) \cdot r \cdot \omega^2 \cdot a} = 1.732$$

$$\vec{M} \updownarrow 0.866\,(-1 + 3) = 1.732$$

$$\leftrightarrow$$

$$M = 0.5 \cdot 1 - 1 \cdot 2 + 0.5 \cdot 3 = 0$$

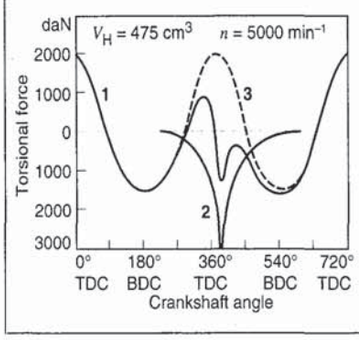
Moments of inertia, 2nd order



$$\frac{M_2}{m_0 \cdot r \cdot \omega^2 \cdot \lambda \cdot a} = 1.732$$

PETITIONER'S EXHIBIT 1002
US PATENT NO. 6,557,540

Torsional-force diagram for a single-cylinder, four-stroke engine
1 Gas and inertial forces, 2 Gas forces, 3 Inertial forces.



Torsional-force diagram for the reciprocating-piston engine

If the periodic gas force acting on the piston and the periodic mass inertial forces acting on the piston, connecting rod and crankshaft assembly are grouped together, they generate a sum of tangential force components at the crankshaft journal. When multiplied by the crank radius, this yields a periodically variable torque value. If this torque value is referred to the piston surface and the crank radius, the result is a value valid for any engine size: tangential pressure. The torsional-force diagram shows the curve for this pressure as a function of crankshaft position. It is one of the most important characteristic curves in assessing dynamic engine behavior.

With multiple-cylinder engines, the tangential-pressure curves for the individual cylinders are superimposed with a phase shift in accordance with the number of cylinders, their configuration, crankshaft design and the firing order. The resulting composite curve is characteristic for the engine design, and covers a full working cycle (i.e., 2 crankshaft rotations for 4-stroke engines). It is also called a tangential-pressure diagram.

Harmonic analysis can be employed to replace the torsional-force diagram with a series of sinusoidal oscillations featuring whole-number multiples of the basic frequencies, and to obtain the "torsional harmonics". When defined according to engine speed these multiples are also called orders. When applied to a four-stroke engine this procedure generates half orders, e.g. the 0.5th order.

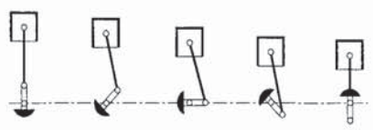
The cyclical fluctuations in torsional force encountered in all reciprocating-piston engines lead to variations in the crankshaft's rotation speed, the so-called coefficient of cyclic variation.

$$\delta_s = (\omega_{max} - \omega_{min})/\omega_{min},$$

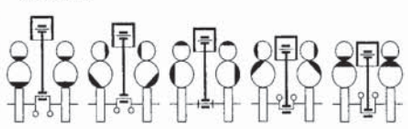
An energy storage device (the flywheel) provides adequate compensation for these variations in rotation rate in normal applications.

Complete 1st and 2nd order balancing of masses in a single-stroke system

Counterweights

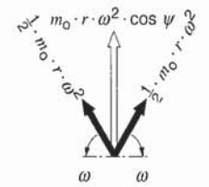


Unbalanced systems rotating in opposite directions



Vector diagrams of the 1st and 2nd order oscillating inertial forces

1st Order



2nd Order



PETITIONER'S EXHIBIT 1002
US PATENT NO. 6,557,540

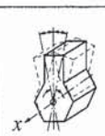
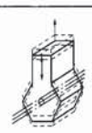
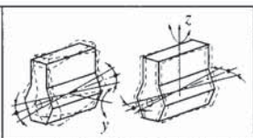
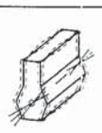
Balancing of masses in the reciprocating-piston engine

Mass balancing encompasses a wide array of measures employed to obtain partial or complete compensation for the inertial forces and moments of inertia emanating from the crankshaft assembly. All masses are externally balanced when no free inertial forces or moments of inertia are transmitted through the block to the outside. However, the remaining internal forces and moments subject the engine mounts and block to various loads as well as deformative and vibratory stresses. The basic loads imposed by gas-based and inertial forces are shown in Table 3.

Balancing of inertial forces in the single-stroke powerplant

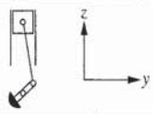
The simplest way to balance rotating masses is to use counterweights to generate an equal force to oppose the centrifugal force. Oscillating masses generate periodic forces. The 1st order forces are propagated at crankshaft speed, while the periodicity of the 2nd order forces is twice the crankshaft's rotation rate. Compensation for these forces is available in the form of a counterweight balance system designed for opposed rotation at a rate equal to or twice that of the crankshaft. The balance forces' magnitudes must equal those of the rotating inertial-force vectors while acting in the opposite direction.

Table 3. Forces and moments applied to the piston, connecting rod and crankshaft assembly

Forces and moments at the engine				
Designation	Oscillating torque, transverse tilting moment, reaction torque	Free inertial forces	Free inertial moment, longitudinal tilting moment about the y-axis (transverse axis) ("pitching" moment) about the z-axis (vertical axis) ("rolling" moment)	Internal flex forces
Cause	Tangential gas forces as well as tangential inertial forces for ordinals 1, 2, 3 and 4	Unbalanced oscillating inertial forces 1st order in 1 and 2 cylinders; 2nd order in 1, 2, and 4 cylinders	Unbalanced oscillating inertial forces as a composite of 1st and 2nd order forces	Rotating and oscillating inertial forces
Design factors	Number of cylinders, ignition intervals, displacement, p_i, ε, p_z, m_0, r, ω, λ	Number of cylinders, crank configuration m_0, r, ω, λ	Number of cylinders, crank configuration,cylinder spacing, counterweight size influences inertial torque components about the y- and z-axes m_0, r, ω, λ, a	Number of throws, crank configuration, engine length, engine-block rigidity
Remedy	Can only be compensated for in exceptional cases	Free mass effects can be eliminated with rotating balancing systems, however this process is complex and therefore rare; crank sequences with limited or no mass effects are preferable		Counterweights, rigid engine block
	Shielding of the environment through flexible engine mounts (in particular for orders ≥ 2)			

PETITIONER'S EXHIBIT 1002
US PATENT NO. 6,557,540

Table 4. Residual 1st order inertial forces with differing balancing rates

		Balancing rate		
		0%	50%	100%
Size of counter-weight	$m_G \triangleq$	m_r	$m_r + 0.5m_0$	$m_r + m_0$
Residual inertial force (z) 1st order	$F_{1z} =$	$m_0 \cdot r \cdot \omega^2$	$0.5 \cdot m_0 \cdot r \cdot \omega^2$	0
Residual inertial force (y) 1st order	$F_{1y} =$	0	$0.5 \cdot m_0 \cdot r \cdot \omega^2$	$m_0 \cdot r \cdot \omega^2$

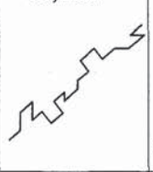
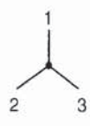
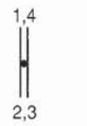
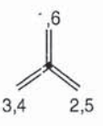
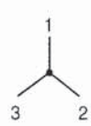
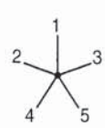
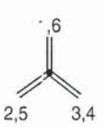
Balancing rate

The forces exerted by the counterweights used to balance the rotating masses can be increased by a certain percentage of the oscillating mass in order to reduce the oscillating forces acting in the direction of the cylinders (z). The percentage of this inertial force which is counteracted then appears in the y-axis. The ratio of the compensated inertial-force component in the z-axis relative to the initial value for the 1st order inertial force is termed the balancing rate (Table 4).

Balancing of inertial forces in the multi-cylinder engine

In multi-cylinder engines the mutual counteractions of the various components in the crankshaft assembly are one of the essential factors determining the selection of the crankshaft's configuration, and with it the design of the engine itself. The

Table 5. Star diagram of the 1st and 2nd order for three- to six-cylinder, in-line engines

	3-cylinder	4-cylinder	5-cylinder	6-cylinder
Crank sequence				
Star diagram 1st Order				
Star diagram 2nd Order				

PETITIONER'S EXHIBIT 1002
US PATENT NO. 6,557,540

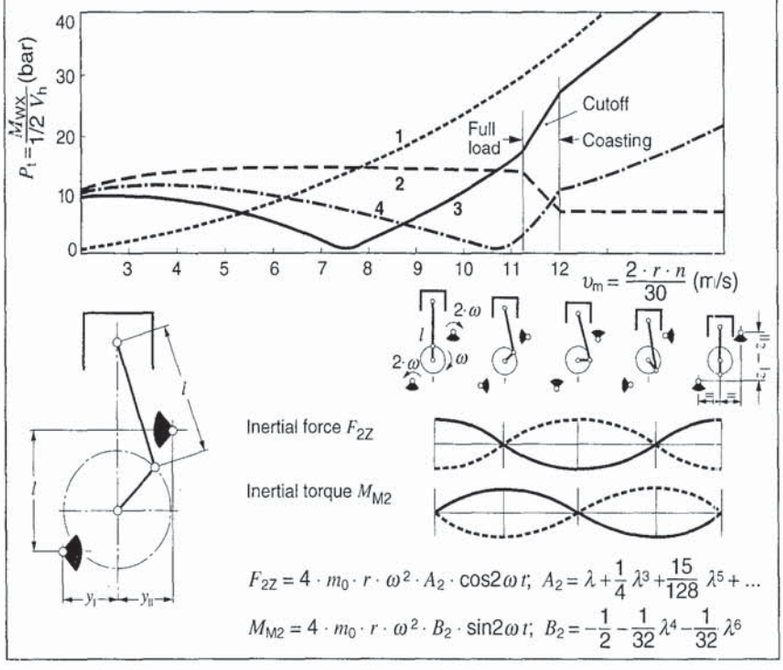
inertial forces are balanced if the common center of gravity for all moving crankshaft-assembly components lies at the crankshaft's midpoint, i.e. if the crankshaft is symmetrical (as viewed from the front). The crankshaft's symmetry level can be defined using geometrical representations of 1st- and 2nd-order forces (star diagrams). The 2nd order star diagram for the four-cylinder in-line engine is asymmetrical, meaning that this order is characterized by substantial free inertial forces. These forces can be balanced using two countershafts rotating in opposite directions at double the rate of the crankshaft (Lanchester system).

Balancing of inertial and gas forces

The tangential gas forces produce yet another periodic torque; this can be detected as reaction torque in the engine block. The composite forces generated in a four-cylinder in-line engine include free mass forces of the 2nd order as well as variable torque forces from the 2nd order mass and gas forces. Compensation for 2nd order mass forces, along with a reduction in the intensity of the 2nd order force transitions, is available from two offset balance shafts.

Balancing 2nd order inertial and transitional forces in a four-cylinder, in-line engine with two offset countershafts

1 Inertial torque only; 2 Gas torque only or complete balancing of inertial torque, $z_I - z_{II} = -2\,B_2/A_2 \cdot r$; 3 Gas and inertial torque without force compensation; 4 Gas and inertial torque with half of the inertial torque balanced, $z_I - z_{II} \approx 0.5 \cdot l$.



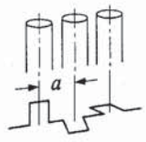
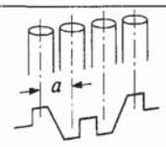
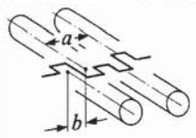
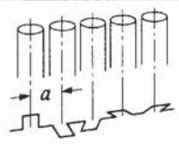
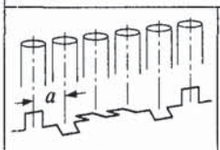
$$F_{2Z} = 4 \cdot m_0 \cdot r \cdot \omega^2 \cdot A_2 \cdot \cos 2\omega t;\quad A_2 = \lambda + \frac{1}{4}\lambda^3 + \frac{15}{128}\lambda^5 + \ldots$$

$$M_{M2} = 4 \cdot m_0 \cdot r \cdot \omega^2 \cdot B_2 \cdot \sin 2\omega t;\quad B_2 = -\frac{1}{2} - \frac{1}{32}\lambda^4 - \frac{1}{32}\lambda^6$$

PETITIONER'S EXHIBIT 1002
US PATENT NO. 6,557,540

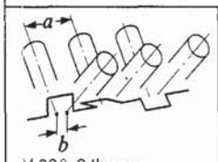
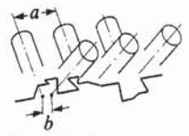
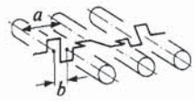
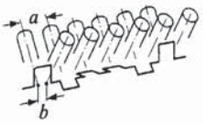
Table 6. Free forces and moments of the 1st and 2nd order, and ignition intervals of the most common engine designs

$F_r = m_r \cdot r \cdot \omega^2 \quad F_1 = m_0 \cdot r \cdot \omega^2 \cdot \cos\alpha \quad F_2 = m_0 \cdot r \cdot \omega^2 \cdot \lambda \cdot \cos 2\alpha$

Cylinder arrangement	Free forces of 1st order[1])	Free forces of 2nd order	Free moments of 1st order[1])	Free moments of 2nd order	Ignition intervals
3-cylinder					
 In-line, 3 throws	0	0	$\sqrt{3} \cdot F_1 \cdot a$	$\sqrt{3} \cdot F_2 \cdot a$	240°/240°
4-cylinder					
 In-line, 4 throws	0	$4 \cdot F_2$	0	0	180°/180°
 Opposed-cylinder (boxer), 4 throws	0	0	0	$2 \cdot F_2 \cdot b$	180°/180°
5-cylinder					
 In-line, 5 throws	0	0	$0.449 \cdot F_1 \cdot a$	$4.98 \cdot F_2 \cdot a$	144°/144°
6-cylinder					
 In-line, 6 throws	0	0	0	0	120°/120°

[1]) Without counterweights.

PETITIONER'S EXHIBIT 1002
US PATENT NO. 6,557,540

Cylinder arrangement	Free forces of 1st order[1])	Free forces of 2nd order	Free moments of 1st order[1])	Free moments of 2nd order	Ignition intervals
6-cylinder (continued)					
 V 90°, 3 throws	0	0	$\sqrt{3}\cdot F_1\cdot a$ [2])	$\sqrt{6}\cdot F_2\cdot a$	150°/90° 150°/90°
 Normal balance V 90°, 3 throws, 30° crank offset	0	0	$0.4483\cdot F_1\cdot a$ 	$(0.966\pm0.256)\cdot\sqrt{3}\cdot F_2\cdot a$ 	120°/120°
 Opposed-cylinder, 6 throws	0	0	0	0	120°/120°
 V 60°, 6 throws	0	0	$3\cdot F_1\cdot a/2$	$3\cdot F_2\cdot a/2$	120°/120°
8-cylinder					
 V 90°, 4 throws in two planes	0	0	$\sqrt{10}\cdot F_1\cdot a^2$ [2])	0	90°/90°
12-cylinder					
 V 60°, 6 throws	0	0	0	0	60°/60°

[1]) Without counterweights.
[2]) Can be completely balanced by using counterweights.

UCLA SELLERS Collection

PETITIONER'S EXHIBIT 1002
US PATENT NO. 6,557,540

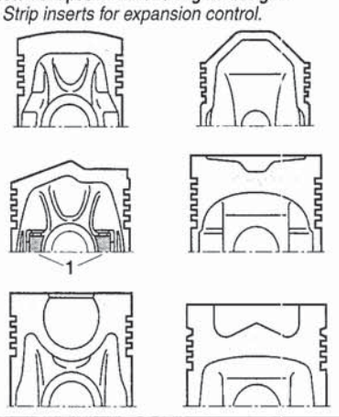
Main components of reciprocating-piston engine

Piston

Pistons in today's motor-vehicle engines must perform a wide range of functions:
- They transmit the force generated by the combustion gas to the connecting rods.
- They serve as crosstails to define the connecting rods' travel paths within the cylinders.
- They support the normal force applied against the cylinder walls while the cylinder pressure is conveyed to the connecting rod.
- Together with their sealing elements, they seal the combustion chamber from the crankcase.
- They absorb heat for subsequent transfer to the cooling system.

Both the piston's design and the wristpin configuration employed to transfer the combustion gas forces to the connecting rod are largely determined by the combustion chamber's shape, including the geometry of the piston crown, while other variables include the selected combustion process and the associated pressure maxima. The priority is to produce the lightest possible piston in a unit capable of withstanding intense forces during operation in an environment with temperatures that can approach the physical limits of the materials used in its manufacture.

Piston shapes in various engine designs
1 Strip inserts for expansion control.

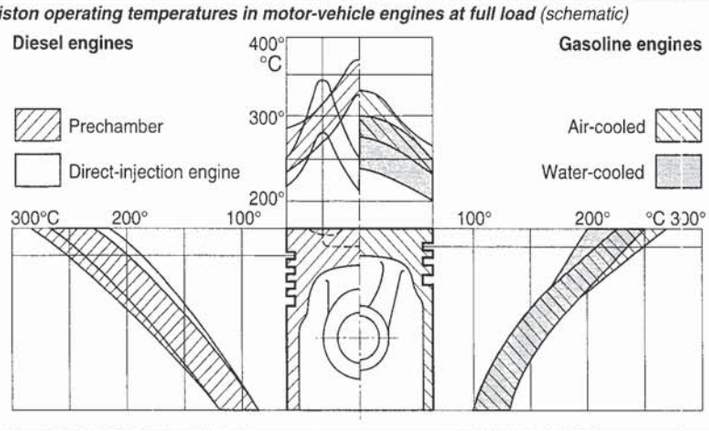


Precise definition of the dimensions for the piston, wristpin and wristpin bushings are essential for achieving this goal.

The most frequently used materials for cylinder liners and pistons are gray cast iron and aluminum. Variations in piston clearance within the cylinder must be minimized to reduce noise (piston slap) and improve sealing, notwithstanding the fact that piston and cylinder liner have different coefficients of expansion. To this end, steel strips or similar elements are sometimes cast into the piston to limit its expansion.

Piston rings form the sealing element between the combustion chamber and the crankcase. The upper two – the compression rings – serve as gas seals. At

Piston operating temperatures in motor-vehicle engines at full load *(schematic)*

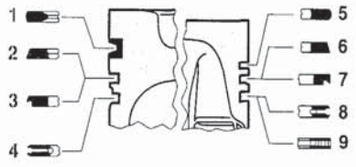


PETITIONER'S EXHIBIT 1002
US PATENT NO. 6,557,540

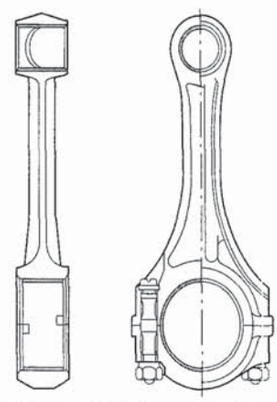
Piston-ring shapes and configurations

Diesel engine: *1 Keystone ring, crowned, 2 Taper-face compression ring with inner bevel, 3 Stepped compression ring, 4 Double-beveled ventilated oil control ring with spiral-type expander.*

Spark-ignition engine: *5 Plain compression ring, crowned, 6 Taper-face compression ring, 7 Stepped ring, 8 Double-beveled ring, 9 Multipart steel oil ring.*



Passenger-car engine connecting rod



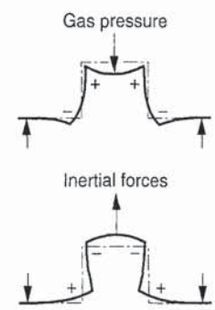
least one additional ring (generally of a different design), the oil control ring, is also present. This is a "scraper" ring and ensures correct lubrication of the piston and compression rings. Owing to the rings' extreme tension and the force that they exert against the cylinder walls, they are a major source of friction within the reciprocating-piston engine.

Connecting rod

The connecting rod (conrod) is the joining element between piston and crankshaft. It is subject to extreme tensile, compression and flex stresses, while it also houses the wristpin bushings and crankshaft bearings. Connecting-rod length is determined by the piston stroke and the counterweight radius; whereby the engine height can also be an important factor (usually the case in vehicle engines).

Crankshaft throw

Primary stresses and deformations due to gas pressure and inertial forces.



Crankshaft

The crankshaft with its rod extensions, or throws, converts the reciprocating motion of the pistons – conveyed to it by the connecting rods – into rotary motion, making effective torque available at the crankshaft's end. The forces acting upon the crankshaft are characterized by highly variable periodicities and vary greatly according to location. These torques and flex forces, and the secondary vibrations which they generate, all represent intense and highly complex stress factors for the crankshaft itself. As a result, its structural properties and vibrational response patterns rely upon precise calculations and carefully defined dimensions. Calculations and dimensioning though are further complicated by the fact that too many multiple journal bearings are practically always installed as a precautionary measure.

The number of crankshaft bearings is primarily determined by overall load factor and maximum engine speed. To accommodate their intense operating pressures, all diesel-engine crankshafts incorporate a main bearing journal between each crankshaft throw and at each end of the crankshaft. This arrangement is also found in high-speed spark-ignition (SI) en-

PETITIONER'S EXHIBIT 1002
US PATENT NO. 6,557,540

gines designed for high specific outputs.

Crankshafts in some smaller SI engines designed for operation at lower load factors sometimes extend the interval between main bearings to 2 cylinders to reduce expense. The number of counterweights also depends upon the criteria cited above.

Stresses and load factors are also primary considerations in the selection of both materials and manufacturing processes. Highly-stressed crankshafts are usually drop-forged. In smaller and less highly stressed engines, cast crankshafts, incorporating the dual advantages of lower weight and less expense, are becoming increasingly popular.

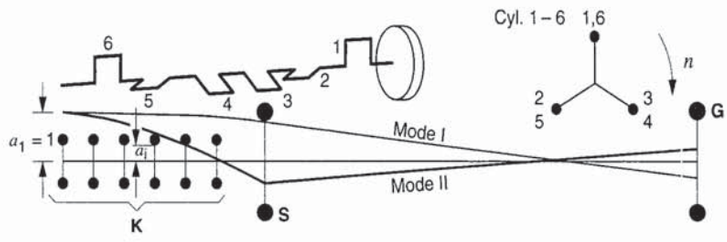
Cast crankshaft



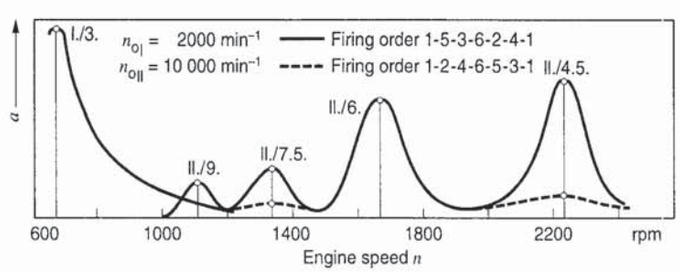
Crankshaft vibrations

Flexural vibration is significant only on engines with a small number of cylinders, because the crankshaft and the necessary large flywheel form an oscillatory system with a low natural frequency. Flexural vibration is not a critical factor on engines of 3 cylinders or more. By logical extension, this also applies to the longitudi-

***Vibrational schematic of a 6-cylinder crankshaft* (K) *with flywheel* (S) *and transmission* (G)**
a Relative amplitudes, n Engine speed.



Order analysis of the crankshaft vibrations of a 6-cylinder engine,
with differing firing orders, a Relative amplitudes



PETITIONER'S EXHIBIT 1002
US PATENT NO. 6,557,540

nal crankshaft vibrations induced by flexural vibrations.

At the same time, the torsional vibrations of the resonant system formed by crankshaft, connecting rods and pistons become increasingly critical with higher numbers of cylinders. This system, in which the mass moments of inertia for connecting rods and pistons vary according to crankshaft angle, can be calculated by reducing it to a smooth, flexible shaft free of inertia with equivalent masses mounted on it. The oscillation reduction model makes it possible to determine both the system's inherent frequency and the intensity of the vibration forces. The oscillations emanate from the tangential forces generated by a combination of gas forces and oscillating mass forces at the crank pin. Vibration dampers are required to reduce the crankshaft's torsional vibrations to acceptable levels (e.g. bonded rubber vibration dampers or viscous vibration dampers).

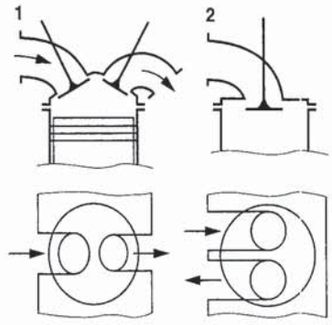
Engine block and crankcase

The block and crankcase unit supports the force-transfer mechanism between cylinder head and crankshaft assembly; it bears the crankshaft assembly's support bearings, and incorporates (or holds) the cylinder sleeves. Also included in the block are a separate water jacket and sealed oil chambers and galleries. The block also serves as a mounting and support surface for most of the engine's ancillary units.

A cast block and crankcase unit is the standard configuration for automotive applications. The cylinder-head bolts oppose the gas forces to facilitate a force transfer of maximum linearity and minimal flexural tendency through transverse support walls and to the main bearings. For greater strength the crankcase is frequently extended to below the crankshaft's center axis. The pistons in spark-ignition engines almost always run in integral cylinders machined from the block casting. In diesel engines, separate dry or wet liners made of special wear-resistant materials are usually used.

Whereas, virtually all blocks for truck engines continue to be manufactured in cast iron, aluminum passenger-car blocks are becoming increasingly popular owing to their weight-savings potential.

Cylinder-head designs according to intake and exhaust tract location
1 Crossflow design,
2 Counterflow design.



Cylinder head

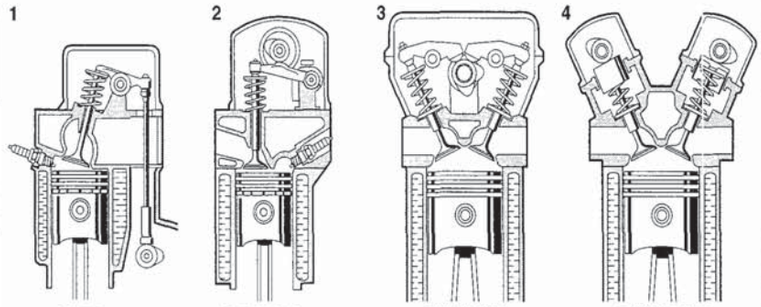
The cylinder head seals off the upper end of the block and cylinder(s). It houses the gas-exchange valves as well as the spark plugs and/or injectors. Together with the piston, it also provides the desired combustion-chamber shape. In the vast majority of passenger-car engines, the entire valve gear is also mounted in the cylinder head. Based on the gas-exchange concepts, one differentiates between two basic design configurations:

- Counterflow cylinder head: Intake and exhaust passages open onto the same side of the cylinder head. This limits the space available for the intake and exhaust gas passages, but due to the short flow tracts this represents a substantial advantage in supercharged applications. This design, with the gas supply and discharge tracts on a single side, also provides practical advantages in transverse-mounted engines.
- Crossflow cylinder head: Intake and exhaust passages are located on opposite sides of the engine, furnishing a diagonal flow pattern for the intake and exhaust gases. This layout's advantages include more latitude in intake and exhaust-tract design as well as less complicated sealing arrangements.

In truck and large industrial engines, individual cylinder heads are often used on each cylinder for better sealing-force distribution and easier maintenance and re-

PETITIONER'S EXHIBIT 1002
US PATENT NO. 6,557,540

Valve-gear designs (source: Hütten "Motoren")
1 Push-rod assembly, 2 Single rocker-arm assembly, 3 Twin rocker-arm assembly, 4 Overhead bucket-tappet assembly, OHV Overhead valves, OHC Overhead camshaft, DOHC Double overhead camshaft.



pair. Separate cylinder heads are also specified for improved cooling efficiency on air-cooled engines.

In passenger-car and low-power engines, one cylinder head is usually employed for all cylinders together. The cylinder heads on water-cooled diesel truck engines are usually made of cast iron.

Superior heat dissipation and lower weight have combined to make aluminum the material of choice in the construction of cylinder heads for air-cooled engines as well as on virtually all spark-ignition and diesel engines for passenger cars.

Valve gear

It is the function of the valve-gear assembly in a 4-stroke engine to permit and to control the exchange of gases in the IC engine (see P. 384). The valve gear includes the intake and exhaust valves, the springs which close them, the camshaft drive assembly and the various force-transfer devices.

Valve-actuation concepts

In the following widely-used designs the camshaft is located in the cylinder head:

- Overhead bucket-tappet assembly, in which a "bucket" moving back and forth in the cylinder head absorbs the cam lobe's lateral force while transferring its linear actuating pressure to the valve stem.
- Cam follower or single rocker-arm assembly actuated by an overhead cam, in which the cam lobe's lateral and linear forces are absorbed and relayed by a cylinder-head-mounted lever rocking back and forth between cam lobe and valve. In addition to transferring forces, the rocker arm can also be designed to magnify the effective lobe profile for greater valve travel.
- Twin rocker-arm assembly actuated by overhead cam, in which the rocker arm's tilt axis is located between the camshaft and the valve. Here too, the rocker arm is usually designed as a cam lift multiplier to produce the desired valve travel.

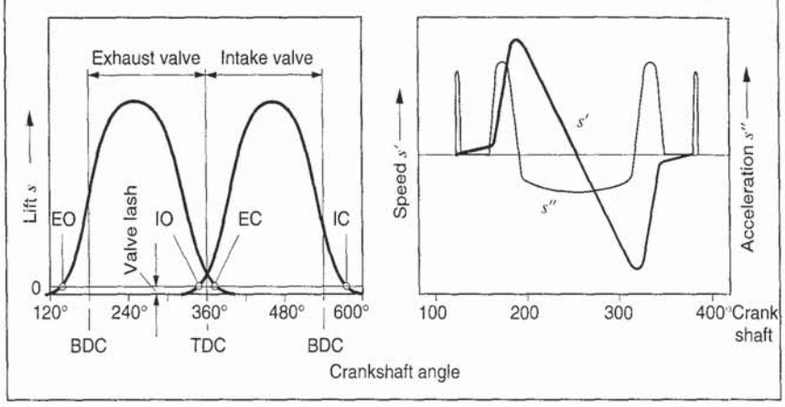
When the camshaft is installed within the block, the camshaft lobe acts against an intermediate lifter and pushrod assembly instead of directly against the valve.

Valve arrangements

The valve control arrangement and the design of the combustion chamber are closely interrelated. Today, nearly all valve assemblies are overhead units mounted in the cylinder head. In diesels and simpler spark-ignition engines, the valves are parallel to the cylinder axis, and are usually actuated by twin rocker arms, bucket tappets or single rocker arms. With increasing frequency, those current spark-ignition engines designed for higher specific outputs tend to feature intake and exhaust valves which are inclined towards each other. This configuration allows larger valve diameters for a given cylinder bore while also providing greater latitude

PETITIONER'S EXHIBIT 1002
US PATENT NO. 6,557,540

Valve timing diagram showing valve lift (s), valve velocity (s′) and valve acceleration (s″)



for optimizing intake and exhaust passage design. Twin rocker-arm assemblies actuated by overhead cams are used most often here. High-performance and racing engines are increasingly using four valves per cylinder and overhead-bucket-tappet valve assemblies.

An engine's valve-timing diagram shows the opening and closing times of the valves, the valve-lift curve with maximum lift, and the valve's velocities and acceleration rates.

Typical valve acceleration rates for passenger-car OHC (overhead camshaft) valve assemblies:

$s'' = 60 \ldots 65$ mm $(b/\omega^2) \triangleq 6400$ m/s² at 6000 min⁻¹ for single and twin rocker-arm assemblies,

$s'' = 70 \ldots 80$ mm $(b/\omega^2) \triangleq 7900$ m/s² at 6000 min⁻¹ for overhead-bucket tappet assemblies. For heavy commercial-vehicle engines with block-mounted camshafts:

$s'' = 100 \ldots 120$ mm $(b/\omega^2) \triangleq 2000$ m/s² at 2400 min⁻¹.

Valve, valve guide and valve seat

The materials employed in manufacturing valves are heat and scale-resistant. The valve seat's contact surface is frequently hardened. A proven method for improving the thermal transfer characteristics of exhaust valves is to fill their stems with sodium. To extend service life and improve sealing, valve-rotating systems (rotocaps) are now in common use.

The valve guides in high-performance engines must feature high thermal conductivity and good antifriction properties. They are usually pressed into the cylinder head and are often supplemented by valve stem seals at their cold ends for reducing oil consumption.

Valve-seat wear is generally reduced by making the valve seats of cast or sintered materials and shrink-fitting them into the cylinder head.

Lobe design and timing dynamics

The cam lobe must be able to open (and close) the valve as far as possible, as fast as possible and as smoothly as possible. The closing force for the valves is applied by the valve springs, which are also responsible for maintaining contact between the cam lobe and the valve. Dynamic forces impose limits on cam and valve lift.

The entire valve-gear assembly can be viewed as a spring/mass system in which the conversion from stored to free energy causes forced vibration. Valve-gear assemblies with overhead camshafts can be represented with sufficient accuracy by a 1-mass system (consisting of the propelled mass, valve-gear assembly stiffness, and the corresponding damping effects).

Dual-mass systems are becoming increasingly popular for use with block-mounted camshafts and pushrods.

The maximum permissible surface pressure, usually regarded as the decisive parameter limiting cam-lobe radius and the rate of opening on the flank, currently lies

PETITIONER'S EXHIBIT 1002
US PATENT NO. 6,557,540

between 600 and 750 N/mm², depending upon the employed material pairings.

Cooling

In order to avoid thermal overload, combustion of the lubricating oil on the piston's sliding surface, and uncontrolled combustion due to excessive component temperatures, the components surrounding the hot combustion chamber (cylinder liner, cylinder head, valves and in some cases the pistons themselves) must be intensively cooled.

Direct cooling

Direct air cooling removes heat directly from the components. The underlying principle is based on intensive air flow, usually through a finned surface. Although primarily used in motorcycle and aircraft engines, this form of cooling is also employed for some passenger-car and commercial-vehicle diesel and spark-ignition engines. Its main advantage is its high reliability and freedom from maintenance. On the negative side, the design measures required to ensure efficient heat dissipation to the cooling air increase the cost of the components.

Indirect cooling

Because water has a high specific heat capacity and provides efficient thermal transition between the materials, most contemporary vehicle engines are water-cooled. The air/water recirculation cooling system is the most prevalent system. It comprises a closed circuit allowing the use of anti-corrosion and anti-freeze additives. The coolant is pumped through the engine and through an air/water radiator. The cooling air flows through the radiator in response to vehicle movement and/or is forced through it by a fan. The coolant temperature is regulated by a thermostatic valve which bypasses the radiator as required.

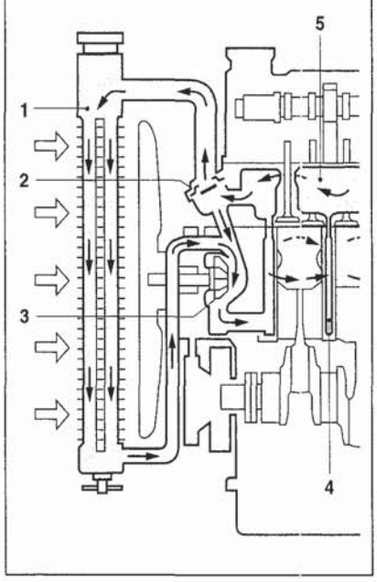
Lubrication

The internal-combustion engine employs oil to lubricate and cool all of the power-transmission components. This oil is also used to remove dirt and neutralize chemically-active combustion products, as well as for transmitting forces and damping vibration. The oil can only fulfill all these requirements if it is transported in adequate quantities to the engine's critical points, and if its properties are adapted to the specific requirements by appropriate measures taken during manufacture (e.g., inclusion of additives).

In total-loss lubrication (fresh-oil lubrication), a metering system supplies oil to the lubrication points, where it is subsequently consumed. A special case of this type of lubrication is mixture lubrication in which oil is either added to the fuel in a ratio ranging from 1:20 to 1:100, or metered to the engine (this process is used primarily in small two-stroke engines).

In most motor-vehicle engines, force-feed lubrication systems are used in combination with splash and oil mist lubrication. The basic force-feed system pumps pressurized oil (usually by gear pump) to all bearing points, while sliding parts are lubricated by splash lubrication systems

Water cooling system with coolant circuit
1 Radiator, 2 Thermostat, 3 Water pump, 4 Water passages in cylinder block, 5 Coolant passages in cylinder head.



PETITIONER'S EXHIBIT 1002
US PATENT NO. 6,557,540